CATÓLICA
UNIVERSIDADE CATÓLICA PORTUGUESA | PORTO
Escola Superior de Biotecnologia

NEW STRATEGIES FOR THE DECELLULARIZATION OF BIOLOGICAL TISSUES

by

Marta Sofia Magalhães Duarte

September, 2019

NEW STRATEGIES FOR THE DECELLULARIZATION OF BIOLOGICAL TISSUES

Thesis presented to *Escola Superior de Biotecnologia* of the *Universidade Católica Portuguesa* to fulfill the requirements of Master of Science degree in Biomedical Engineering

by

Marta Sofia Magalhães Duarte

Place: Escola Superior de Biotecnologia, Universidade Católica Portuguesa

Supervision:

Prof. Ana Leite Oliveira

Dr. Nilza Ribeiro

September, 2019

Resumo

O início do século 21 tem sido marcado pelo aumento das doenças crónicas. Este desenvolvimento resultou num crescimento do interesse na criação de novas terapias, com foco na recuperação de tecidos através da transplantação do tecido danificado por matrizes "inteligentes" desenvolvidas recorrendo ao uso da Engenharia Biomédica. A descelularização, um processo que visa a remoção de material celular imunogénico de um tecido ou órgão, tem-se tornado num meio atraente para o desenvolvimento de novas matrizes funcionais e bioativas.

A presente tese teve como objetivo explorar novas metodologias para a descelularização de tecidos biológicos. Para este propósito, é apresentada uma revisão da literatura relevante e um estudo que investiga o potencial de três diferentes protocolos para a descelularização de osso trabecular porcino usando o fosfato de tri-n-butilo (TnBP), dióxido de carbono supercrítico ($scCO_2$), e uma combinação de ambos. O uso do TnBP como um agente de descelularização, ao invés do uso de produtos químicos mais prejudiciais como os detergentes, pode levar a uma maior preservação da matriz extracelular (ECM), tal como a propriedades bioquímicas e mecânicas mais desejáveis para a matriz resultante. O uso do $scCO_2$ pode, também, resultar num processo de descelularização mais rápido, levando não só a uma redução do tempo de exposição dos tecidos a produtos químicos potencialmente prejudiciais, mas também a uma redução do preço financeiro deste processo.

No total foram implementados e examinados cinco protocolos diferentes: 1% (v/v) TnBP durante 48 horas, $scCO_2$ durante 1 hora e 3 horas, e $scCO_2$ com 0.1% (p/v) TnBP com durante 1 hora e 3 horas. Devido à natureza inovadora deste projeto, usaram-se variáveis temporais para estudar qualquer efeito prejudicial devido ao efeito da exposição prolongada ao $scCO_2$.

Os resultados obtidos revelaram que tanto o TnBP como o $scCO_2$ conseguiram diminuir a quantidade de DNA presente nas amostras, mas esta diminuição foi maior nos protocolos que onde o TnBP foi usado. A análise às propriedades mecânicas dos tecidos sujeitos a TnBP revelaram um aumento da força máxima e da tensão de limite elástico, o que poderá significar que ocorreu crosslinking das fibras de colagénio. Já o uso do $scCO_2$ resultou na desidratação das amostras, aumentado os valores para o módulo de Young e força máxima. O protocolo de combinação $scCO_2$-TnBP causou uma diminuição para metade da quantidade de DNA presente nas amostras tratadas em comparação a não-tratadas, demonstrado o potencial desta metodologia inovadora e abrindo novas possibilidade para otimizações futuras.

Palavras-chave: descelularização, dióxido de carbono supercrítico, TnBP, osso trabecular

Abstract

The beginning of the 21st century has been marked by the rise of chronic diseases. This development has led to increased interest in the development of new therapies that focus on restoring normal tissue function through transplantation of injured tissue with biomedically engineered smart matrices. Decellularization, a process that focuses on the removal of immunogenic cellular material from a tissue or organ, has become an appealing methodology for the creation of functional and bioactive scaffolds.

The present thesis focused on the creation of new methodologies for the decellularization of biological tissues. For this purpose, the author reviewed current decellularization literature and put forward a study that investigated the potential of three different decellularization protocols for porcine trabecular bone tissue using Tri(n-butyl) phosphate (TnBP), supercritical carbon dioxide ($scCO_2$), and a combination of both. The use of TnBP as a decellularization agent, instead of harsh chemicals such as detergents, could lead to better preservation of the extracellular matrix (ECM), and better biochemical and mechanical properties to the resulting scaffold. As well, the use of supercritical fluids could lead to faster decellularization times, not only reducing the time tissues are exposed to potentially harmful agents, but also reducing the financial cost of the process.

In total, five different protocols were implemented and examined: 1% (v/v) TnBP treatment for 48 hours, $scCO_2$ treatment for 1 hour and 3 hours, and $scCO_2$ treatment with 0.1% (w/v) TnBP for 1 hour and 3 hours. Due to the innovative nature of this work, time variants to protocols were implemented to investigate any possible harmful effects caused by prolonged exposure to $scCO_2$ treatment.

Results revealed that both TnBP and $scCO_2$ led to the removal of DNA content, but this effect was more pronounced in treatments that used TnBP. Mechanical analysis of TnBP-treated samples revealed a higher ultimate strength and yield strain, suggesting some degree of crosslinking of collagen fibers occurred. Meanwhile, the use of $scCO_2$ led to dehydration of samples, increasing values for Young's Modulus and ultimate strength. The combined protocol of $scCO_2$-TnBP led to a decrease in DNA content to about half of that measured for untreated samples, demonstrating the potential of this methodology and opening new possibilities for future optimizations that could achieve required decellularization levels.

Keywords: decellularization, supercritical carbon dioxide, TnBP, trabecular bone

Acknowledgments

Throughout the creation and writing of this thesis, I have received immeasurable support from my supervisors, colleagues, family, and friends. While words will never be enough to express my gratitude, I would like to acknowledge their work here.

To begin with, I would like to thank my supervisor, Professor Ana Oliveira, whose patience, time and expertise were indispensable in the writing of this work. As well, I would like to extend my gratitude to Dr. Nilza Ribeiro, who was always available to help me in the execution of my work.

I would also wish to acknowledge Rossana Correia (Histology and Electron Microscopy, Instituto de Investigação e Inovação em Saúde), Ana Rita Malheiro (Histology and Electron Microscopy, Instituto de Investigação e Inovação em Saúde), Rui Fernandes (Histology and Electron Microscopy, Instituto de Investigação e Inovação em Saúde), and Juliana Dias (Unidade Orgânica de Investigação, Politécnico de Leiria), for lending their services and expertise.

In addition, I would like to thank my colleague, Inês Vasconcelos, for her invaluable counsel and time spent in my aid.

Finally, I wish to acknowledge the tremendous efforts of my parents, who have always been there for me. As well, my friends, who have provided me with happy distractions from my work, allowing for some well-needed respite.

Contents

List of Figures

List of Tables

Table of Abbreviations

ASTM - American Society for Testing and Materials

CAGR - Compound annual growth rate

DBM - Demineralized bone matrix

dECM - Decellularized extracellular matrix

DNA - Deoxyribonucleic acid

ECM – Extracellular matrix

EMA - European Medicines Agency

FDA - Food and Drug Administration

GAGs – Glycosaminoglycans

H&E - Hematoxylin and eosin

HHP - High hydrostatic pressure

ISO - International Organization for Standardization

PAA - Peracetic acid

RT – Room temperature

$scCO_2$ – Supercritical carbon dioxide

SDS - Sodium dodecyl sulfate

SEM - Scanning electron microscope

SIS - Small intestine submucosa

TEM - Transmission electron microscopy

TnBP - Tri(n-butyl) phosphate

UBM - Urinary bladder matrix

USA – United States of America

1. Introduction

The rise of chronic disease has been a major preoccupation within the majority of developed countries. Populations are becoming older, a consequence of increasing life expectancy and decreasing birth rates, and this has led to an increase of age-associated diseases that represent some of the most complicated therapeutic challenges in medicine [1]. This development has led to an increased interest in the therapies provided by regenerative medicine, a field of medicine that focuses on restoring normal tissue function through the enhancement of endogenous tissue repair or via direct transplantation of injured tissue [1].

The paradigm of health in Portugal has largely followed global trends. Portugal has an aging population, as more seniors (≥65) than young (≤15) are currently residing in the country [2]. This statistic, and the rise of obesity, has contributed to the prevalence of chronic diseases in Portugal. Chronic diseases are responsible for 80% of mortality in countries belonging to the European Union [2]. Musculoskeletal diseases are one of the most widespread conditions affecting Portuguese people, while cardiovascular problems caused approximately 29,7% of deaths in Portugal in 2015 [2]. Additionally, Portugal has one of the lowest numbers of years of healthy life after the age of 65 [2]. In response to these concerns, the Ministério da Saúde [2] has increased funding for scientific investigation within the biomedical field, through the creation of funds and agencies such as the "Fundo para a Investigação em Saúde" and "Agência de Investigação Clínica e Inovação Biomédica".

1.1 The importance of decellularized extracellular matrix

1.1.1 Current challenges in Regenerative Medicine

The term "Regenerative Medicine" refers to a branch of tissue engineering and molecular biology with the aim of directly replacing or regenerating injured tissue, rather than just treating disease symptoms. At present, the field has focused on two areas: tissue engineering, and stem cell research.

Stem cells are currently used as a therapeutic strategy. Often these cells are infused directly into injured tissue, as to minimize or prevent damage, and to enhance the healing process. A typical example would be the injection of autologous bone marrow stem cells after myocardial infarction for heart tissue regeneration [3]. A major attraction of the use of stem cells as a therapeutic modality is their capacity to differentiate according to environmental cues. However, stem cell therapy usually involves injecting stem cells directly into damaged areas that often have an already compromised microstructure or other pathologic hinderances [4]. This limitation could be improved, or removed entirely, by using matrices engineered in a way that would provide the appropriate cues needed for stem cell growth.

Another way to replace injured tissue is organ transplantation. However, this method suffers from a limited pool of donors and the possibility of immune complications [3,5]. It has been shown that even residual cellular material can cause an inflammatory response and reverse any of the potential advantages of their implantation [6]. This limitation has led to a rise in interest in tissue engineering, a field where tissues or whole organs are engineered or otherwise modified in a laboratory for later implantation. The advantages of this approach are clear, since engineered tissues can be tailored to have the properties that best fit specific clinical needs. With the fast development of technology, the focus has shifted to designing functional biomaterials, such as smart 3D biomimetic scaffolds, that have the capacity to actively interact with human stem cells in a way that mimics the natural interactions that occur between the extracellular matrix and cells [7]. However, much of the mechanisms behind the interactions between the extracellular matrix and cells are still shrouded in mystery even to this day. This lack of knowledge makes the process of recreating a perfect copy of this complex matrix and its effects on cells an arduous task.

1.1.2 The Extracellular Matrix

The extracellular matrix (ECM) is a three-dimensional network of several extracellular macromolecules that support the cells that surround it. This matrix forms the intercellular space that borders cells, binding them to it, and is present in some form for all cells through all or most of their development [8].

The ECM is composed of a variety of macromolecules, such as proteins (like collagen and elastin), glycoproteins, glycosaminoglycans (GAGs), proteoglycans and polysaccharides [9]. Several growth factors (such as fibroblast growth factors or vascular endothelial growth factors) are also bound to the proteins within the matrix [8]. While this composition can vary between species, the main components of ECM are highly conserved between individuals of the same species or in the same biological class, like in the case of mammals [10].

The composition, mechanics, and geometry of the extracellular matrix play a vital role in determining what biochemical and mechanical properties a tissue will have as they modulate cell function and influence many physiological processes [8,11]. The ECM not only provides structural support but plays an essential role in cell migration, proliferation, cell development, differentiation, and even angiogenesis [11–16]. It seems likely that the combination of the matrix's three-dimensional structure, surface topology, and varied biochemical composition all contribute to these effects (Figure 1.1).

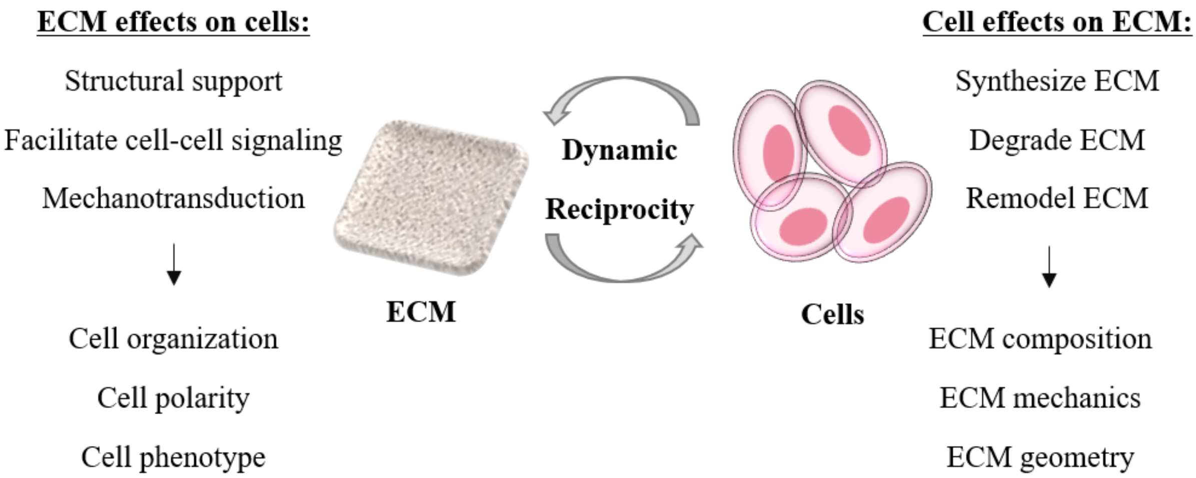

Figure 1.1 Illustrative chart of the feedback loop interactions between the extracellular matrix and cells. Adapted from [10].

Several studies have pointed to the ability of the ECM to affect cell organization, motility, proliferation, polarity, and phenotype [8,11–22]. This dynamic is reciprocated by the cells inhabiting the matrix, which, in their turn, are continually degrading, secreting, and consequently remodeling the ECM, affecting its composition, mechanics, and geometry [10]. This remodeling process is continuous, and as such the ECM is regarded as a highly dynamic structure [16,18].

This capacity for remodeling and regeneration, indispensable for reconstructing tissue architecture after injury, attracts high interest, both for the development of new therapeutic methods and for the advancement of the field of tissue engineering. Products derived from the extracellular matrix, like collagen or fibrinogen, have already proven to stimulate regenerative healing and are currently available commercially [12,23,24].

1.1.3 Could dECM be the ideal scaffold?

Decellularized extracellular matrices (dECM) derived from tissues or whole organs could be the solution to the conundrum presented above. Decellularization consists in the removal of all immunogenic cellular material from a tissue or organ, leaving the non-immunogenic extracellular matrix behind. By using this method, it becomes possible to create a functional and bioactive scaffold, with the complexity and advantages provided by ECM, without the immunogenic drawbacks of transplantation of unprocessed tissue or organs.

dECMs can be prepared from any organ or tissue and have already been successfully obtained from the bladder [25–27], heart valves [28–30], lungs [31–33], liver [34], and even whole hearts [35,36]. The resultant scaffold is a complex structure of vascular networks, signaling molecules, and unique tissue-specific architecture that can mimic nature and be recognized appropriately by cells [4]. There has been a rising interest in producing dECMs from several tissue types, and studies have shown that these scaffolds have promising remodeling potential [37]. dECMs can be obtained from tissues of several different animal species, like pigs, cows, horses, or humans. It is even possible to use decellularize tissues from one organ and then utilize the obtained scaffold in a completely different anatomical site. However, since different tissues have different biochemical and mechanical properties, it is necessary to carefully consider the tissue source of dECMs that best suit each clinical application.

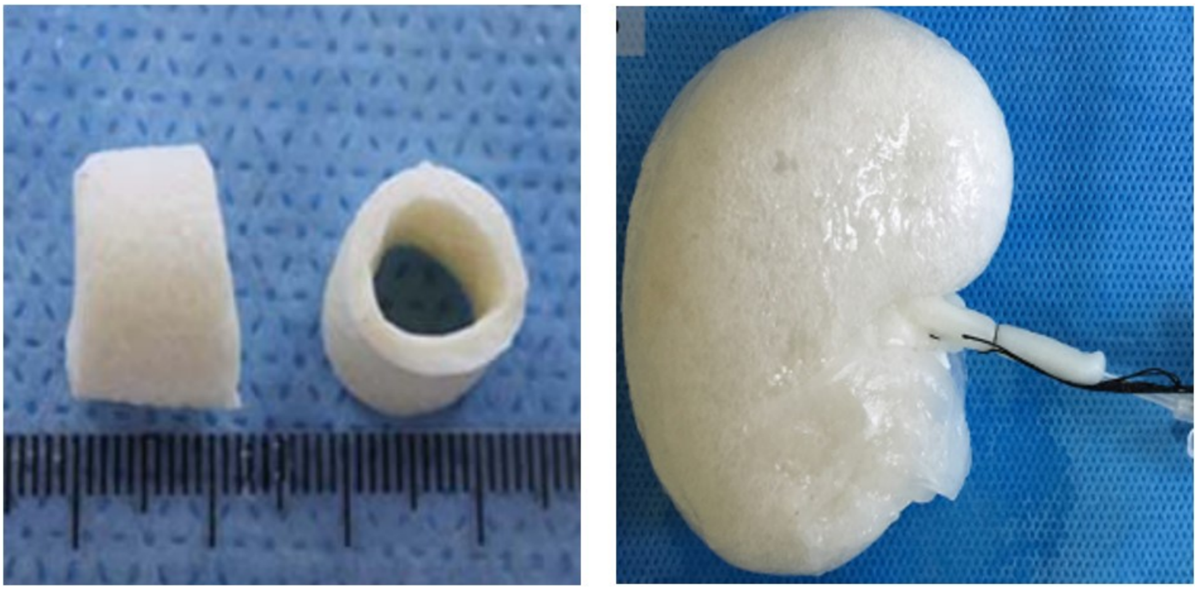

Figure 1.2 Examples of scaffolds obtained from decellularized extracellular matrices. **Left:** an ovine aorta [38]. **Right:** an ovine kidney [39].

Decellularization is a complex procedure, often requiring the use of several decellularization agents (either chemical, biological, or physical) over multiple steps. This intricacy leads to a process that needs to be rigorously tested and optimized for each tissue source. Finally, bioactivity and architecture, among other tissue properties, are affected to some extent via these treatments. Therefore, it is crucial to obtain a detailed characterization of each decellularized matrix before they see clinical use.

1.1.4 Clinical applications

Currently, there are numerous commercially available products derived from decellularized extracellular matrices (see Appendix I). These products are marketed worldwide for use in the repair of soft tissues (cardiac, neurological), wound management, or even as part of prosthetics. Naturally derived extracellular matrices can be obtained from several different sources. When these tissues come from humans, they are called allografts, when other animals are the source, they are considered xenografts. A list of some of the currently available decellularized ECM-derived products is available within Table 1.1 (a more detailed list can be consulted in Appendix I).

Table 1.1 Examples of commercially available decellularized ECM-based products grouped by their tissue of origin.

Tissue Type	Available Products
Dermis	AlloMax™, AlloPatch HD®, DermACELL®, DuraMatrix®, FlexHD®, Graft Jacket®, Integra® HuMend™, PerioDerm™, SurgiMend™, XenMatrix™, Zimmer® Collagen Patch
Urinary Bladder Matrix	Acell Vet®, MatriStem®
Small Intestine Submucosa	Oasis®, AxoGuard®, Biodesign®, Cor™Patch
Heart Valves	CryoValve® SG, Hancock® II, Mosaic™

Although decellularized matrices have been prepared from various tissue types, only a small niche is available commercially (Figure 1.3).

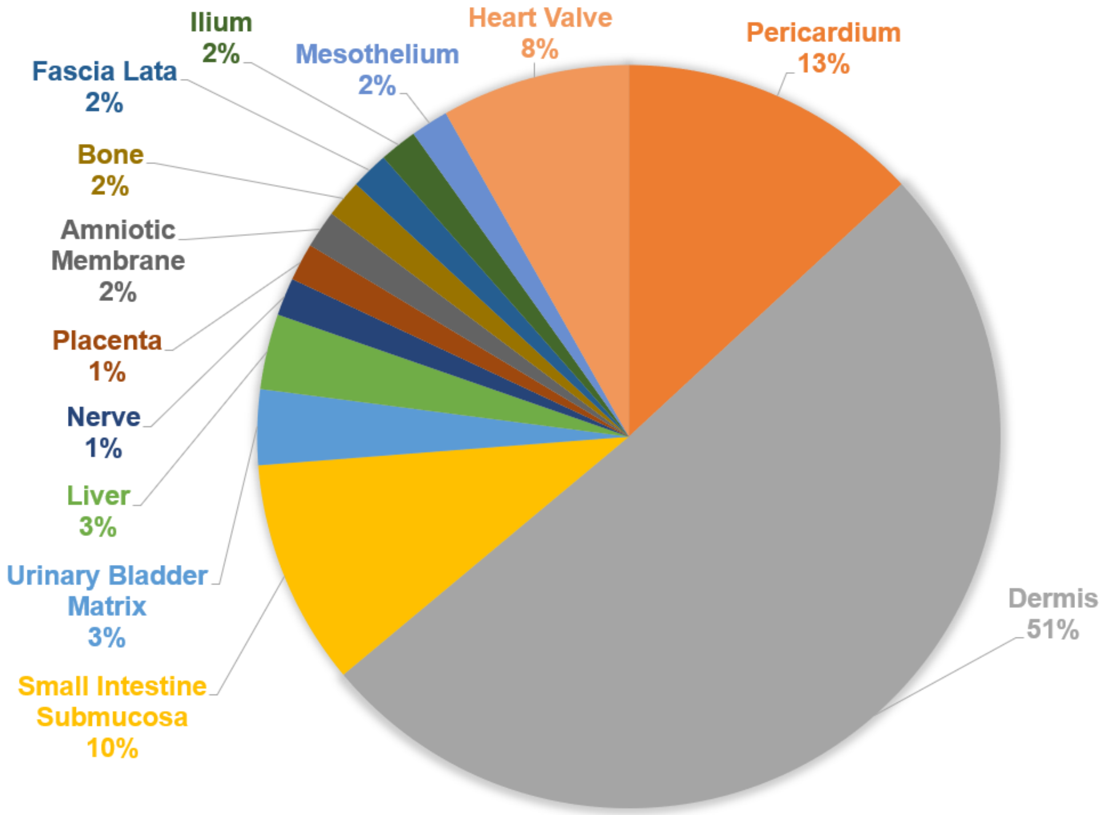

Figure 1.3 Tissue type source of commercially available decellularized ECM-based products. Based on the list provided in Appendix I.

The majority of decellularized ECM-based products are obtained from the skin (Figure 1.3). Most are patches, rich in collagen as well as elastin, and with preserved dermal architecture. These products are made for direct application in wounds or to help repair soft tissue after surgeries. Other commonly used tissues are the small intestine submucosa (SIS), the urinary bladder matrix (UBM), and cardiovascular tissues, such as the pericardium and the heart valve. Hard tissues, such as bone or enamel, have been explored much less. This limitation makes current ECM-based products unusable in osteochondral clinical applications since hard tissue differs significantly in biochemical composition and mechanical properties from soft tissue. Another weakness of the current market lies with neurological tissues, which is very complex and possesses unique properties, and is therefore not easily replaced by other tissue types.

Since the ECM is highly preserved between different species from the same biological class, it is interesting to observe that currently, there seems to be split between allograft and xenograft ECM-derived products (Figure 1.4).

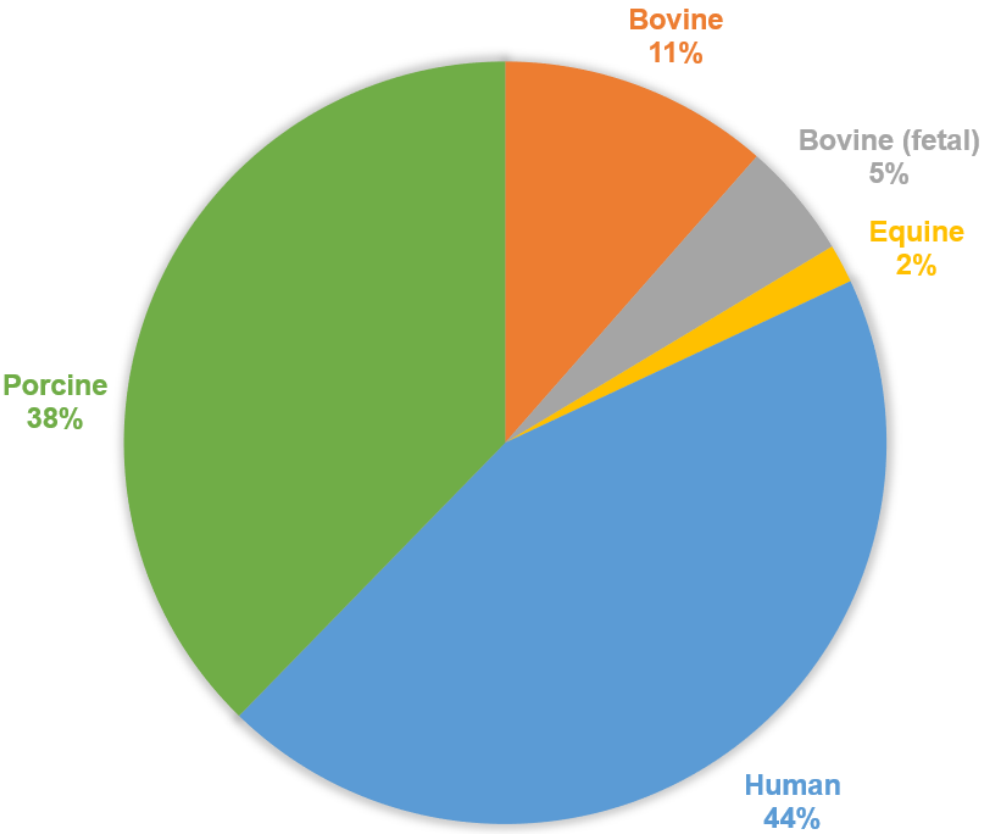

Figure 1.4 Animal source of commercially available decellularized ECM-based products. Based on the list provided in Appendix I.

Even so, in 2017, porcine-derived ECM products saw the largest revenue share in the market [40]. This domination is likely due to the wide availability of porcine materials, resulting in better accessibility of research and development of new products. Human-derived ECM products rely on donations of human dermis, reducing supply when compared with animal-sourced products. There is currently some discussion concerning the choice between an allogenic or xenogenic source for dECM products, as it has been suggested that human-sourced products could be safer than xenogenic ones, due to reduced immunogenic potential in the case of incomplete decellularization [41]. Research concerning this issue could potentially change the outlook of the ECM market when it comes to the raw material used to produce these products.

A final analysis concerns the intended applications of decellularized ECM-based products (Figure 1.5).

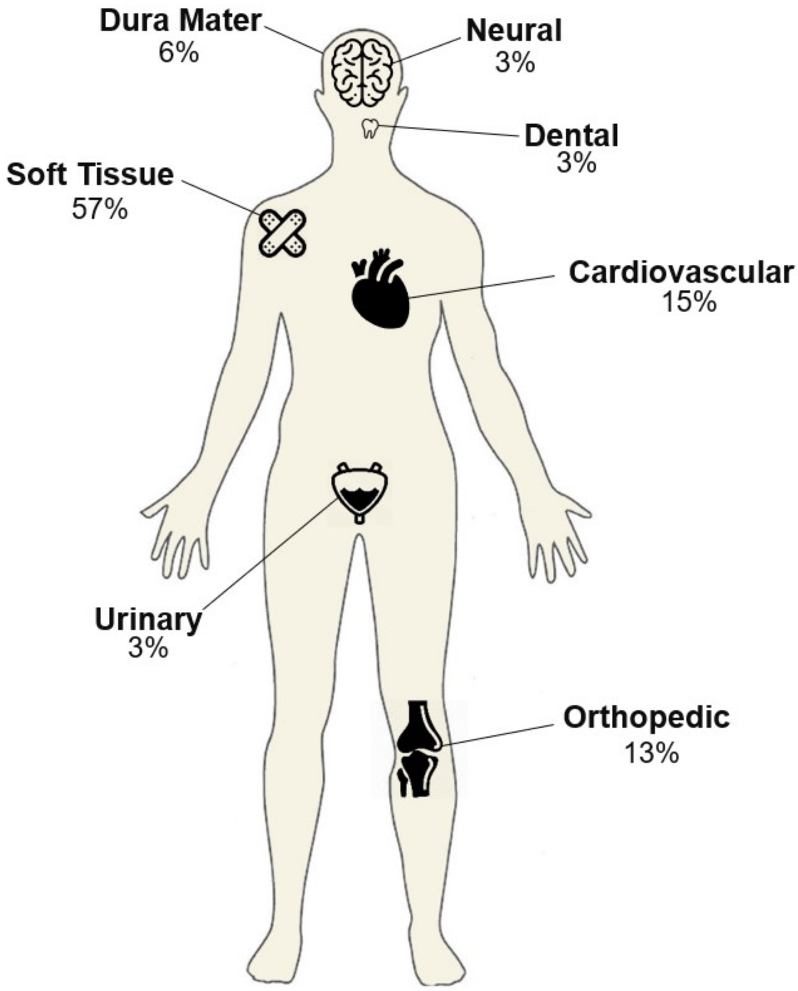

Figure 1.5 Intended applications of commercially available decellularized ECM-based products. Based on the list provided in Appendix I.

The most representative involves soft tissue (~57%), followed by cardiovascular (~15%) and orthopedic (~13%). Less commonly are applications involving neurosurgery, with most products applied in the repair of the dura mater (~6%), and some in the replacement or repair of nerves (~3%). dECMs are also used in the treatment of prolapse or stress urinary incontinence (~3%) and dental procedures (~3%).

1.1.5 Brief market outlook

The global market for decellularized extracellular matrices was worth 24.30 million dollars in 2018 and is estimated to grow with a compound annual growth rate (CAGR) of 8.2% until 2027, where it is estimated to reach 47.46 million dollars [42].

While, currently, applications in soft tissue repair account for the largest revenue share, the fastest growth is expected to be seen in the segment of vascular repair [40]. Figure 1.6 shows this rapid evolution, reflected in the market within the United States.

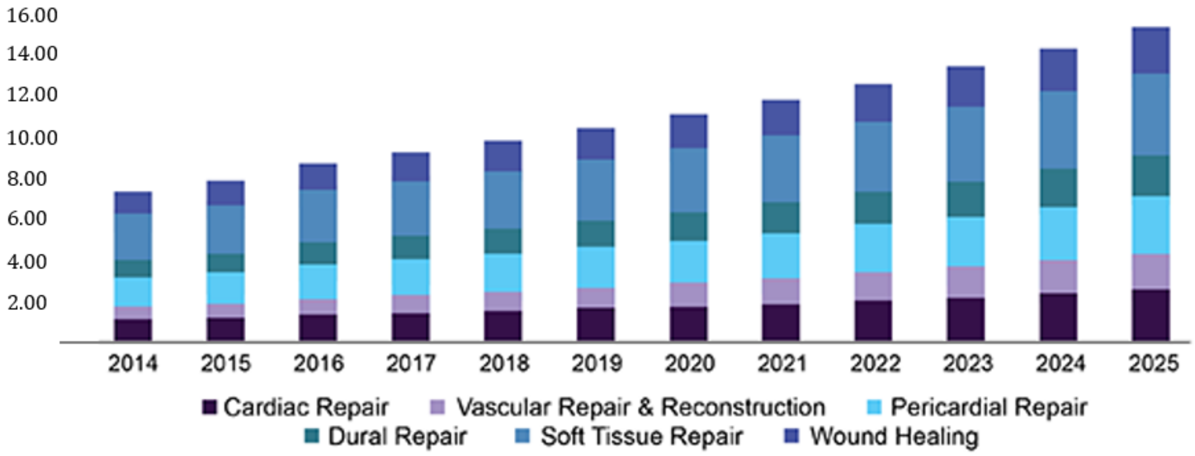

Figure 1.6 United States extracellular matrix market size (USD million) by application, from 2014-2025. Adapted from [40].

Forecasts justify this predicted boost in demand for cardiac repair applications due to the ever-increasing geriatric population, the prevalence of vascular disease and, consequently, the increasing number of vascular surgeries [40]. The many public and private organizations that support research in this area, like the European Society for Vascular Surgery, are also vital aspects of the rise expected for this market segment [40].

While the overrepresentation of specific segments of the dECM market makes any analysis of less represented tissues (e.g., bone) a difficult hurdle, it is possible to develop predictions based on secondary but related markets. The global orthobiologics (biological products used in orthopedic medicine) market was valued in 2017 at 5 billion dollars and is expected to grow at a CAGR of 7.5% from 2014 to 2025 [43]. This industry is currently driven by the surging number of orthopedic procedures, a consequence of a rising geriatric population and obesity [43]. Currently, viscosupplementation treatments dominate the market, but demineralized bone matric and synthetic bone substitutes are well represented as well (Figure 1.7).

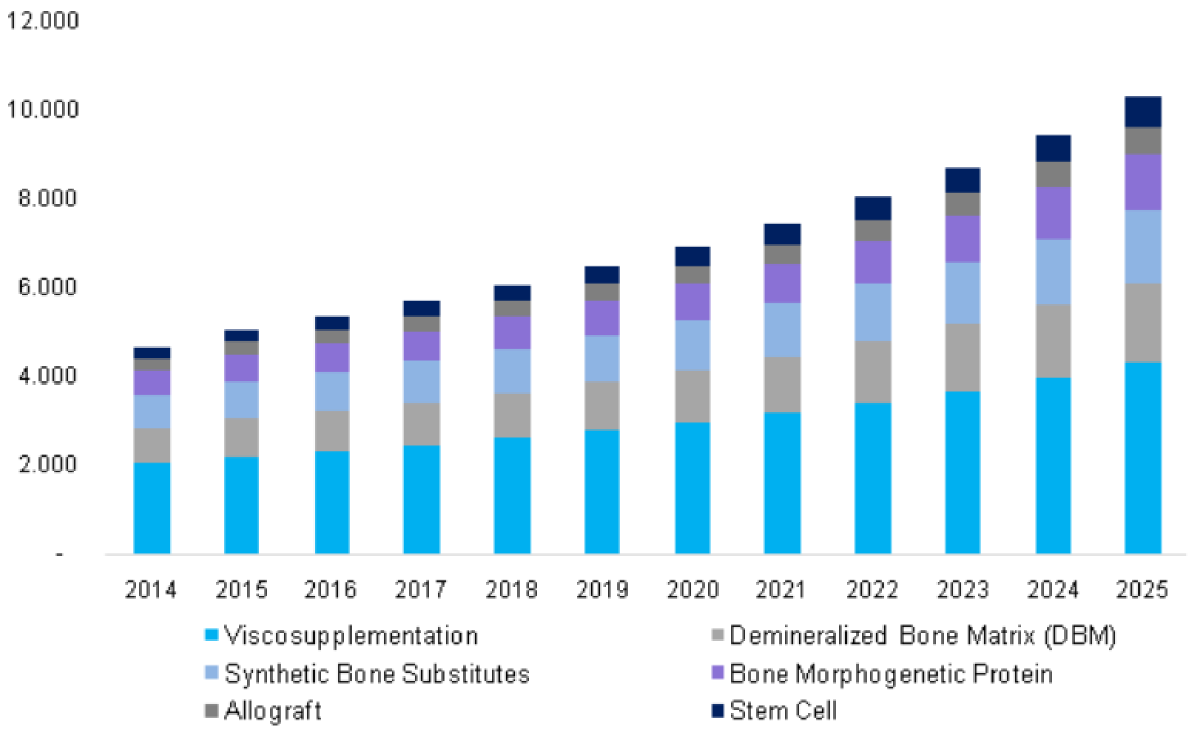

Figure 1.7 Orthobiologics market by product from 2014-2025 in USD billion. Adapted from [43].

Decellularized matrices developed from bone tissue could eventually come to surpass current products obtained from demineralized bone matrices or be used as bone graft substitutes instead of the synthetic alternatives. With the advancement of decellularization technology and the rising interest in developing protocols for unrepresented tissue types, dECMs can penetrate such markets as the one presented above. These opportunities reveal the full potential of decellularized extracellular matrices, that goes beyond the current use of patches to help soft tissue repair.

1.2 The decellularization process

Designing a decellularization protocol is a complex affair. Current decellularization literature lists many possible agents and application techniques that need to be combined to design a decellularization protocol that fits each kind of tissue.

1.2.1 Decellularization agents

1.2.1.1 Chemical agents

Acids and bases

Acids and bases are used in decellularization protocols to cause or catalyze hydrolytic degradation of biomolecules by solubilizing the cytoplasmatic components of cells and disrupting nucleic acids. However, these chemical agents can cause damage to collagen fibers, glycosaminoglycans, and growth factors [44]. Some of the acids commonly used in decellularization protocols are peracetic acid, acetic acid, and deoxycholic acid (see Appendix II).

Peracetic acid (PAA) is an organic peroxide that is highly corrosive and a strong oxidizer. This acid is commonly used as a disinfectant but has been used to decellularize thinner tissues, such as the small intestine submucosa [45]. However, some studies have failed to achieve the decellularization evaluation criteria proposed by Crapo *et al.* (2011) [46] using peracetic acid alone [45–47]. Syed *et al.* (2014) [45] also found that peracetic acid significantly altered the mechanical properties of small intestine submucosa. Deoxycholic acid is a secondary bile acid known to cause DNA damage via oxidative stress [48]. Its sodium salt, sodium deoxycholate, can be used as a biological detergent since it solubilizes cell membranes and intracellular components [49]. Ozeki *et al.* (2006) [50] reported that esophagi treated with deoxycholic acid exhibited superior DNA extraction and ECM preservation. Bloch *et al.* (2012) [51] were also able to achieve efficient cell lysis using deoxycholic acid, without affecting the integrity of the proteoglycan network or a reduction of GAG content in aortic heart valves. Acetic acid is a synthetic carboxylic acid that has been found to damage collagen fibrils, leading to an altered ultrastructure and a reduction in the scaffold's ultimate strength [44].

Hypertonic and hypotonic solutions

Hypertonic and hypotonic solutions, such as saline solutions or deionized water, can be used to provoke cell lysis via osmotic shock, usually with very minimal effects on ECM composition and architecture [52–54]. Hypertonic solutions can also osmotically disrupt nuclear membranes, and help to fragment DNA and dissociate it from proteins with the aid of detergents [55,56]. Hypotonic solutions cause cell swelling due to the movement of water into the cell and, eventually, membrane rupture [57]. Often, tissues are immersed alternatively in hypertonic and hypotonic solutions for multiple cycles, to exacerbate osmotic stress [26,52,55,58–61]. Alternatively, hypertonic and hypotonic solutions may be used after cell lysis has occurred to help remove residues within the cells after membrane rupture. However, the use of these agents alone cannot effectively remove cellular remnants, acting merely in synergetic support to other decellularization agents, such as detergents [53,61,62].

Detergents

Detergents are amphipathic compounds, possessing both hydrophobic and hydrophilic groups, with unique properties in aqueous solutions where they spontaneously form micellar structures [63]. Detergents can solubilize membrane proteins by creating a mimic of the lipid bilayer, where they are generally found [63]. There are four major categories of detergents, but decellularization protocols mostly involve one or more of these three: non-ionic detergents, ionic detergents, and zwitterionic detergents.

Nonionic detergents are those that have an uncharged hydrophilic head group. These detergents are generally considered to be milder and relatively non-denaturing since they disrupt lipid-lipid and lipid-protein interactions while leaving protein-protein interactions mostly unaltered [63]. Triton X-100 has been used for cell removal in several studies (see Appendix II) since 1987, achieving mixed results [64]. However, it appears to be less effective than sodium dodecyl sulfate (SDS) in achieving total decellularization, particularly in cases of denser tissues such as tendons [65–67]. At least one study (Kajbafzadeh *et al*., 2019) [39] has proposed that a hybrid treatment of Triton and SDS can result in a decellularized scaffold with better properties than that achieved by using just SDS at a higher dose. Triton X-100 can also be used as a washing step to remove residuals of other detergents, like SDS [68]. However, in terms of ECM preservation, Triton X-100 may lead to loss of elastin, GAGs, and disruption of collagen fibers, leading to an altered ultrastructure [28,66,69].

Ionic detergents contain a hydrophilic head group that can be either negatively (anionic) or positively (cationic) charged. These detergents are very effective as solubilizing membrane proteins but always lead to some degree of protein denaturation [63]. Sodium dodecyl sulfate (SDS) is an anionic detergent that is commonly used in decellularization treatments (see Appendix II). This detergent has proven to be highly effective in removing cellular components and nuclear remnants in several studies [26,30,70–72]. However, it can also cause drastic alterations to the ECM due to the extensive damage to collagen and content and the removal of GAGs and growth factors [30,73,74].

Zwitterionic detergents contain both negatively and positively charged atomic groups and combine the properties of ionic and nonionic detergents. Their strength of action is intermediate between ionic and nonionic detergents [63]. They are more efficient than nonionic detergents at breaking protein-protein interactions but have a denaturing effect less harsh than ionic detergents. CHAPS (3-[(3-cholamidopropyl)dimethylammonio]-1-propanesulfonate) is a zwitterionic detergent that has been used to decellularize thinner tissue, such as lungs [31,33,75]. Some studies have shown that CHAPS is less effective in achieving complete decellularization than the ionic detergent SDS, but has less harmful effects on ECM composition and morphology [76,77]. In some studies (Petersen *et al.*, 2010 and Petersen *et al.*, 2012) [31,33] CHAPS was shown to preserve collagen and elastin content, two significant determinants on the overall mechanical properties of tissues. GAGs were, however, largely lost from these decellularized scaffolds [31].

<u>Alcohols</u>

Alcohols, such as ethanol and methanol, are polar organic compounds that are used as decellularization agents due to their capacity to dehydrate cells and, consequently, cause cell lysis [78,79]. Their hydroxyl group allows for good solubility with many other organic compounds, while their carbon chain gives alcohols the ability to dissolve nonpolar substances such as lipids [80]. Alcohols are often used to remove lipids from tissues and have generally be found to be more efficient than enzymatic treatments for this purpose [81–83]. Certain alcohols, such as ethanol, have been used to remove phospholipids from heart valves and other conduits, preventing tissue calcification and eventual prosthesis failure [80,84]. Ethanol has also been used as a final treatment to remove residual surfactants after tissue decellularization [85]. However, alcohols cause dehydration, which can result in stiff and brittle tissue, endangering the utility of scaffolds processed with the use of these agents [81,86]. Nevertheless, a recent study using supercritical carbon dioxide ($scCO_2$) with an ethanol *entrainer* (a solvent added to $scCO_2$ to provide a significant boost in solubility) has suggested that pre-saturating the environment with water may maintain tissue hydration [87]. It is also well established that certain alcohols like ethanol and methanol can cause protein precipitation since they are often used as cell fixatives for histological analysis [88].

<u>Tri(n-butyl) phosphate</u>

Tri(n-butyl) phosphate, also known as TnBP, is an organophosphorus compound currently used as an extractant and plasticizer. It forms stable hydrophobic complexes with some metals, disrupting protein-protein interactions, thus facilitating the removal of cells. TnBP has also been used for many years as an organic solvent to inactivate viruses in the blood [89,90]. For decellularization of denser tissues, such as tendon, TnBP seems to be more effective than the use of detergents, like Triton X-100 and SDS, or certain acids at removing cell nuclei while leaving structure and composition intact [47,91]. However, at least one study (Pridgen *et al.*, 2011) [92] has reported inadequate removal of DNA from flexor tendons after TnBP treatment. There are also conflicting reports on the effect of TnBP on ECM composition. While some studies (Pridgen *et al.*, 2011, Cartmell and Dunn, 2000, Deeken *et al.*, 2011) [47,66,92] found no statistically significant differences in collagen content in tendon tissues treated with TnBP, Woods and Gratzer (2005) [72] reported a significant decrease of collagen in porcine bone–anterior cruciate ligament–bone grafts after the use of TnBP.

1.2.1.2 Biological agents

Enzymes

Many decellularization protocols involve the use of enzymes as a step to aid the removal of cells and other ECM residues from tissues. Several types of enzymes have been used in decellularization studies), but the most commonly used are nucleases and trypsin.

Nucleases, like DNase and RNase, cleave the phosphodiester bonds between nucleic acids and are used in decellularization protocols as a step to aid the removal of nucleic material after cell lysis [25,26,93]. Ribonucleases have also been used to help with virus inactivation [71]. Trypsin is a serine protease that hydrolyzes proteins by cleaving the peptide chains of the carboxyl group of lysine and arginine. Trypsin needs long incubation times to help achieve complete cell removal [71,79,94,95]. However, long exposition times to trypsin can cause a disruption of ECM ultrastructure and composition, including GAGs, elastin, and collagen degradation [28,58,79,94,95]. Nevertheless, some disruption of ECM ultrastructure can be desirable for denser tissues, such as tendons, where exposure to trypsin is done as a preliminary step to allow other decellularization agents to penetrate cells [96–98]. Dispase is a protease that cleaves fibronectin and certain collagen types. It has been reported that the use of dispase with other decellularization agents may aid cell removal better than trypsin when used with specific decellularization techniques [79]. Dispase has been used to isolate a viable corneal epithelium, but results showed a disruption of the basal lamina, which suggests a possible deteriorating effect on ECM structure [99]. At least one study (Hopkinson *et al.*, 2008) [100] has suggested that thermolysin may be a better alternative than dispase for preserving basement membrane.

1.2.1.3 Physical agents

Temperature

Decellularization methods that rely on sharp temperature changes, such as freeze-thaw processing, can effectively cause cell lysis [101]. Freeze-thawing is a form of thermal shock treatment that entails the rapid snap-freezing of a tissue followed by thawing. This rapid freezing causes ice crystals to form in the interior of cells, which disrupt membranes and lead to cell lysis. Usually, multiple cycles of freeze-thaw are introduced as a step to aid cell lysis in decellularization protocols [82,102–104]. However, subsequent treatments using other decellularization agents are still needed for the removal of the resulting membranous debris and intracellular contents [101,104–106]. Thermal shock treatments that utilize rapid freezing can disrupt or fracture ECM due to the formation of ice crystals, resulting in changes in the scaffold's ultrastructure or mechanical strength [79,100,103]. For denser, mechanically bearing tissues, such as tendons or ligaments, freeze-thawing used in association with other agents proved to effectively decellularize with minimal disruption of ultrastructure, biochemical composition, and mechanical properties of natural ECM [101,106,107].

Force

Direct application of force, like the application of gentle pressure on tissues, can be used to induce cell lysis with the aid of other decellularization agents [83,108,109]. Removing cells from a surface of a tissue or organ mechanically, like scraping of brushing, can also be used following decellularization processing [100,110]. However, these methods can severely compromise the mechanical integrity of the resulting scaffold [100].

Hydrostatic pressure

Methods using hydrostatic pressure, like High Hydrostatic Pressure (HHP) or Ultrahigh Hydrostatic Pressure (UHP) can be used to provoke cell lysis or to aid in the removal of cellular material from tissues [111–113]. Usually, HHP alone cannot achieve complete decellularization, and another method to remove DNA remnants is necessary [112]. It has also been reported that high hydrostatic pressure can inactivate certain microorganisms and viruses, so this method could also provide a sterilizing effect at certain pressure levels [114]. Pressurization or depressurization may induce the formation of ice inside tissues, so it is crucial to strictly control these rates as to avoid drastic increases or decreases of temperature [112].

Supercritical carbon dioxide

Supercritical technology has been recently used to improve current decellularization methods. The use of supercritical carbon dioxide ($scCO_2$) to substitute or hasten specific decellularization steps is of high interest. Carbon dioxide (CO_2) can achieve its critical point at relatively low temperature and pressure (31.1ºC and 7.39 MPa), and has no surface tension, providing a better permeation into a wide range of materials with porous and complex structures [115]. CO_2 is also non-toxic, non-flammable and inert in most situations and can be easily removed by degassing and does not leave toxic residues behind.

It has been theorized that $scCO_2$ can induce cellular death without the use of aggressive surfactant solutions, or even help specific decellularization agents to achieve greater penetration of tissues, helping to expedite the process of decellularization [81,87,116,117]. CO_2 is apolar, so a co-solvent may be necessary to eliminate some charged molecules such as phospholipids. Sawada *et al.* (2011) [81] reported that decellularization using $scCO_2$ with an ethanol *entrainer* managed to suitably remove cell nucleus and cell membranes in porcine aorta within 20 minutes under mild conditions (15 MPa, 37ºC). Guler *et al.* (2017) [38] also observed complete cell removal after $scCO_2$ treatment of aortas with an ethanol *entrainer*. However, other works (Casali *et al.*, 2018 and Antons *et al.*, 2018) [87,116] have not managed to reproduce these results using $scCO_2$ processing alone. Casali *et al.* (2018) [87] hypothesized that $scCO_2$ treatment is not enough to adequately provoke cell lysis, leading to reduced cell penetration and incomplete cell removal. Studies utilizing hybrid detergent/$scCO_2$ treatments or extensive pre-treatments to achieve cell lysis have managed to obtain complete decellularization, giving some credibility to the above-described hypothesis [87,116]. However, $scCO_2$ has been proven to inactivate certain bacteria, spores, fungi and viruses. While the exact mechanism of inactivation remain unclear, at least one study (Enomoto *et al.*,1997) [118] has presented proof that cell rupture occurs during pressurization with high-pressure carbon dioxide treatment. Other studies have suggested that $scCO_2$ may just accumulate in the cell membrane and increase its permeability, permitting an easier entry to CO_2 and a co-solvent into the cell, leading to its inactivation [119].

Ethanol is the most commonly used *entrainer* for $scCO_2$ decellularization, but for denser tissues, a stronger solvent may be necessary to achieve complete cell removal [116]. $scCO_2$ processing usually leads to a dehydrated final product with altered properties [38,81]. However, saturating the environment with water may allow for maintenance of the hydration state of the ECM, even in the presence of other additives [87]. As in the case of hydrostatic pressure treatment, it is essential to mind the pressure used during the $scCO_2$ process, since high pressure levels can disrupt the ultrastructure of ECM [38,81].

1.2.2 Decellularization techniques

The decellularization agents presented above can be applied to tissues and organs using several different techniques. This confers another layer of complexity to designing a decellularization protocol, as not only one must take care to choose the decellularization agents most adequate for each tissue, but also the best technique to apply these agents. The most commonly used techniques seen in decellularization literature are presented in Table 1.2.

Table 1.2 Commonly used decellularization techniques and their advantages.

Technique	Advantage
Immersion and agitation	Agitation provides increased exposure of cellular components to decellularization agent
Osmotic gradient	Osmotic gradient disrupts cell membranes
Pressure gradient	Pressure gradient can help steer enzyme movements
Whole organ perfusion	Transport of decellularization agent through the vasculature is more efficient than immersion
Supercritical fluid	High transfer rate and high permeability potentiate faster decellularization times

1.2.3 Decellularization protocols

Decellularization protocols can be classified as physically-based, chemically-based, or biochemically-based processes [120]. Most decellularization protocols are, in fact, combination processes, using a mixture of physical, chemical and enzymatical steps [121]. Although protocols look very different from each other on the surface, most essentially follow the same logic [121]: Initially, there will be a step to lyse the cell membrane and break up cells. Following that, a treatment to separate the cellular component from the extracellular matrix. Finally, several washing steps to remove both the cellular debris and residual chemicals from the treated tissue.

To find the optimal protocol one must always consider the properties of the tissue to be decellularized. Thickness, density, and composition all have deep effects on the efficiency of decellularization agents [46]. Also, the intent of use of the resulting decellularized matrix needs to be considered. Clinical applications that do not require mechanically strong matrices have different requirements than the ones that need load-bearing strength. Some examples showcasing how the complexity and length of decellularization vary depending on the tissue to be decellularized are shown in Figure 1.8.

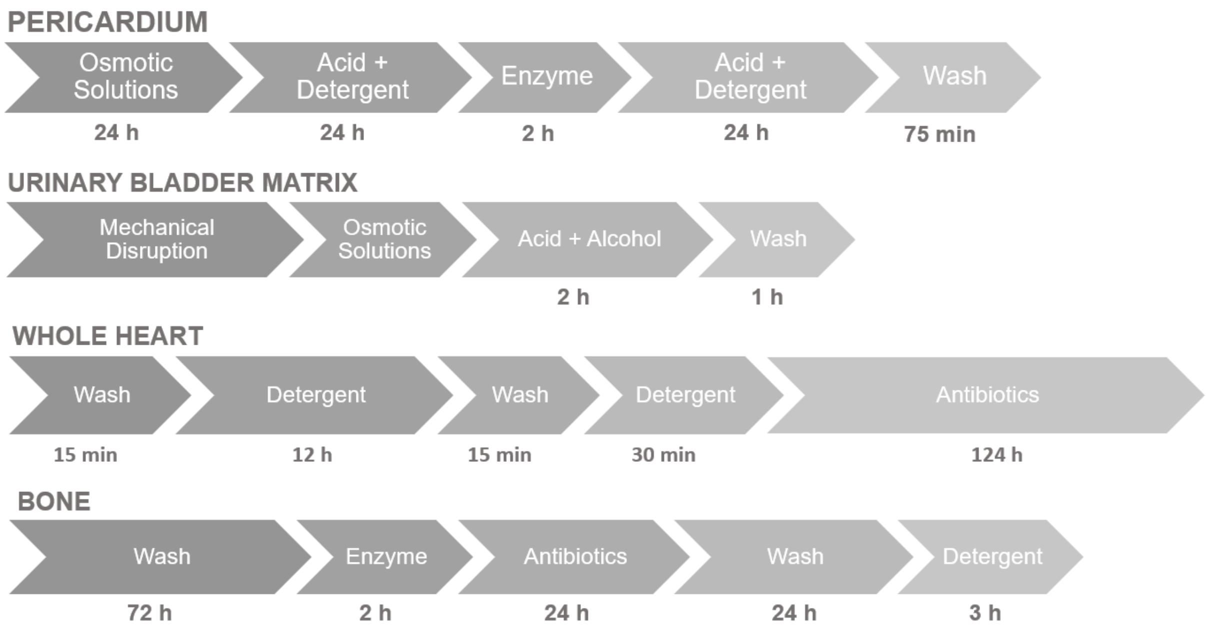

Figure 1.8 Examples of decellularization protocols for the pericardium, urinary bladder matrix, whole heart and bone. Each step is categorized according to the main agent used. Time is omitted when not clarified within source. Protocols referenced: Pericardium [58]; UBM [110]; Whole heart [36]; Bone [122].

Generally, the complexity and length of a decellularization protocol will run proportional to the degree of geometric and biological conservation desired for the resulting decellularized matrix [46]. Except for thin membranes, decellularization is often a time-consuming affair (Figure 1.8). One of the current challenges in the field lies in shortening the length of these treatments, while simultaneously not increasing the harmful effects of decellularization treatments.

1.3 Evaluating decellularization

What constitutes successful decellularization is not thoroughly defined at present [46,123]. As previously explained, a decellularization process should be highly dependent on the tissue's type, source, and final function, so different measures of evaluation have been used throughout the field. Currently, the evaluation of decellularized tissues is separated into two main objectives: verifying the removal of cellular components from the tissue and assessing the quality and integrity of the remaining original ECM. However, guidelines detailing what should or should not be present in the acellular scaffold materials and how their properties should be measured are still limited and not fully wide-spread [124].

1.3.1 Immunogenicity

When it comes to cellular components in decellularized scaffolds, less is more. Residual dead cells or cellular material can activate the immune system and trigger a host response, potentially leading to the scaffold's failure [6,125–127]. Even a relatively low-level immune response can lead to a hindered healing process and tissue regeneration *in vivo*, causing the scaffold to fail [128]. As such, reducing a scaffold's immunogenetic potential is arguably the most critical requirement of successful decellularization.

Studies [125,129,130] have shown that the presence of DNA is directly correlated to adverse host reactions, even at low levels. Any level of residual cell remnants is capable of eliciting an inflammatory response within the host. However, Gilbert *et al.* (2009) [129] showed that even scaffold materials available commercially contained minimal amounts of remnant DNA. Since this DNA was only present as small fragments, the study concluded that it was unlikely that they would cause any adverse effects on the tissue remodeling response [129]. Crapo *et al.* (2011) [46] suggested that any remaining DNA should be inferior to 50 ng per mg of ECM dry weight and shorter than 200 bp in fragment length. However, not many studies have thoroughly examined what amount of DNA in decellularized scaffolds will lead to an increased probability of eliciting an immune response. In particular, more long-term clinical studies focusing on potential side-effects of the use of decellularized scaffolds are needed.

Furthermore, most decellularization literature focuses on remaining cellular components being the sole cause of immune potential. However, this assumption is flawed [127]. Even ECM components are capable of eliciting an adverse immune response, as at least one study (Ellingsworth *et al.*, 1986) [131] has observed that bovine collagen resulted in an allergic reaction in 3% of the population. Griffiths *et al.* (2008) [132] also identified several non-collagenous antigenic proteins that were matrix-bound. These results show the need for *in vivo* studies of the immune potential of decellularized scaffolds, instead of the reliance on DNA quantification alone. Since a strong inflammatory response to these scaffolds can be clinically dire, the importance of a rigorous standard is easily perceived [123,133].

1.3.2 Other biological and mechanical properties

Another important focus of decellularization lies in the preservation of the appealing biological and mechanical properties of the extracellular matrix. As such, it is evident that it is necessary to study the effect that decellularization agents have on the tissues themselves to effectively evaluate decellularization.

Preserving the mechanical integrity of tissues is often a big concern. Some of the primary properties of interest include the elastic modulus and ultimate strength. Ultimately, the nature of the tissue itself and the purpose of application of the scaffold is what will determine the range of properties to be tested [134]. Therefore, a universal standard for evaluating decellularization via mechanical integrity may be not enough, but a consensus between tissues with similar origins and intended function may still be possible to achieve in the future.

Decellularization agents, both chemical and physical, have been shown to have a detrimental effect on certain elements of the ECM (such as collagen and GAGs, among others), which in turn can affect the mechanical integrity of these tissues. Presently, a consensus on the adverse effects that these agents may have on the properties of ECM has still not been reached. It seems progressively more likely that conflicting reports will continue to appear in literature since observable side-effects vary depending on numerous parameters (e.g., tissue source, type, and thickness, the concentration of agent used, duration of the decellularization procedure or, even, the pre-treatment protocol used) [46,134,135]. Understanding the extent of the loss caused by decellularization and the effects this loss will ultimately reflect on the efficacy of these decellularized tissues *in vivo* is of vital importance.

1.3.3 Attempts at a universal evaluation standard

It is vital to reach a consensus on what a successful decellularized tissue truly means and how to accurately quantify it and, so far, there are no legally accepted criteria establishing how to evaluate decellularization [46,135]. As explained by Crapo *et al.* (2011) [46], a standard for tissue decellularization could allow researchers and manufacturers to evaluate the effectiveness of their protocols and facilitate proper comparison of obtained results between different sets of teams. Furthermore, rigorous legal guidelines need to be established and used across the field for a substantial clinical translation of these decellularized products to occur.

Some attempts have been made at providing a universal standard for evaluation of decellularization. In 2011, Crapo *et al.* [46] suggested that, in order to avoid adverse host responses, the following minimum criteria need to be accomplished to satisfy the intent of decellularization:

1. < 50 ng dsDNA per mg ECM dry weight;
2. < 200bp DNA fragment length;
3. lack of visible nuclear material in tissue sections stained with 4',6-diamidino-2-phenylindole (DAPI) or hematoxylin and eosin (H&E).

However, these criteria do not readily provide a solution to all previously presented dilemmas. First, a lack of visible nuclear material in tissues stained with DAPI or H&E does not necessarily mean that a material is rid of cellular debris. In one study by Simon *et al.* (2003) [133], previously thought acellular heart valves were found to have multiple cellular remnants when observed by scanning electron microscopy.

Second, as previously explained, even a very low amount of residual cellular components may still trigger an adverse host reaction. This fact means that a tissue that has been proven to observe all minimal proposed criteria may still fail after *in vivo* application. While a perfect guarantee of safety from host reactions will never be an accomplishable goal, it should be possible to establish an assurance level based on the probability of an adverse host reaction occurring. A more throughout research needs to be carried out, particularly on host tissue reactions of decellularized tissues after *in vivo* implementation.

Last, the proposed standard concerns only on the presence of DNA in decellularized tissues. While this focus is corroborated by studies showing that the presence of DNA is directly correlated to adverse host reaction [125,129,130], it is insufficient to prove the absence of an antigenic potential [127]. Nonetheless, the criteria proposed above has proven to be an important standard for evaluating a decellularization protocol's effectiveness on the removal of cellular material.

In 2018, M. Kawecki *et al.* [135] proposed the following accompanying criteria for evaluating the effectiveness of decellularization:

1. lack of intracellular membrane compartments (e.g., mitochondria);
2. lack of cell membrane elements;

3. presence of unremoved and undamaged ECM elements (such as collagen, GAGs or fibronectin);
4. lack of cytotoxicity of the obtained ECM scaffold.

These criteria expand the definition of successful decellularization beyond the reduction of the tissue's immunogenicity potential to encompass the preservation of biological and mechanical properties. However, they do not provide a precise, quantifiable measure that can be used by researchers to evaluate the effectiveness of a decellularization protocol or to compare with other protocols in the literature. As previously explained, some ECM degradation is always bound to occur from the use of decellularization agents, so it is vital to reach a proper quantifiable standard for a threshold of removed vs. damaged elements, even if specific for a tissue type, source, and function. As such, the lack of established metrics for proposals 3 and 4, in particular, could lead to confusion between different teams at what an acceptable threshold for ECM preservation or scaffold cytotoxicity might be.

1.3.4 Regulation of decellularized matrices

At present, there are no regulations delineated specifically for decellularized products. Instead, the existing regulations established for the use of biomaterials have been applied to these products. In the European Union, such regulations would include Good Manufacturing Practices directives [136], directives concerning medical devices [137], or, in the case of human-sourced products, directives that set standards of quality on procurement, processing, and distribution of human tissues or cells [138]. These regulations are usually of a general nature, concerned chiefly with the safety and biocompatibility of these products, and thus do not focus on specific requirements for these biomaterials [139]. In the United States, many of these matrices will be classified as medical devices or combination products by the Food and Drug Administration (FDA) and need to navigate the regulatory requirements of the FDA in both pre-market and post-market environments [140]. On a global scale, these products will often seek to follow the standards set by organizations like the American Society for Testing and Materials (ASTM) and the International Organization for Standardization (ISO), such as the requirements set for the characterization and testing of biomaterial scaffolds [141], quality management systems [142], medical devices [143], or their biological evaluation [144].

More work is needed for a guideline or standard designed explicitly for decellularized scaffolds to be established. Criteria need to be thoroughly researched, and scientifically-proven evidence needs to be present to give weight to any proposal to be put forward. Furthermore, international and recognized standards organizations like ASTM, ISO, or other expert bodies like the FDA or the European Medicines Agency (EMA) need to be involved as to facilitate a translation of these products from a laboratory to a clinical setting.

1.4 Decellularization of bone

1.4.1 The bone's extracellular matrix

The bone's extracellular matrix is composed of organic compounds (~20 to 40%), inorganic minerals (~50 to 70%), water (~5 to 10%) and lipids (<3%) [145]. Within the organic phase, collagen is present in the biggest amount (~85 to 90%), predominantly type I collagen, with some trace amounts of type V and III [145,146]. The extracellular bone matrix proteins are divided into two categories: structural proteins, such as collagen and fibronectin, and proteins with other specialized functions, like growth factors or enzymes [146]. Although collagen provides some amount of load-bearing strength to bone, it is primarily responsible for its elasticity and flexibility [145].

The mineral content of bone is mostly composed by hydroxyapatite [$Ca_{10}(PO_4)_6(OH)_2$], but also includes carbonate, magnesium, and acid phosphate in small amounts. This inorganic phase surrounds and impregnates with collagen fibers, providing mechanical rigidity and load-bearing strength to bone [145]. The amount and arrangement of these components have a substantial impact on the final properties of each type of bone.

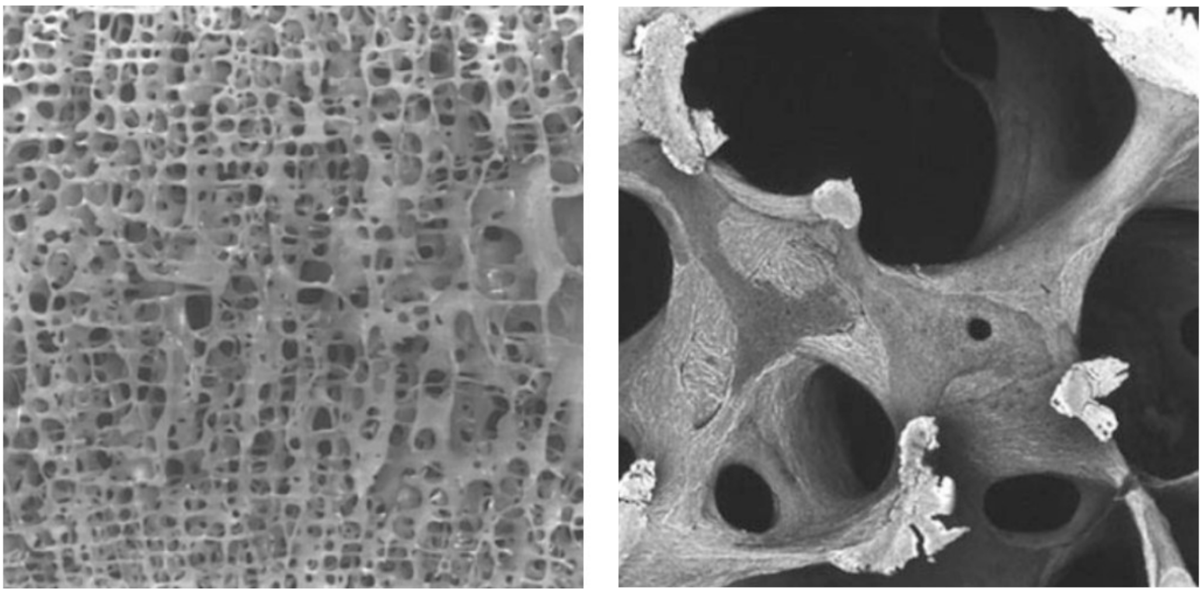

Figure 1.9 Scanning electron microscopy of bone [147]. **Left:** Very low magnification (wide field) micrograph of trabecular bone. **Right:** Bone packet distribution by BSE-SEM.

Finally, cells that reside in this intricate matrix can originate from two cell lineages. The mesenchymal stem cell lineage gives rise to preosteoblasts, osteoblasts, and osteocytes, while the hematopoietic stem cell lineage creates monocytes, preosteoclasts, and osteoclasts [148]. These cells interact with the extracellular matrix, secreting new organic matter and driving matrix mineralization (more on the interactions between cells and ECM is on Chapter 1.1.2 "The Extracellular Matrix").

1.4.2 Bone grafts and substitutes

At present, an orthopedic surgeon has a very limited array of options when faced with an injury requiring bone replacement. The "gold standard" has been the use of autologous bone grafts, usually harvested from the iliac crest, but there are severe disadvantages to this method. The supply of autologous bone graft is minimal, especially in the case of massive segmental bone loss or others that require multiple harvests [149]. Another drawback is the morbidity associated with this type of intervention, with one study (Younger and Chapman, 1989) [150] placing it at around 8.6% for major complications, like infection, prolonged wound drainage, large hematomas and severe pain, and around 20.6% for minor complications such as superficial infection, temporary sensory loss or mild pain. Nonetheless, autologous bone grafts set the standard to which all substitute bone grafts are compared to, due to their excellent osteogenic, osteoconductive, and osteoinductive properties [149]. Allogenic bone grafts have also been used, and although they come with the advantage of eliminating donor-site morbidity and a broader supply, there is a risk of severe immune complications or disease transmission, and they are slower to integrate with native tissue when compared to autologous grafts [148].

It is due to the limitations associated with allografts that the interest in using scaffold substitutes has risen, such as naturally derived biopolymers, like collagen or chitosan, and demineralized ECM-based materials. Independent of the method used, any product intended to use as a bone graft substitute should have present the following essential components [149]:

1. osteoconductive matrix;
2. osteoinductive proteins;
3. osteogenic cells (such as osteoblasts or osteoblast precursors).

Collagen and ECM-degenerated proteins (such as gelatine) were initially sought for use in bone tissue engineering due to their excellent biocompatibility, biodegradability, and cell-binding properties [151]. However, these naturally derived biopolymers came with severe drawbacks like poor mechanical integrity and a high degradation rate *in vivo* [151].

Bioceramics, such as calcium phosphates and bioactive glasses, are also a popular alternative used as synthetic bone grafts due to their bioactivity, ability to bond directly to the surrounding bone tissue, and good osteoconductivity. However, their mechanical strength and biodegradability rates run opposite to each other: materials with strong mechanical integrity (such as crystalline hydroxyapatite) are practically bioinert, and biodegradable materials (such as bioactive glasses) are often very fragile [151].

Finally, demineralized bone matrix (DBM) is a type of allograft bone graft material that has had the inorganic mineral component of the extracellular matrix removed. Currently, demineralized bone matrix products are available commercially and have been applied clinically, usually for filling in bony defects. DBM products are available in a variety of forms, such as powder, putty, chips, crushed granules, or gel-filled syringes [152]. DBM has osteoconductive and osteoinductive properties that prompt bone regeneration, but the lack of the mineral component significantly reduces the mechanical properties of bone [153]. Commercially available DBM is also often very expensive (one millimeter often costs above 100 euros), making it cost prohibitive for the treatment of large bone defects.

1.4.3 Decellularized bone Extracellular Matrix research

So far, there has not been much work done concerning the decellularization of xenogenic and allogenic bone extracellular matrices (Table 1.3). Nevertheless, a gradual increase in interest in bone dECM can be observed throughout the years examined in this work.

Table 1.3 Summary of the current works on decellularized bone extracellular matrices, highlighting the tissue source and size of scaffolds and the respective step-by-step decellularization protocol. (Note: washing steps were omitted when the time was not specified or less than 1 hour).

Scaffold Details	Decellularization Protocol		Ref.
Tissue source: Porcine femur *Scaffold size:* Small pieces (size not specified)	1. High-hydrostatic pressurization (980 MPA, 30ºC) 2. DNase I + antibiotics 3. 80% v/v ethanol	10 min 3 weeks 3 days	154

Tissue source: Bovine tibae *Scaffold size:* Fragments (4 x 4 x 4 mm)	1. 0.5 N HCl 2. 1:1 chloroform/methanol 3. 0.05% trypsin + 0.02% EDTA 4. 1% w/v penicillin/streptomycin	24 h 1 h 24 h 24 h	155
Tissue source: Bovine femur *Scaffold size:* Granules (0.25 –1 mm)	1. Thermal shock treatment (x 4) 2. 1% Triton X-100 3. 0.1% Triton X-100 4. Immersion in ddH_2O 5. Ethanol (50%, 70%, 96%, 100%)	65 h 20 m 8 h 16 h 48 h 8 h	103
Tissue source: Human femur *Scaffold size:* Cubes ($1cm^3$)	1. Sonication in dH_2O, 60ºC 2. Wash-centrifuge steps, 1850 x g, 60ºC (x3) 3. Sonication in 3% v/v H_2O_2 + 0.02% PAA, 60ºC 4. Sonication in 70% v/v ethanol 5. Centrifugation at 1850 x g	15 m 2 h 15 m 10 m 10 m 15 m	156
Tissue source: Mice calvaria *Scaffold size:* Particles (size not specified)	1. 0.5% SDS + 0.1% NH_4OH	3 weeks	157
Tissue source: Bovine femur *Scaffold size:* Fragments (15 x 4 x 2 cm)	1. 0.9% saline solution 2. 0.01, 0.1 and 1% SDS 3. 1% Triton X-100 4. Rinse in PBS 5. 2:1 and 1:2 chloroform/ethanol	12 h 72 h 2 h 4 h 48 h	158
Tissue source: Porcine femur *Scaffold size:* Plugs (Ø ~9.5 mm)	1. Wash in dH_2O 2. 0.05% trypsin-EDTA 3. penicillin/streptomycin 4. Wash in dH_2O 5. 1.5% PAA + 2.0% Triton X-100	72 h 2 h 24 h 24 h 3 h	122
Tissue source: Human femur *Scaffold size:* Pieces (0.3×0.3 cm)	1. 0.6 N HCL 2. Thermal shock treatment (x 6) 3. 0.25% trypsin 4. 2.5% SDS	4 days 42 m 18 h 26 h	102

Tissue source: Bovine knee joint *Scaffold size:* Cylinders (Ø 10mm)	1. PBS + 0.1% EGTA 2. 0.1% Triton X-100 3. $scCO_2$ at 30 MPa, 50 ºC	1 h 2 h 30 m	159
Tissue source: Bovine metacarpus *Scaffold size:* Cylindrical plugs (Ø 4 mm)	1. PBS + 0.1% EDTA 2. Tris + 0.1% EDTA 3. Tris + 0.5% SDS 4. Tris + DNAse + RNAse 5. PBS + 70% ethanol	1 h 12 h 24 h 6 h 10 m	160

Hashimoto *et al.* (2011) [154] reported for the first time, a method to decellularize bone/bone marrow using high-hydrostatic pressurization (HHP) method followed by enzymatic and alcohol washes to remove cell debris and lipid content better. The cellular content from both cortical and trabecular bone/bone marrow was successfully removed by this method. Afterward, the resulting scaffold was re-seeding with rat mesenchymal stem cells (rMSCs), allowing a better proliferation and osteogenic differentiation promotion than the one observed in tissue culture polystyrene dishes [154]. No mechanical assays were used to characterize these scaffolds.

Sawkins *et al.* (2013) [155] applied a stringent decellularization process to decellularize bone matrix, to produce a hydrogel-shaped dECM. For this purpose, they used an enzymatic-based decellularization method involving trypsin. DNA content of the decellularized material was lower than the upper limit recommended for complete decellularization (<50 ng of DNA per mg of dry ECM). However, the hydrogels formed using this decellularized bone matrix had significantly lower storage moduli than those formed by demineralized bone matrix or collagen type I hydrogels [155].

From 2015 on, there was substantial progress in bone decellularization methods. Gardin *et al.* (2015) [103] developed a novel protocol for decellularization and depilation of bovine bone granules based on multiple steps of thermal shock, washes with detergent, and dehydration with alcohol. This protocol was successful in reducing both DNA and RNA content by 90%, and the resulting granules were found to be biocompatible, osteoinductive, and osteoconductive in *in vitro* and *in vivo* experiments [103]. The treatment of samples with ethanol appeared to be vital for the total removal of cellular debris and thus conferred superior biocompatibility. Since the objective of this work was to produce a guided bone regeneration (GBR) membrane, the mechanical integrity of the granules after decellularization was not analyzed.

In another work by Smith *et al.* (2015) [156], the decellularization protocol used was based on multiple wash-centrifuge and sonication steps. This method was notable since it did not make the use of detergents, even though chemical agents (hydrogen peroxide and peracetic acid) were still present during sonication. The removal of around DNA was 99.2%, and the resulting scaffold was considered biomechanically stable, even with a significant increase in Young's modulus and a small insignificant increase in stiffness [156].

The following year, Lee *et al.* (2016) [157] optimized the experimental parameters to decellularize small bone particles using 0.5% sodium dodecyl sulfate (SDS) and 0.1% ammonium hydroxide (NH_4OH). The obtained graft material had a decreased mechanical strength (15.51% lesser than control samples) and protein content but was able to stimulate rMSC's osteogenic differentiation in vitro [157]. *In vivo* implantation of the particles in critical-sized defects of rat calvaria yielded a synergic effect that enhanced bone regeneration, with the newly formed bone showing good integration at the interface between the host bone and the particles in the defect [157].

Karalashvili *et al.* (2017) [158] designed three-dimensional bone grafts from decellularized bovine femoral bone for the reconstruction of large size maxillofacial bone defects. Residual DNA was lesser than 1.4%, and scanning electron micrographs showed that the intricate mesh of collagen fibers of the decellularized bone fragments appeared intact [158]. A large decellularized bone graft was also fashioned for implementation on a 54-year-old female patient's zygomatic bone defect, and the graft retained its shape, structure, and integration with the host's bone during four years after transplantation [158].

Later, Bracey *et al.* (2018) [122] engineered a trabecular bone dECM from porcine femurs that had been subjected to several immersions in detergents and biological decellularization agents. The processed bone plugs had a 98% decrease in DNA content. Its micro-architecture appeared to be preserved and similar to the natural bone, although the density had been significantly lowered. The scaffolds were less stiff and had a greater deformation at failure. Notable in this work was the use of mass spectrometry to analyze the protein composition of bone scaffolds to compare it against human demineralized bone matrix. Since DBM is already a proven clinical product with osteoconductive and osteoinductive potential, the data derived from this analysis could serve to demonstrate the potential of decellularized bone scaffolds. Results derived from this analysis showed a similar composition between dECM and DBM, with a bigger presence of hematopoietic proteins detected in the decellularized scaffolds [122].

As well, Abedin *et al.* (2018) [102] produced a demineralized and decellularized human epiphyseal bone matrix to be used as a scaffold for bone generation. The research group demineralized the human epiphyseal bone using hydrochloric acid and decellularized it through a combination of physical, enzymatic, and chemical methods. Histological staining revealed a total removal of nuclear materials from the decellularized scaffold while maintaining the overall structure of the extracellular matrix. DNA quantification confirmed the presence of less than 50 ng of DNA per mg of ECM [102]. Different combinations of physical and chemical processes were also examined, but complete decellularization was not observed until the addition of the enzymatic stage [102].

You *et al.* (2018) [159] developed a combined decellularization technique based on supercritical carbon dioxide ($scCO_2$) technology to produce and characterize a natural bone scaffold. The grafts were washed with Triton X-100 and then subjected to a $scCO_2$ treatment at 30 MPa, 50ºC for 30 minutes. The group reported that a large number of cell impurities were effectively removed, with only a limited amount of fibrous material remaining within the micropores [159]. The immunogenicity of these decellularized grafts was studied by implanting them in mice, and the lack of the usual immune rejection in response to this implantation was taken as proof of the efficiency of the decellularization protocol. The group also raised the possibility of a simultaneous decellularization and sterilization process due to the use of $scCO_2$, but, in this work, cobalt-60 was used for this purpose instead [159].

Last, Sladkova *et al.* (2018) [160] utilized a combination protocol that made use of chemical and biological agents to decellularize human cadaveric and bovine bone. The scaffolds were then compared for engineering bone grafts using human induced pluripotent stem cell-derived mesodermal progenitor cells [160]. The results showed that scaffolds derived from both cow and human equally supported cell viability, tissue growth, and formation of a mineralized bone matrix [160]. These findings suggest that bone scaffolds derived from xenogenic sources could be a suitable and convenient alternative to human-derived grafts.

This analysis elucidates on the potential and opportunities for future research of decellularization on bone tissue. The creation of scaffold materials that could work as bone graft substitutes is an exciting outcome, but more work is necessary before such grafts are made commercially available.

1.5 Objective

Within the scientific and economic context presented through this introduction, the main objective of the present thesis is to propose new and more effective decellularization strategies for bone tissue, using a porcine trabecular bone model.

2. Materials and Methods

2.1. Animal tissue processing

Femurs from freshly slaughtered (< 24 hours) female pigs were obtained from a local slaughterhouse. The distal ends of the femurs were cut into slices approximately 3 to 4 millimeters tall using a band saw machine. The bones were transported to the laboratory properly conditioned and refrigerated to prevent tissue degradation. Afterwards, the slices were cut into small cylindrical pieces (Ø 6 mm) using a biopsy punch (Kai Medical, Japan). Any pieces containing articular or subchondral elements were immediately discarded. Afterwards, samples were rinsed 3 times with deionized water before being frozen at -20 ºC until further use.

2.2. Cell lysis treatment

A freeze-thaw step was done to induce cell lysis in bone samples before the decellularization treatment. Initially, samples were thawed at room temperature (RT) for 30 minutes and rinsed 3 times with deionized water. Afterwards, the bone pieces underwent six cycles of rapid freeze-thaw, each comprising of a freezing step in liquid nitrogen (-196 ºC) for 2 minutes and a rapid melting step in a water bath at room temperature for 5 minutes. Lastly, samples were rinsed 3 times in deionized water.

To study the effects of the freeze-thaw treatment, 2 samples were immediately put in a formaldehyde solution for further histological analysis via hematoxylin and eosin (H&E) staining, and another 2 samples were immersed in a fixing solution (4% glutaraldehyde and 6% formaldehyde) for later examination via transmission electron microscopy (TEM). The remaining samples were frozen at- 20 ºC until further use.

2.3. Decellularization

Three different approaches to decellularize trabecular bone tissue were analyzed in this work: i) immersion in tri-n-butyl phosphate (TnBP); ii) supercritical CO_2 treatment; and iii) a combined $scCO_2$-TnBP treatment. In total, five different protocols (Figure 2.1) were implemented and examined: 1% (v/v) TnBP treatment for 48 hours, $scCO_2$ treatment for 1 and 3 hours, and $scCO_2$ treatment with 0.1% (w/v) TnBP for 1 and 3 hours.

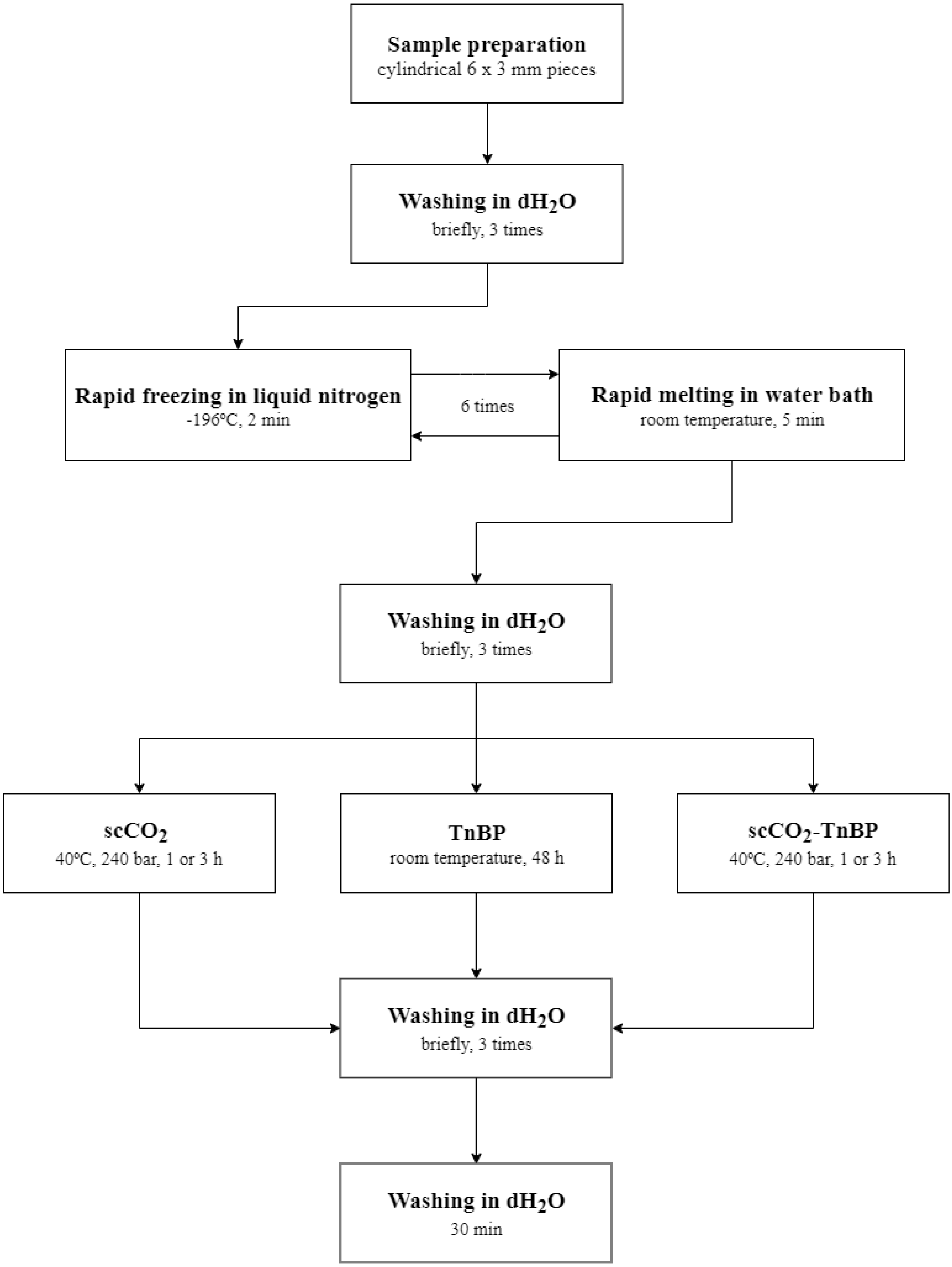

Figure 2.1 Flow-chart detailing the decellularization process and protocol variants. Samples were subjected to one of three different treatment types: TnBP for 48 hours, $scCO_2$ for 1 hour or 3 hours, and $scCO_2$-TnBP for 1 hour or 3 hours. On total, five different protocols were examined.

2.3.1. TnBP treatment

The TnBP treatment was adapted from a protocol by Cartmell *et al.* (2000) [66]. Bone samples were incubated with 1% (v/v) TnBP for 48 hours under continuous agitation (230 rpm). The solution was changed after 24 hours.

Afterwards, the samples were rinsed in deionized water 3 times and washed for 30 min in deionized water under continuous agitation. Representative samples (n=2) were set immediately aside and immersed in a formaldehyde solution for H&E staining. The remaining samples were frozen at -20ºC until further use.

2.3.2. $scCO_2$ treatment

Samples were sealed in sterilization pouches (Tyvek, USA) and placed inside the pressure vessel of a Parr Instruments series 4540 high pressure reactor (Parr Instrument Company, Illinois, USA). Premium CO_2 Liquid Premier with 99.995 % of purity (Gasin Air Products, Portugal) was introduced into the pressure vessel via a high-pressure pump at 50 g/min and pressure was set to 240 bar. The temperature was adjusted to 40 ºC and the rotation motor speed was set at 600 rpm. Pressurization took approximately 30 minutes to complete. After 1 or 3 hours, the vessel was slowly depressurized using a manually operated valve. Depressurization took approximately 25 minutes to complete.

After treatment, the samples were subjected to the same washing and storage procedures as described in section 2.3.1.

2.3.3. $scCO_2$-TnBP treatment

The $scCO_2$-TnBP hybrid treatment followed the conditions described in section 2.3.2. with the addition of 0.1% (w/v) TnBP (Merck Millipore) into the pressure vessel before $scCO_2$ treatment.

2.4. Transmission Electron Microscopy

In this work, TEM was used to confirm if cell lysis had been successfully induced after freeze-thaw treatment. Samples were fixed via immersion in 2.5% (v/v) glutaraldehyde and 2% (v/v) paraformaldehyde in 0.1M sodium cacodylate buffer (pH 7.4) solution for 5 days. Afterwards, samples were washed and decalcified in MoL-DECALCIFIER (EDTA-based decalcifying solution) for 48 hours and post-fixated in 2% (v/v) osmium tetroxide in 0.1M sodium cacodylate buffer (pH 7.4) solution for 2 hours. Samples were then incubated with 1% (v/v) uranyl acetate

O/N, washed in buffer and dehydrated through a graded series of ethanol, and finally embedded in Epon (EMS). Ultrathin sections were cut at 50 nm and prepared on an RMC Ultramicrotome (PowerTome, USA) using a diamond knife and recovered to 200 mesh Formvar Ni-grids, followed by 2% (w/v) uranyl acetate and saturated lead citrate solution. Visualization was performed at 80 kV in a JEM-1400 microscope (JEOL, Japan) and digital images were acquired using a CCD digital camera Orious 1,100 W (Japan) using 8,000x and 12,000x magnifications.

2.5. Micro Computed Tomography

Control and treated samples were scanned in a Skyscan 1174 (Brucker, USA) with an image pixel size of 9.55 μm, exposure time of 8500 milliseconds and a rotation step of 0,9º. The three-dimensional reconstructions were made using CTan and CTvox, while the transversal plane views were made using Dataviewer. Porosity measurements were derived from micro-CT reconstructions. Pore sizes were measured from transversal plane views and presented as the mean (n=7) of pore sizes from one sample for each treatment group.

2.6. Scanning Electron Microscopy

Samples were coated with Au/Pd with a sputter coater (Quorum Technologies, UK) for 45 seconds and imaged on a Vega3-LM scanning electron microscope (TESCAN, Czech Republic). Visualization was performed at 15kV and digital images were acquired at 50x magnification.

2.7. Mechanical Compression Testing

Mechanical properties of treated and control samples (n = 6) were assessed via uniaxial compression testing using a texturometer equipment (TA.XT PLUS, Texture Analyzer, UK). Initially, the height of samples was measured using a 200mm digital caliper (Mitutoyo, Japan) to allow for correction for sample's geometry. Compression was done using a 5 mm cylinder stainless probe (Stable Micro Systems Ltd, UK) and a 30 kg compression load cell. Testing was done using a crosshead speed of 1 mm/s until fracture or 90% strain was reached. Results were obtained as a stress versus strain for strain rate curve and subsequently analyzed in Microsoft Excel (Microsoft, USA). Young's modulus was derived from the slope of the stress-strain curve's linear portion, while yield point was obtained from the first of the stress-strain curve's non-linear portion.

2.8. Histology

For tissue fixation, bone samples were previously fixed in 10 % (v/v) buffered formalin for a minimum of 24 hours and de-calcified in EDTA for 48 hours. Samples were then routinely processed in an automated system and embedded in paraffin using a Microm STP-120 spin tissue processor (Thermo Scientific, USA). Sequential sections for hematoxylin and eosin staining were made at 4 µm in adhesive slides using a Shandon Finesse 325 (Thermo Scientific, USA).

2.9. DNA quantification

DNA content was analyzed from control and treated bone samples (n = 5) to access decellularization efficiency. Samples were frozen in liquid nitrogen (-196 ºC) and grinded into small particles using a mortar and pestle. PureLink™ Genomic DNA Mini Kit (Thermo Fisher Scientific, USA) was used to extract genomic DNA from known masses of bone samples following the manufacturer's protocol. DNA yield was then measured using a microplate spectrophotometer (BioTek, USA) by UV absorbance at 260 nm using the following equations:

$$\text{Concentration } (\mu g/ml) = A_{260} \times Dilution\ Factor \times 50\ \mu g/ml \tag{2.9.1}$$

$$\text{DNA yield } (\mu g) = Concentration\ (\mu g/ml) \times Total\ Sample\ Volume\ (ml) \tag{2.9.2}$$

2.10. Statistical analysis

Statistical analysis was conducted using IBM® SPSS® Statistics (International Business Machines Corporation, USA). Significant differences were identified at $p \leq 0.05$ using independent samples t-tests.

3. Results

3.1 Assessment of cell lysis

3.1.1 Macroscopic images

In Figure 3.1 are presented the macroscopic field pictures of untreated samples (Fig. 3.1 a) and samples subjected to the cell lysis treatment (Fig. 3.1 b).

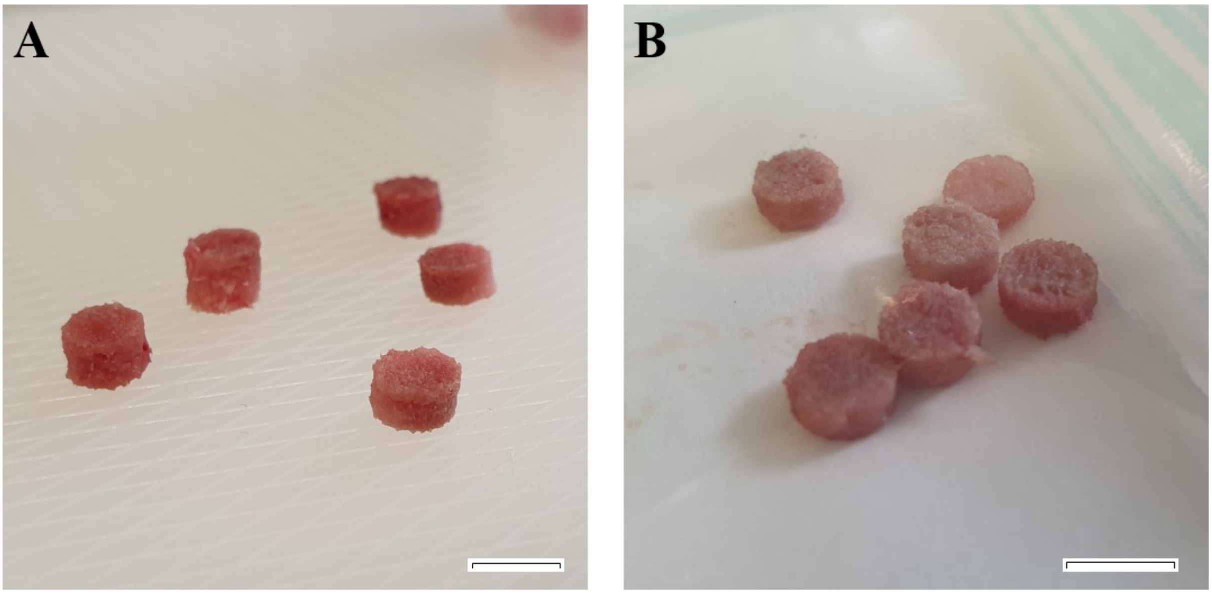

Figure 3.1 Macroscopic field photographs: **(A)** Untreated samples; **(B)** Samples subjected to cell lysis treatment. Scale bar indicates 6 mm.

Analysis of the samples' morphology revealed no significant differences in color, shape or texture between untreated samples (Figure 3.1 a) and samples that had been subjected to the cell lysis treatment (Figure 3.1 b).

3.1.2 Transmission Electron Microscopy

TEM imagining revealed a distinct morphology between osteocytes present in untreated samples (Figure 3.2 a) and in the samples subjected to a freeze-thaw cycle treatment to induce cell lysis (Figure 3.2 b).

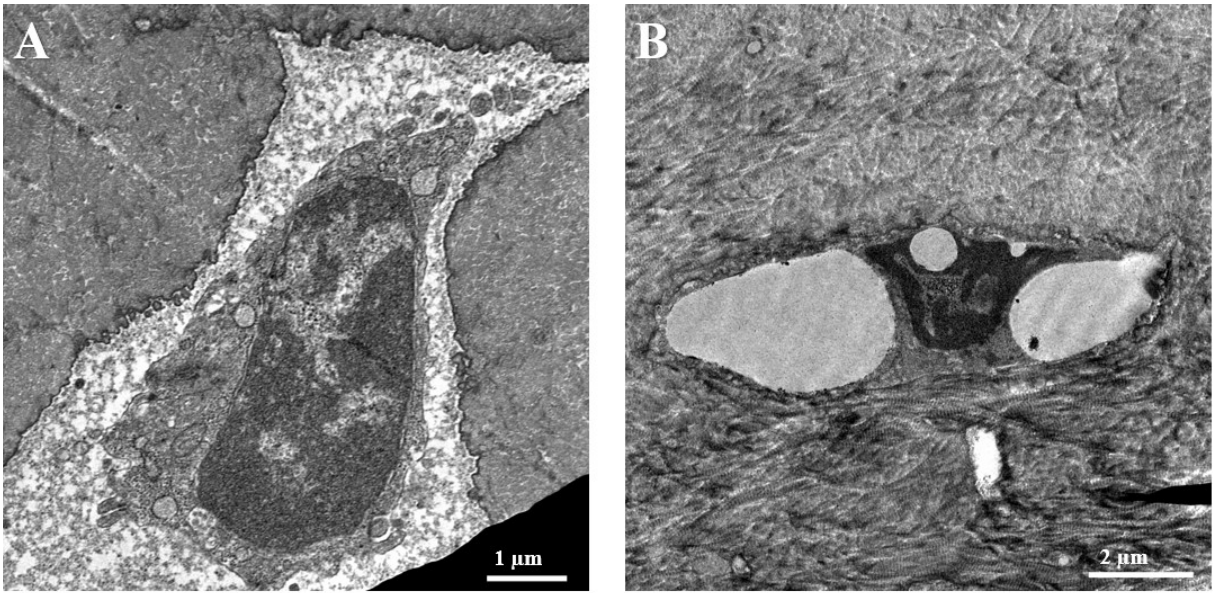

Figure 3.2 TEM micrographs of osteocytes: **(A)** untreated sample (12,000x); **(B)** sample subjected to cell lysis treatment (8,000x). Scale bars indicate 1 µm in **(A)** and 2 µm in **(B)**.

The cells observed in untreated samples exhibited a normal morphology with outlined cell components, while no such distinctions were found in the cells from treated samples. The cells from treated samples were also shrunken and smaller than cells found in untreated samples.

3.2 Integrity and structure of decellularized bone

3.2.1 Macroscopic images

Figure 3.3 presents the macroscopic images of untreated trabecular bone samples and samples subjected to one of the following decellularization protocols: TnBP for 48 hours, $scCO_2$ for 1 hour and 3 hours, and $scCO_2$-TnBP treatment for 1 hour and 3 hours.

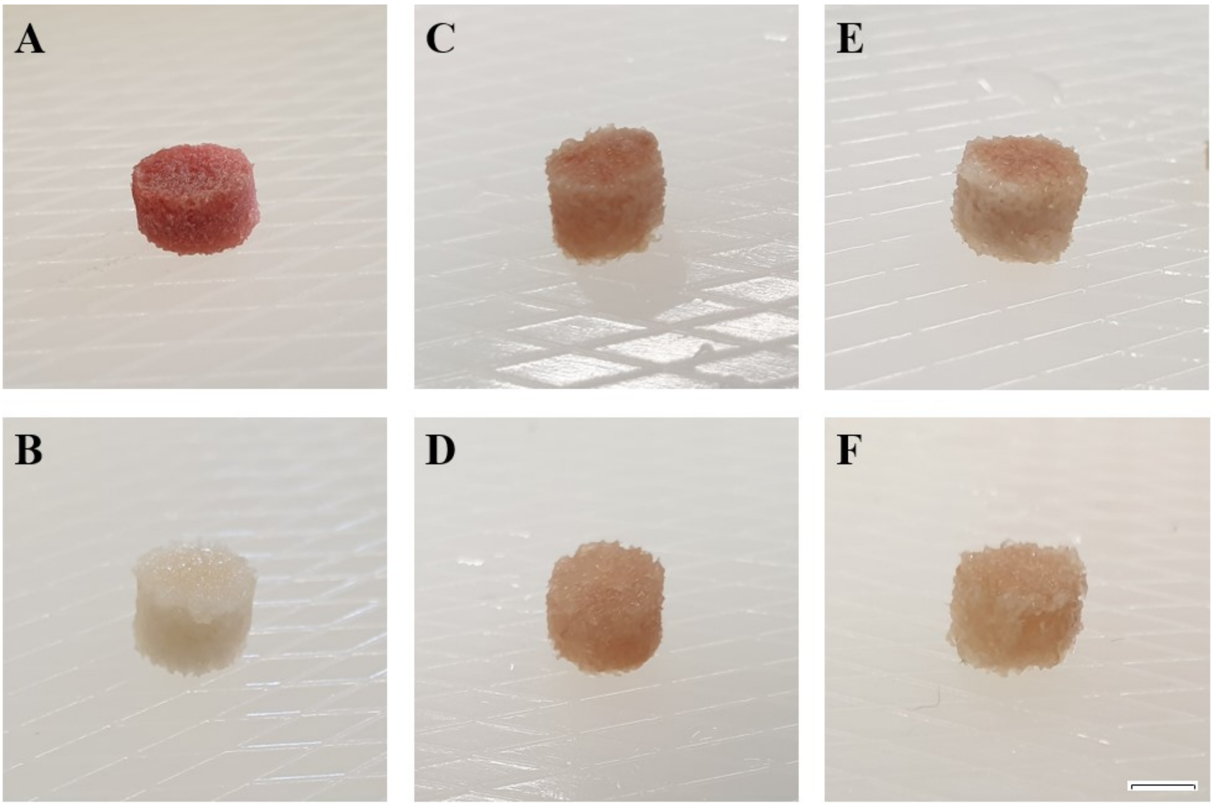

Figure 3.3 Macroscopic field images: **(A)** Untreated sample; **(B)** TnBP treatment for 48h; **(C)** $scCO_2$ treatment for 1 hour and **(D)** 3 hours; **(E)** $scCO_2$-TnBP treatment for 1 hour and **(F)** 3 hours. Scale bar indicates 3 mm.

The untreated bone samples had an intense red color and a uniform texture (Figure 3.3 a). All samples exhibited some degree of discoloration after being subjected to their respective treatments. However, this loss of color was most distinct for samples that undergone the TnBP treatment (Figure 3.3 b), and less pronounced for samples subjected to $scCO_2$ treatments (Figure 3.3 c,d). As for the samples subjected to the hybrid $scCO_2$-TnBP treatment (Figure 3.3 e,f), the extent of discoloration was higher than $scCO_2$ treatment, but lesser than that of TnBP treatment. Texture appeared to be similar between all samples.

3.2.2 Micro-Computed Tomography

3.2.2.1 Micrographs

Micro-CT revealed similar microarchitecture between untreated and treated samples (Figure 3.4).

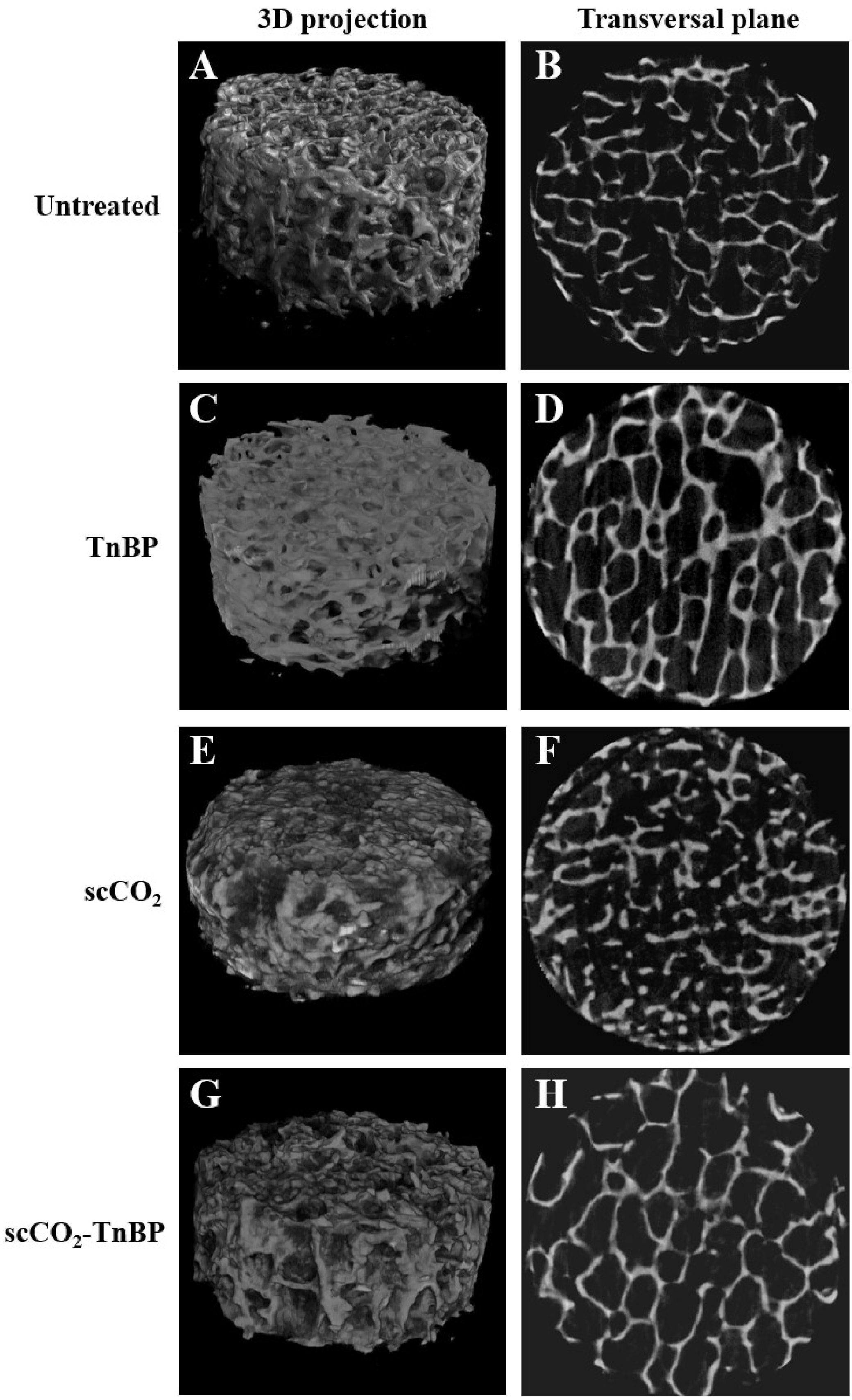

Figure 3.4 Micro-CT imaging of untreated and treated samples showing 3-dimensional projections and transversal plane views: **(A, B)** Untreated; **(C, D)** TnBP treatment; **(E,F)** $scCO_2$ treatment for 1 hour**;** **(G,H)** $scCO_2$-TnBP treatment for 1 hour.

However, substantial changes to the microstructure were observed in the sample subjected to the $scCO_2$ treatment for 3 hours, as the trabeculae appeared substantially separated from each other (Figure 3.5 c).

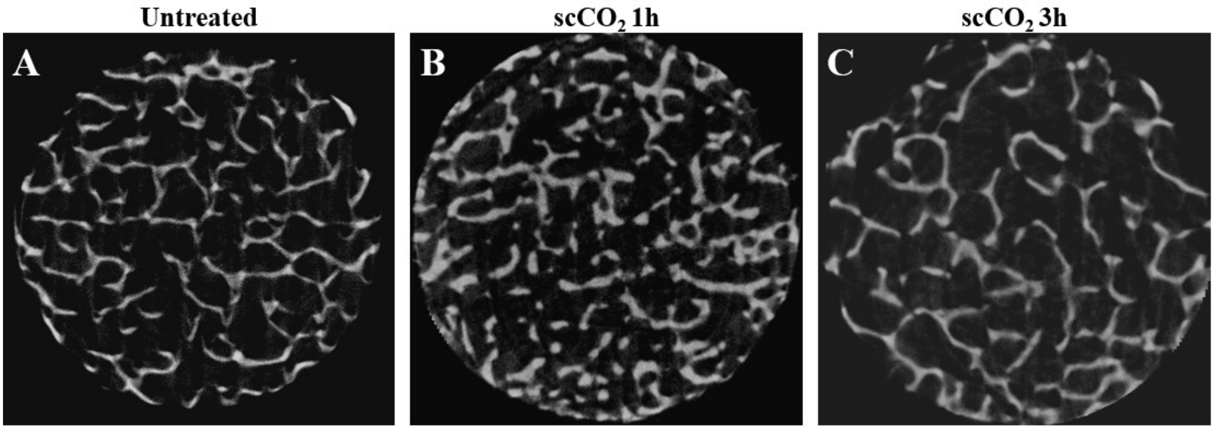

Figure 3.5 Micro-CT transversal plane view of samples: **(A)** Untreated sample; **(B)** $scCO_2$ treatment for 1 hour; **(C)** $scCO_2$ treatment for 3 hours.

3.2.2.2 Measurements

Porosity measurements derived from Micro-CT imaging are presented in Table 3.1.

Table 3.1 Porosity and mean pore size values for untreated and treated samples. Mean pore size is presented as the mean ± standard deviation.

Treatment	Porosity (%)	Mean Pore Size (µm)
Untreated	48.8	392.8 ± 87.2
TnBP 48h	66.7	406.6 ± 81.4
$scCO_2$ 1h	58.0	420.1 ± 97.3
$scCO_2$ 3h	61.7	508.7 ± 169.0
$scCO_2$-TnBP 1h	66.2	481.1 ± 95.0
$scCO_2$-TnBP 3h	52.7	341.4 ± 66.3

Significant differences to untreated samples are indicated with a $^*p \leq 0.05$ as compared by independent samples t-tests.

Porosity measured in treated bone samples was higher than in untreated samples. Mean pore size of treated samples was superior to untreated samples for all groups except for the $scCO_2$-TnBP for 3 hours treatment, but this increase was not statistically significant.

3.2.3 Scanning Electron Microscopy

SEM micrographs clearly show the porous complex network of the bone extracellular matrix for untreated and treated samples (Figure 3.6).

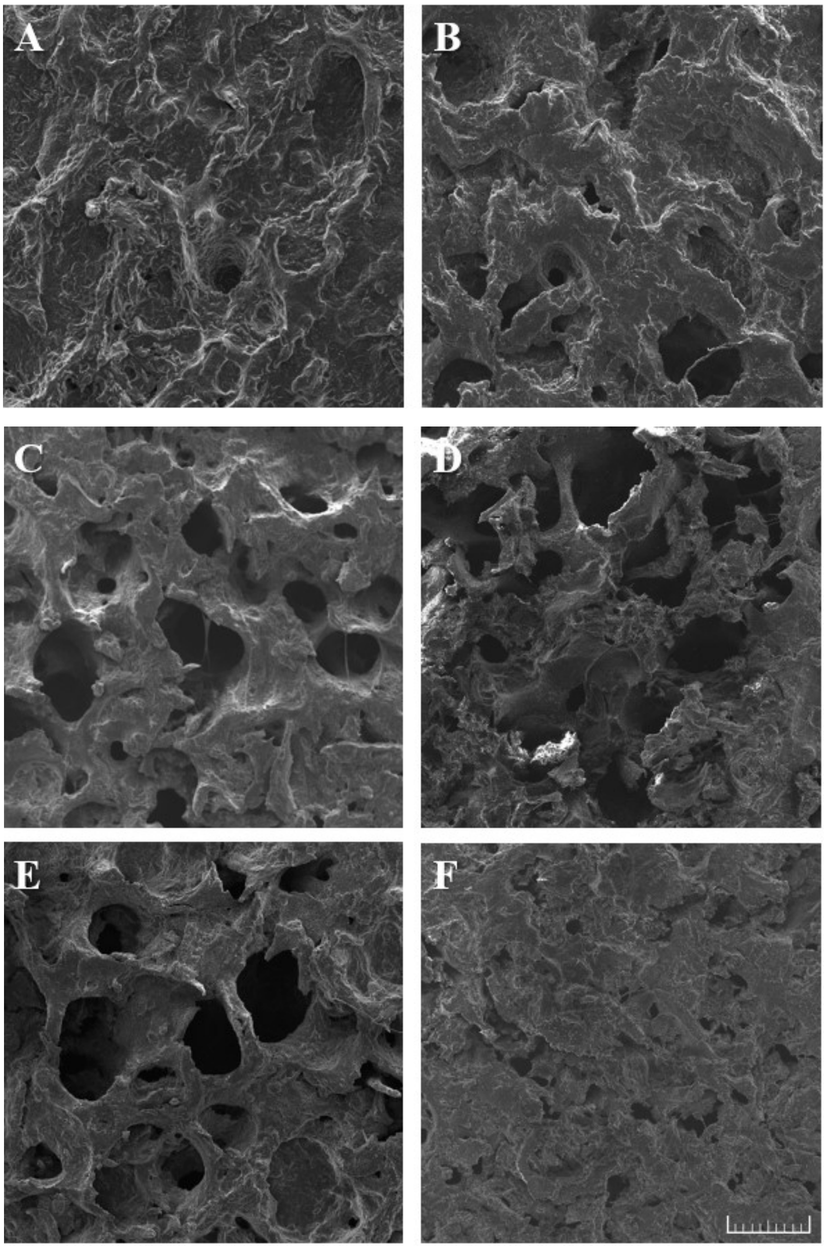

Figure 3.6 SEM micrographs of samples for each treatment type (50x): **(A)** Untreated; **(B)** TnBP treatment; **(C)** $scCO_2$ treatment for 1 hour and **(D)** 3 hours; **(E)** $scCO_2$-TnBP treatment for 1 hour and **(F)** 3 hours. The scale bar indicates 500 µm.

The micrographs of untreated samples showed that the marrow spaces appear to be filled with marrow content, partially obscuring the pores from view (Figure 3.6 a), unlike the treated samples where these pores were easy to observe (Figure 3.6 b-f). The surface topology for the sample subjected to the TnBP for 48 hours protocol (Figure 3.6 c) appeared distinct from that observed in other treatment types. As for the samples subjected to the $scCO_2$-TnBP treatment for 3 hours treatment (Figure 3.6 f), these appeared to be significantly different from other samples, as marrow spaces were much more compact, and pores appeared much smaller.

3.2.4 Mechanical properties

Table 3.3 shows the data obtained from mechanical compression testing for Young's modulus, strength, yield strain, and failure strain.

Table 3.2 Young's Modulus and Yield Point values obtained for each treatment group. Young's Modulus and Yield Point are presented as mean ± standard deviation.

Treatment	Young's Modulus (MPa)	Ultimate Strength (MPa)	Yield Strain	Failure Strain
Untreated	47.61 ± 4.25	4.00 ± 0.61	0.20 ± 0.024	0.68 ± 0.069
TnBP 48h	57.31 ± 3.66*	7.01± 0.81**	0.27 ± 0.073*	0.68 ± 0.098
$scCO_2$ 1h	66.24 ± 8.10*	7.81 ± 1.15**	0.25 ±0.053	0.62± 0.063
$scCO_2$ 3h	65.94 ± 6.39*	7.35 ± 1.40**	0.26 ± 0.048*	0.70 ± 0.033
$scCO_2$-TnBP 1h	62.70 ± 6.70*	7.01 ± 0.71**	0.22 ± 0.043	0.69 ± 0.054
$scCO_2$-TnBP 3h	49.16 ± 4.41	4.15 ± 0.53	0.19± 0.061	0.68± 0.019

Significant differences to untreated samples are indicated with a $^*p \leq 0.05$ as compared by independent samples t-tests.

A significant increase in Young's modulus was observed for all treatments except for the $scCO_2$-TnBP for 3 hours treatment. Similarly, ultimate strength was significantly superior to untreated samples for all treatments except for the $scCO_2$-TnBP for 3 hours treatment. The ductility of the samples did not appear significantly altered, but for treatments $scCO_2$ for 3 hours and TnBP for 48 hours, the values for yield strain were superior to untreated samples.

3.3 Extent of cell removal

3.3.1 Histology

Hematoxylin and eosin (H&E) staining of representative sections of untreated and treated samples are presented in Figure 3.7.

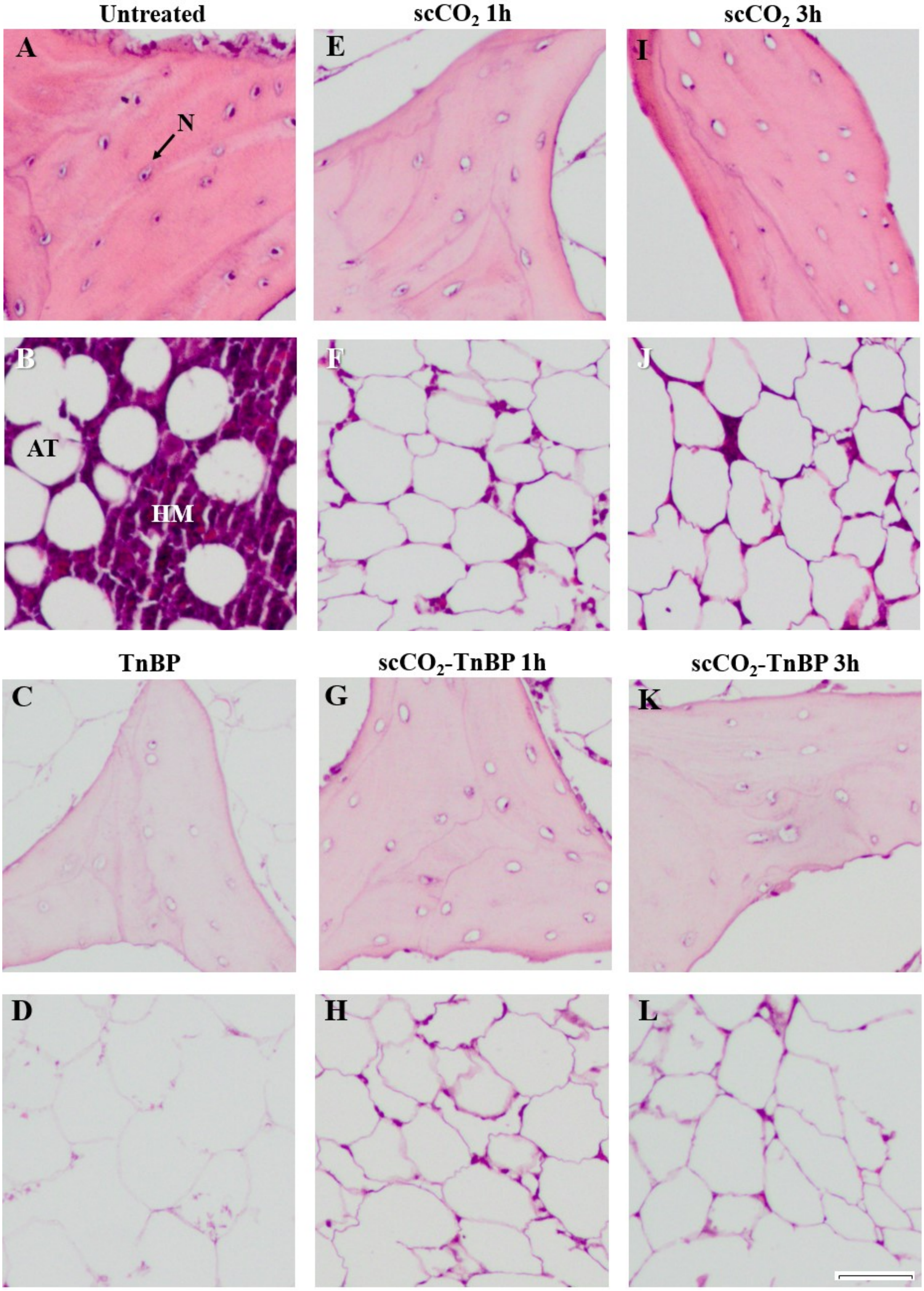

Figure 3.7 H&E staining of untreated and treated samples (10x): **(A,B)** Untreated; **(C,D)** TnBP treatment; **(E,F)** $scCO_2$ treatment for 1 hour and **(I,J)** 3 hours**;** **(G,H)** $scCO_2$-TnBP treatment for 1 hour and **(K,L)** 3 hours. Highlights: **(AT)** Adipose tissue; **(HM)** Hemopoietic marrow; **(N)** Cell nuclei. The scale bar indicates 50 μm.

Two sections are shown for each treatment type: a section focusing on the trabeculae (Figure 3.7 a,e,i,c,g,k) and another focusing on the marrow spaces (Figure 3.7 b,f,j,d,h,l). As shown in Figure 3.7, the extracellular matrix of the untreated tissue was stained pink, and cell nuclei stained dark purple. For all treatments, some degree of cell removal was observed (Figure 3.7 c-l), though this was more pronounced within the bone marrow. Cell removal was more extensive in treatments that used TnBP (Figure 3.7 c,d,g,h,k,l) compared to treatments that only used $scCO_2$ (Figure 3.7 e,f,i,j). No treatment was able to remove completely cellular material that was embedded within the trabeculae.

3.3.2 DNA quantification

DNA concentration values for untreated and treated samples are presented in Figure 3.8 and Table 3.2.

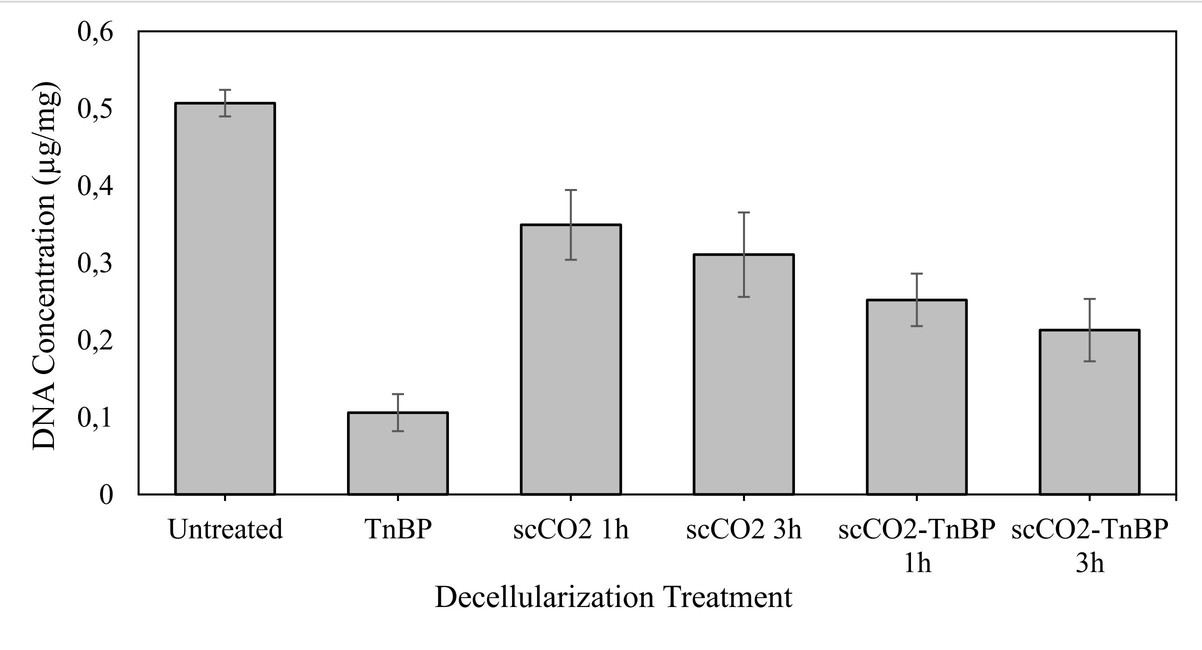

Figure 3.8 Mean DNA Concentration (µg/mg) present in samples after each decellularization treatment. Error bars display standard deviation error for all mean values.

Table 3.3 DNA concentration and corresponding percentage DNA removal compared to untreated samples for each treatment group. DNA concentration is presented as the mean ± standard deviation.

Treatment	DNA Concentration (µg/mg)	Percentage of DNA Removal
Untreated	0.507 ± 0.017	-
TnBP 48h	0.106 ± 0.024	79%
$scCO_2$ 1h	0.349 ± 0.045	31%
$scCO_2$ 3h	0.311 ± 0.055	39%
$scCO_2$-TnBP 1h	0.252 ± 0.034	50%
$scCO_2$-TnBP 3h	0.213 ± 0.040	58%

These results revealed there was a percentage decrease of DNA content for all samples that underwent treatments, being more marked for TnBP 48 hours treatment.

4. Discussion

The main objective of the present work was to investigate the potential of three innovative protocols to decellularize porcine trabecular bone tissue without the use of harsh decellularization agents such as detergents.

For this purpose, an adaptation of Cartmell and Dunn (2000)'s protocol [66] was attempted for the first time on porcine trabecular bone tissue. This protocol had been previously used to successfully decellularize tendons from rat tails, using only a 48 hours immersion period in 1% (v/v) TnBP. As well, the merits and effects of using supercritical carbon dioxide as a decellularization agent were also investigated, without the addition of any *entrainer* or secondary agent. Finally, a combined decellularization strategy using supercritical carbon dioxide and TnBP was herein proposed and studied. While $scCO_2$ has been used previously to aid in the decellularization of bovine bone, this protocol also involved the use of Triton X-100, a non-ionic detergent that is known to disrupt the ultrastructure of ECMs [46,159]. Additionally, different testing periods of both the $scCO_2$-TnBP and $scCO_2$ methods were tested to investigate any possible harmful effects on the extracellular matrix caused by prolonged exposure to $scCO_2$ treatment.

To the author's knowledge, there have been no other studies reporting on the effects of TnBP on bone tissue. On the other hand, the combination of this compound with $scCO_2$ has also not been reported in the literature for bone tissue or otherwise.

4.1. The importance of cell lysis

The induction of cell lysis is usually the first step in a decellularization protocol [121]. Specifically, for the decellularization of bone, freeze-thawing appears to be a popular initial step [102,161,162]. Casali *et al.* (2017) [87] reported a significant increase in the decellularization efficiency for their $scCO_2$-based protocol after the addition of a step to induce cell lysis. As such, in this work, particular focus was taken to induce cell lysis before decellularization using a rapid freeze-thawing methodology adapted from Abedin *et al.*'s (2018) work [102]. Freeze-thawing processing was chosen since it has been proven to lyse cells from several tissues without severely impacting ECM composition and ultrastructure [46]. The intracellular ice crystals that form during rapid freezing disrupt cell membranes, leading to their rupture. This method is also believed to cause minimal impact on mechanical properties for load-bearing tissues, an essential factor for creating a scaffold to serve as a bone graft substitute [46,93]. In fact, in this study, no significant changes in the color or texture of the samples were observed after they were subjected to the cell lysis treatment, suggesting some degree of tissue preservation.

Transmission electron micrographs showed significant differences between cells within untreated samples, and those present in samples subjected to the rapid freeze-thaw treatment being the latest shrunken, as most of the cytoplasm was eliminated from these cells. This morphology has been associated with non-viable bone cells after freeze-thaw treatment [163]. These results demonstrate that the treatment proposed was successful in inducing cell lysis.

4.2 Impact of decellularization on bone properties

One of the most critical features of the extracellular matrix of trabecular bone is its complex microarchitecture with its high surface area, allowing efficient nutrient diffusion and contact with various growth factors [164]. Not only does bone architecture play a role in osteogenic promotion and differentiation, but it also impacts the final mechanical properties of trabecular bone, which is why any scaffold used as a bone substitute should aim to imitate it [164–166]. Even pore size can have a significant effect on osteoblast survival and bone formation. Excessively small pore sizes can lead to decreased oxygen and nutrient diffusion, affecting osteoconductivity, therefore larger pore sizes (200-600 μm) are considered optimal for bone repair and regeneration [167]. Porosity in trabecular bone is also highly variable and can fluctuate between 50-90% depending on several factors, such as anatomic site, age, disease, or other interspecimen variations [168]. Excess porosity (>90%) decreases the mechanical strength of the scaffold, so a careful balance between the need for adequate diffusion of nutrients and oxygen and the mechanical properties of the scaffold needs to be found for every type of bone graft substitute [164].

In this work, the complex architecture observed in untreated samples appears to have been preserved for all treatments except for the treatment of scCO_2 for 3 hours, where bone struts appear to have significantly drifted apart from each other, creating large open areas between them. Porosity appears to have increased with the degree of decellularization, except for the treatment of scCO_2-TnBP for 3 hours, where it was significantly lesser than its corresponding 1 hour treatment. This result was not expected but may be explained by the considerable variability of porosity seen in trabecular bone, a high heterogeneous tissue. Samples subjected to the treatment of scCO_2-TnBP for 3 hours might came from a denser, more compact tissue region (and SEM imaging appears to confirm this hypothesis). Even so, the levels of porosity obtained for all treatments were within the range of porosity reported for trabecular bone tissue [164]. For the treatments of $scCO_2$-TnBP for 1 hour and TnBP for 48 hours, porosity was similar to what has been reported for demineralized bone matrix (62.24%) [169]. All treatments also resulted in an increase in the mean pore size except for that of $scCO_2$-TnBP for 3 hours. High variability was encountered when measuring pore sizes, evidenced by the high value of standard deviation seen for all means. Again, the high heterogeneity of trabecular bone may explain both the high variability of pore sizes and the smaller size of pores in the sample subjected to the $scCO_2$-TnBP for 3 hours treatment. It is worth noting that, for all treatments, the range of pore sizes observed was still within the typical 200-600 µm range previously established as optimal [167].

As discussed above trabecular bone is one of the most heterogeneous biological tissues. Its biomechanical properties, like ultimate strength or elasticity modulus, can differ widely even in the same species, such as both within and across anatomical sites, after the advent of disease, or with age [170]. Even intraspecimen variations in tissue properties can have biomechanical consequences: trabecular thickness, for example, can alter the apparent modulus to the equivalent extent of ten years of bone loss [170]. For this reason, it can be difficult to establish a standard value of comparison when it comes to mechanical parameters such as Young's Modulus or Yield Stress. Studies have pointed out to values of around 50 to 389 MPa for Young's Modulus of human trabecular bone [171,172]. Porcine bone also appears to have modulus values similar to those seen in human bones, which is why it is a popular alternative for bone grafting [172]. Regarding yield stress and strength values in trabecular bone, this property appears to be heterogeneous (varying with anatomic location, age, disease, among others), anisotropic (depend on loading direction), and asymmetric (compression versus shear) [170].

In this study, the values for Young's modulus were on the lower range of those presented in literature. These results may be explained by the geometry of the tested samples. Due to equipment limitations, some restrictions were imposed on the handling of bone samples, which resulted in a non-standard sample geometry (cylindrical 6 x 3 mm pieces) for mechanical compression testing. The geometry of trabecular bone specimens has been previously found to significantly impact their mechanical behavior [173,174]. Since the same methodology was used to test untreated and treated samples, this study focused on the comparison between the values obtained through this work.

The samples treated with TnBP had a superior ultimate strength, Young's modulus and yield strain compared to untreated samples. TnBP has been known in some studies to damage collagen content [46,175], but in this work, the stiffness and ductility of these scaffolds were not negatively impacted. A significant difference in the strain at yield was observed, marking an increase in the extensibility for these samples. It is not the first time this increase has been observed for tissues treated with TnBP, as Deeken *et al*. (2011) [47] and Xing *et al*. (2014) [176] reported similar results with TnBP decellularized tendons. Deeken *et al*. (2011) [47] suggested that a possible motive for this increase was that the removal of cellular content from tissues allowed the collaged fibers an easier sliding past one another, or that a low level of collagen crosslinking might have occurred during treatment. While the strength of bone depends mostly on its mineral phase, collagen crosslinking can affect the post-yield mechanical properties of bone, mainly its toughness and stiffness [177]. Crosslinking can significantly increase the ultimate strength of tissues composed of collagen fibers [178]. In this work, samples subjected to TnBP treatment also had higher ultimate strength than that observed in untreated samples. Cartmell and Dunn (2000) [66] also observed an increase in strength in tendons decellularized with 2% (v/v) TnBP, with no changes found for modulus or failure strain.

The samples that underwent both $scCO_2$ treatments had a significant increase in Young's modulus compared to those observed in untreated samples (66.24 MPa for 1 hour and 65.94 MPa for 3 hours). A likely explanation for this increase is that $scCO_2$ treatment is known to cause dehydration, which severely impacts values for both Young's modulus and ultimate strength [81,87]. In this work, all samples were hydrated after decellularization treatment for 30 minutes, but a more extensive period of rehydration might be necessary to mitigate the effects of dehydration. An increase in the extensibility was detected for samples subjected to the 3 hours protocol variant, as they sustained more strain before yield. It is possible that the alterations to the microstructure observed in micro-CT imagining were the cause of this change. No significant differences in the ductility were observed between untreated and $scCO_2$-treated samples, as failure strains remained consistent.

As for the hybrid $scCO_2$-TnBP protocol, a significant increase in modulus and ultimate strength were observed after 1 hour of treatment. While yield strain was higher than that of untreated samples, this increase was not considered significant. Modulus was higher than the one detected for TnBP-treated samples and lower than $scCO_2$-treated ones. It is possible that adding TnBP to the treatment chamber may have reduced the degree of dehydration of the samples. However, the differences in modulus and ultimate strength for samples treated with $scCO_2$-TnBP for 1 hour, and those treated with $scCO_2$, were not considered significant. Mostly, the mechanical properties of samples treated with $scCO_2$-TnBP followed those exhibited by $scCO_2$-treated samples, with slightly lower values for modulus, strength, and yield strain. The most considerable differences were observed after $scCO_2$-TnBP treatment for 3 hours, where no increase in modulus or strength compared to untreated samples was detected. While these results may seem initially discordant, structural imaging done to this sample group revealed lower porosity, smaller mean pore size compared to other treated samples and significantly different morphology compared to other sample groups. As previously explained, trabecular bone is a highly heterogeneous tissue. Although care was taken to diminish the variability between samples (only female pigs with similar age were selected, and samples were cut from the same anatomical site), certain sample groups were mostly or entirely composed of bone discs taken from femurs belonging to the same animal. As such, it is possible that samples belonging to the $scCO_2$-TnBP for 3 hours group were taken from tissue that was significantly different in both microstructure and mechanical properties than the tissues used for other samples.

4.3 Decellularization efficacy

In the present work, the highest decrease in DNA concentration was observed after the TnBP treatment for 48 hours, resulting in a 79% decrease in DNA content compared to untreated samples. Nonetheless, at a DNA concentration of 0.106 µg/mg, this value was still higher than the proposed maximum of 0.05 µg/mg to be considered successful decellularization [46]. Histological analysis confirmed these findings, showing an almost empty marrow space, with very little cellular debris visible (Figure 3.7 h). Also notable was how almost all lacunae appeared clear from nuclear material (Figure 3.7 g). Nevertheless, a complete absence of nuclear material was not observed.

The $scCO_2$ protocol resulted in a 31% (0.349 µg/mg) and 39% (0.311µg/mg) reduction of DNA content for 1 hour and 3 hours of treatment time, respectively. Histological analysis also confirmed that a significant amount of cellular content remained in the tissue after treatment (Figure 3.7 c-f). This outcome was similar to the results of Sawada *et al*. (2008) [81] and Casali *et al*. (2018) [87], where the use of $scCO_2$ alone was ineffective at totally removing cells from extracellular matrices. It has been hypothesized that $scCO_2$ removes cellular materials through supercritical extraction and may need the addition of a polar CO_2 soluble additive, also known as an *entrainer*, to effectively remove cells from tissues, since CO_2, a nonpolar molecule, cannot properly interact with cellular materials that are charged [46,87]. While Sawada *et al.* (2008) [81] and Guler *et al*. (2017) [38] reported complete removal of cell nuclei after using $scCO_2$ containing ethanol, Casali *et al.* (2018) [87] were unable to reproduce this result and observed that the addition of ethanol alone did not substantially intensify the extent of decellularization, perhaps due to $scCO_2$ being unable to destroy the cell membrane. Similarly, Antons *et al.* (2018) [116] suggested that ethanol may not have the required counteractive solvent strength needed for the decellularization of denser tissues, such as cartilage or tendons, recommending the use of a CO_2-philic detergent as a decellularization aid.

The $scCO_2$-TnBP protocol resulted in a 50% reduction in DNA content after 1 hour of treatment time, and a 58% reduction after 3 hours, resulting in a DNA concentration of 0.252 µg/mg and 0.213 µg/mg, respectively. The addition of TnBP into the pressurization chamber for the $scCO_2$-TnBP treatment marked a significant improvement in cell content removal (~20% more effective) compared to the $scCO_2$ protocol. However, this result was still below the proposed minimum threshold of DNA content put forward by Crapo *et al.*(2011), which determines that less than 0.05 µg of DNA per mg of ECM dry weight is needed to satisfy the intent of decellularization [46]. Histological analyses showed extensive removal of marrow content, but evidence of remaining nuclear content was still found on bone samples that were subjected to this treatment. Moreover, in the trabeculae, a significant amount of the lacunae (where osteocytes are located) still appeared to have nuclear material within. This difference in the efficiency of cell removal might be explained by the significant denser composition of the trabeculae, while bone marrow is located in easily accessible open spaces.

These results suggest that more parameters, other than the amount of TnBP added to the pressure chamber, need to be re-adjusted in the hybrid $scCO_2$-TnBP protocol since even a 10-fold increase in TnBP concentration was not enough to remove all nuclear material from trabecular bone tissue. These include the pressure used during $scCO_2$ treatment and, not less important, the time of exposure. Another possibility would include the addition of a more effective washing step, involving the use of a biological decellularization agent (such as nucleases), to achieve complete decellularization.

5. Conclusions

The present work investigated the potential of three different protocols using TnBP, supercritical carbon dioxide, or a combination of both as decellularization strategies for trabecular bone tissue.

The use of TnBP instead of harsh chemicals such as detergents, known to damage collagen content, has shown to be a promising methodology to better preserve the extracellular matrix while ensuring the elimination of cellular content from trabecular bone in a high extent. Mechanical analysis of TnBP-treated samples revealed a higher ultimate strength, yield strain, and in modulus. These results suggest that TnBP could be causing some degree of crosslinking of the collagen fibers. To the author's knowledge, there have been no previous works examining the effects of TnBP on bone tissue. These results suggest the need for further studies to better understand the effect of TnBP on collagen and, consequently, on the mechanical properties of bone.

The proposed treatment that used pure $scCO_2$ has proven to cause some removal of DNA content, however to levels considerably below the currently held standard for successful decellularization of 50 ng/mg [46]. Moreover, $scCO_2$ resulted in the dehydration of trabecular bone tissue, which affected its macrostructure and mechanical properties. The use of $scCO_2$ as both a decellularization agent and a vehicle for the delivery of TnBP was herein explored for the first time. This new methodology could lead to a faster decellularization process while making use of lower concentrations of this reagent when compared to currently published literature. Not only would this approach be economically more valuable, but it would also reduce the amount of time these tissues are exposed to potentially harmful treatments.

The combined protocol of $scCO_2$-TnBP induced a decrease in DNA content to about half of that measured for untreated samples, while no significant changes to the microstructure of trabecular bone tissue were observed after treatment, suggesting possible preservation of the extracellular matrix. The mechanical analysis revealed an increase in Young's modulus and ultimate strength of the treated samples. The potential of combined $scCO_2$-TnBP treatment was herein demonstrated, opening new possibilities and future optimizations that could achieve required decellularization levels.

6. Future Work

The work carried out in this thesis not only clearly demonstrated the potential of a combined $scCO_2$-TnBP treatment for the decellularization of trabecular bone, but also allowed for a new understanding of various parameters that need to be readjusted in further studies.

Regarding the design of the decellularization protocol itself, there are several possible improvements which can be made. First, the results showed that samples may have suffered dehydration while exposed to $scCO_2$ treatment. A proposed improvement then lies in the implementation of a more rigorous rehydration of samples at the end of the decellularization protocol. Secondly, the efficiency of DNA removal needs to be improved. Some parameters that could be readjusted are the pressure and exposure time used during $scCO_2$ treatment. As well, it would be interesting to analyze the addition of a more effective washing step, such as the addition of nucleases after $scCO_2$-TnBP treatment, to compare decellularization efficiency.

For a more accurate evaluation of structural and mechanical properties, another point of improvement lies in the mitigation of the effects of high heterogeneity of trabecular bone. In future work it would be recommended that samples be obtained from a higher number of animals. Sample geometry can also deeply affect the mechanical behavior of trabecular bone specimens, so future work should only use 2:1 cylinders. In addition, the use of more recent and high accuracy techniques for measuring mechanical properties would be recommended, such as nano-indentation or Finite Element Analysis (paired with micro-CT imagining).

Since very little work exists that focus on the effect of TnBP as a decellularization agent, it would also be interesting to properly measure the effect of TnBP on trabecular bone tissue, specifically regarding its effect on collagen content and crosslinking. The suggested future work could find use not only for studies in bone but for other collagen rich tissues.

Appendix I. Decellularized ECM-based Products

There is a wide range of products derived from decellularized extracellular matrices that are currently available for sale. Table 1 presents a list of 60 of these dECM-based products.

Table 1. List of currently available commercial decellularized ECM-based products, with references, issuing company, tissue and animal of origin, and intended clinical application.

Ref.	Product	Company	Origin	Tissue Type	Clinical Use
179	Acell Vet®	Acell, Inc.	Porcine	Urinary Bladder Matrix	Treatment of canine arthritis, tendon and ligament repair
180	AlloMax™	Becton, Dickinson and Company	Human	Dermis	Soft tissue repair
181	AlloMend®	AlloSource	Human	Dermis	Soft tissue repair
182	AlloPatch HD®	CONMED/Musculoskeletal Transplant Foundation	Human	Dermis	Orthopedic repair
183	AlloSkin™ AC	AlloSource	Human	Dermis	Soft tissue repair
184	Architect®	Harbor MedTech	Porcine	Dermis	Soft tissue repair
185	ArthroFlex®	Arthrex	Human	Dermis	Soft tissue repair
186	Avance® Nerve Graft	Axogen	Human	Nerve	Nerve repair
187	Axis™ Dermis	Coloplast	Human	Dermis	Treatment of prolapse or stress urinary incontinence

188	AxoGuard®	Axogen	Porcine	Small Intestine Submucosa	Nerve repair
189	Biodesign®	Cook® Medical	Porcine	Small Intestine Submucosa	Soft tissue repair
190	BIOVANCE®	Celularity, Inc.	Human	Amniotic Membrane	Soft tissue repair
191	CardioGRAFT®	LifeNet Health	Human	Heart Valve	Cardiovascular repair
192	Chondrofix	Zimmer Biomet	Human	Bone	Osteochondral repair
193	Cor™Patch	CorMatrix®	Porcine	Small Intestine Submucosa	Epicardial tissue support and repair
194	Cortiva®	RTI Surgical	Human	Dermis	Soft tissue repair
195	CryoPatch® SG	CryoLife, Inc	Human	Heart Valve	Cardiovascular repair
196	CryoValve® SG	CryoLife, Inc	Human	Heart Valve	Pulmonary heart valve replacement and repair
197	DermACELL®	Stryker	Human	Dermis	Soft tissue repair
198	Dermacell AWM	LifeNet Health	Human	Dermis	Wound management
199	DermaMatrix™	DePuy Synthes	Human	Dermis	Soft tissue repair
200	DermaSpan™	Zimmer Biomet	Human	Dermis	Orthopedic and soft tissue repair
201	Dermavest®	AediCell®	Human	Placenta	Soft tissue repair
202	Dura-Guard®	Baxter International Inc.	Bovine	Pericardium	Dura mater repair
203	DuraMatrix®	Stryker	Bovine	Dermis	Dura mater repair
204	Durepair®	Medtronic Inc.	Bovine (fetal)	Dermis	Repair of dura mater

205	DynaMatrix® Plus	Keystone Dental	Porcine	Small Intestine Submucosa	Soft tissue repair
206	FlexHD®	Musculoskeletal Transplant Foundation - Biologics	Human	Dermis	Connective and soft tissue repair
207	Fortiva®	RTI Surgical	Porcine	Dermis	Soft tissue repair
208	Glyaderm®	Euro Skin Bank	Human	Dermis	Dura mater and soft tissue repair
209	Graft Jacket®	Wright Medical	Human	Dermis	Tendon and ligament reinforcement
210	Integra® HuMend™	Integra LifeSciences	Human	Dermis	Integumental tissue repair
211	Integra® Reinforcement Matrix	Integra LifeSciences	Porcine	Dermis	Orthopedic and soft tissue repair
212	Hancock® II	Medtronic Inc.	Porcine	Heart Valve	Valve replacement
213	Matrix HD®	RTI Surgical	Human	Dermis	Orthopedic and soft tissue repair
214	Matrix Patch™	Auto Tissue Berlin GmbH	Equine	Pericardium	Pediatric cardiac repair
215	MatriStem®	ACell, Inc.	Porcine	Urinary Bladder Matrix	Soft tissue repair
216	Medeor®	DSM	Porcine	Dermis	Soft tissue repair
217	Meso BioMatrix™	DSM	Porcine	Mesothelium	Soft tissue repair
218	MIRODERM®	MiroMatrix Medical Inc.	Porcine	Liver	Wound management
219	MIROMESH®	MiroMatrix Medical Inc.	Porcine	Liver	Soft tissue repair
220	Mosaic™	Medtronic Inc.	Porcine	Heart Valve	Valve replacement

221	Oasis®	Smith & Nephew, Inc.	Porcine	Small Intestine Submucosa	Wound management
222	OraGRAFT®	LifeNet Health	Human	Ilium	Dental procedures
223	Peri-Guard®	Baxter International Inc.	Bovine	Pericardium	Pericardial and soft tissue repair.
224	Perimount®	Edwards Lifesciences LLC	Bovine	Pericardium	Valve replacement
225	PerioDerm™	Musculoskeletal Transplant Foundation - Biologics	Human	Dermis	Dental, integumental, and soft tissue repair
226	Permacol™	Medtronic Inc.	Porcine	Dermis	Soft tissue repair
227	PriMatrix™	Integra LifeSciences	Bovine (fetal)	Dermis	Wound management
228	ProxiCor™	Aziyo Biologics	Porcine	Pericardium	Cardiovascular repair
229	Strattice™ RTM	Allergan, Inc.	Porcine	Dermis	Soft tissue reinforcement
230	SureDerm®	Hans Biomed	Human	Dermis	Orthopedic and soft tissue repair
231	SurgiMend™	Integra LifeSciences	Bovine (fetal)	Dermis	Soft tissue repair
232	Suspend®	Coloplast	Human	Fascia Lata	Treatment of prolapse or stress urinary incontinence
228	Tyke®	Aziyo Biologics	Porcine	Small Intestine Submucosa	Neonatal pericardial repair

233	Tutopatch®	RTI Surgical	Bovine	Pericardium	Soft tissue repair
234	Vascu-Guard®	Baxter International Inc.	Bovine	Pericardium	Vascular reconstruction
235	Veritas®	Baxter International Inc.	Bovine	Pericardium	Pelvic floor reconstruction
236	XCM BIOLOGIC®	DePuy Synthes	Porcine	Dermis	Soft tissue repair
237	XenMatrix™	Becton, Dickinson and Company	Porcine	Dermis	Soft tissue repair
238	Zimmer® Collagen Patch	Zimmer Biomet	Porcine	Dermis	Rotator cuff repair

Appendix II. Decellularization Agents

Table 1 presents a summary of Chapter 1.2.1 "Decellularization Agents", as well as all published works referenced in the making of the chapter.

Table 1. List of decellularization agents, their mechanism of action, possible effects to the extracellular matrix, and published works that reference said agent. Based and expanded from Crapo *et al.* (2011) [46].

Agent/Technique	Mechanism of Action	Effects on ECM	Ref.
Chemical Agents			
Acids and Bases	• Solubilize cytoplasmatic components of cells • Disrupt nucleic acids	• Can damage collagen fibers, reducing tissue's mechanical properties • Can cause loss of GAGs and growth factors • Variable efficiency	25,27,35,44,45,47,50,51,72,79,83,110,130,239–245
Hypertonic and Hypotonic Solutions	• Osmotic shock leads to cell lysis	• Leaves residues in ECM unless combined with other agents.	26,27,44,50,52–55, 57–62,74, 82,246,247
Alcohols	• Solubilizes lipids • Cause cell dehydration that leads to cell lysis	• Dehydration of ECM can cause brittleness • Can cause protein precipitation	52,79,81–83,85–87, 240, 247–252
Tri(n-butyl) phosphate (TnBP)	• Forms hydrophobic complexes with metals • Disrupts protein-protein interactions	• Can cause loss of GAGs and collagen content • Leaves DNA residues	47,66,72,91, 176,253,254

Nonionic detergents			
Triton X-100	• Disrupts lipid-lipid and lipid-protein interactions	• May cause loss of elastin, GAGs and collagen content	26,28–30,34–36,39, 44,47,50,52–55,58–61, 65–72,74,76,83,86,97, 98,109,112,130,239, 240,243,244,246,254–264
Ionic detergents			
SDS	• Solubilizes membrane proteins • Disrupts protein-protein interactions	• May dramatically alter ECM composition and mechanical properties • Loss of GAGs, growth factors and collagen	25–27,30,32,36,39,45, 47,53,55,57,60,62,65, 66,68,70–72,74,76,77, 83,85,86,93,112,240,258,260,263–269
Zwitterionic detergents			
CHAPS	• Disrupts lipid-lipid and lipid-protein interactions • Mild effect on protein-protein interactions	• Collagen content is preserved somewhat • Loss of GAGs	31–33,61,75–77
Biological Agents			
Enzymes			
Trypsin	• Hydrolyzes proteins by cleaving the peptide chains of lysine and arginine	• Long exposition times may lead to disruption of ECM ultrastructure • GAGs, elastin and collagen degradation	26,30,35,58–60,71,79, 83,94–98,112,130, 240,246,255,269,270
Nucleases	• Cleave the phosphodiester bonds between nucleic acids	• Can provoke an immune response when not removed properly from tissue	25,26,44,50,52,55,58, 71,74,82,83,93,112, 113,243,265,271–273

Dispase	• Cleaves fibronectin and certain collagen types	• Deteriorating effect on ECM ultrastructure due to loss of collagen	79,100,269
Mechanical Agents			
Temperature	• Rapid freezing forms ice crystals inside of cells that disrupt membranes, leading to cell lysis	• Ice crystal can disrupt ECM ultrastructure	79,82,93,100–107, 116,130,270,274–281
Force	• Mechanical abrasion removes cells from tissues	• Direct application of force may severely compromise the mechanical integrity of scaffold	26,83,100,108–110, 282
Pressure	• Pressure causes cells to burst	• Rate of pressurization can cause drastic temperature changes and formation of ice crystals • Pressure used can be harmful to ECM ultrastructure • Leaves DNA residues	111–113,263
Supercritical Carbon Dioxide ($scCO_2$)	• Supercritical properties may help CO_2 and other additives achieve a higher penetration power • Direct pressure can cause cells to burst	• Extraction of volatile substances, like water • Pressure used can disrupt ECM ultrastructure	38,81,87,116,117,159, 283–286

Bibliography

1. Blair NF, Frith TJR, Barbaric I. Regenerative Medicine: Advances from developmental to degenerative diseases. In: El-Khamisy S, editor. Personalised medicine. 1st ed. Cham: Springer; 2017. p. 225–39.

2. Ministério da Saúde. Retrato da saúde [Internet]. Lisbon: Governo de Portugal, Ministério da Saúde; 2018 [cited 2019 Jul 28]. Available from: https://www.sns.gov.pt/retrato-da-saude-2018/

3. Vacanti JP, Otte J-B, Wertheim JA. Regenerative medicine and solid organ transplantation from a historical perspective. In: Orlando G, Lerut J, Soker S, Stratta RJ, editors. Regenerative medicine applications in organ transplantation. 1st ed. Cambridge: Academic Press; 2014. p. 1–15.

4. Taylor DA, Sampaio LC, Ferdous Z, Gobin AS, Taite LJ. Decellularized matrices in regenerative medicine. Acta Biomater. 2018 Jul 1;74:74–89.

5. Mao AS, Mooney DJ. Regenerative medicine: Current therapies and future directions. Proc Natl Acad Sci U S A. 2015 Nov 24;112(47):14452–9.

6. Zhang Q, Raoof M, Chen Y, Sumi Y, Sursal T, Junger W, et al. Circulating mitochondrial DAMPs cause inflammatory responses to injury. Nature. 2010 Mar 4;464(7285):104–7.

7. Khan F, Tanaka M. Designing smart biomaterials for tissue engineering. Int J Mol Sci. 2017 Dec 21;19(1):17.

8. Hynes RO. Extracellular matrix: Not just pretty fibrils. Science (80-). 2009 Nov 27;326(5957):1216–9.

9. Özbek S, Balasubramanian PG, Chiquet-Ehrismann R, Tucker RP, Adams JC. The evolution of extracellular matrix. Mol Biol Cell. 2010 Dec 15;21(24):4300–5.

10. Scarritt M, Murdock M, Badylak SF. Biologic scaffolds composed of extracellular matrix for regenerative medicine. In: Atala A, Lanza R, Mikos AG, Nerem R, editors. Principles of regenerative medicine. 3rd ed. Cambridge: Academic Press; 2019. p. 613–26.

11. Bornstein P, Sage EH. Matricellular proteins: extracellular modulators of cell function. Curr Opin Cell Biol. 2002 Oct 1;14(5):608–16.

12. Vorotnikova E, McIntosh D, Dewilde A, Zhang J, Reing JE, Zhang L, et al. Extracellular matrix-derived products modulate endothelial and progenitor cell migration and proliferation in vitro and stimulate regenerative healing in vivo. Matrix Biol. 2010 Oct;29(8):690–700.

13. Engler AJ, Sen S, Sweeney HL, Discher DE. Matrix elasticity directs stem cell lineage specification. Cell. 2006 Aug 25;126(4):677–89.

14. Smith LR, Cho S, Discher DE. Stem cell differentiation is regulated by extracellular matrix mechanics. Physiology. 2018 Jan 1;33(1):16–25.

15. Nelson CM, Bissell MJ. Of extracellular matrix, scaffolds, and signaling: tissue architecture regulates development, homeostasis, and cancer. Annu Rev Cell Dev Biol. 2006 Nov;22(1):287–309.

16. Mongiat M, Andreuzzi E, Tarticchio G, Paulitti A. Extracellular matrix, a hard player in angiogenesis. Int J Mol Sci. 2016 Nov 1;17(11):1822.

17. Humphrey JD, Dufresne ER, Schwartz MA. Mechanotransduction and extracellular matrix homeostasis. Nat Rev Mol Cell Biol. 2014 Dec 22;15(12):802–12.

18. Lu P, Takai K, Weaver VM, Werb Z. Extracellular matrix degradation and remodeling in development and disease. Cold Spring Harb Perspect Biol. 2011 Dec 1;3(12):a005058.

19. Xu R, Boudreau A, Bissell MJ. Tissue architecture and function: dynamic reciprocity via extra- and intra-cellular matrices. Cancer Metastasis Rev. 2009 Jun 23;28(1–2):167–76.

20. Ringer P, Colo G, Fässler R, Grashoff C. Sensing the mechano-chemical properties of the extracellular matrix. Matrix Biol. 2017 Dec;64:6–16.

21. Sapir L, Tzlil S. Talking over the extracellular matrix: How do cells communicate mechanically? Semin

Cell Dev Biol. 2017 Nov;71:99–105.

22. Song I, Dityatev A. Crosstalk between glia, extracellular matrix and neurons. Brain Res Bull. 2018 Jan;136:101–8.

23. Macarak EJ, Howard PS. Adhesion of endothelial cells to extracellular matrix proteins. J Cell Physiol. 1983 Jul;116(1):76–86.

24. Dejana E, Colella S, Languino LR, Balconi G, Corbascio GC, Marchisio PC. Fibrinogen induces adhesion, spreading, and microfilament organization of human endothelial cells in vitro. J Cell Biol. 1987 May 1;104(5):1403–11.

25. Bolland F, Korossis S, Wilshaw S-P, Ingham E, Fisher J, Kearney JN, et al. Development and characterisation of a full-thickness acellular porcine bladder matrix for tissue engineering. Biomaterials. 2007 Feb;28(6):1061–70.

26. Yang B, Zhang Y, Zhou L, Sun Z, Zheng J, Chen Y, et al. Development of a porcine bladder acellular matrix with well-preserved extracellular bioactive factors for tissue engineering. Tissue Eng Part C Methods. 2010 Oct;16(5):1201–11.

27. Rosario DJ, Reilly GC, Ali Salah E, Glover M, Bullock AJ, MacNeil S. Decellularization and sterilization of porcine urinary bladder matrix for tissue engineering in the lower urinary tract. Regen Med. 2008 Mar;3(2):145–56.

28. Grauss RW, Hazekamp MG, van Vliet S, Gittenberger-de Groot AC, DeRuiter MC. Decellularization of rat aortic valve allografts reduces leaflet destruction and extracellular matrix remodeling. J Thorac Cardiovasc Surg. 2003 Dec;126(6):2003–10.

29. Korossis SA, Booth C, Wilcox HE, Watterson KG, Kearney JN, Fisher J, et al. Tissue engineering of cardiac valve prostheses II: Biomechanical characterization of decellularized porcine aortic heart valves. J Heart Valve Dis. 2002 Jul;11(4):463–71.

30. Kasimir M-T, Rieder E, Seebacher G, Silberhumer G, Wolner E, Weigel G, et al. Comparison of different decellularization procedures of porcine heart valves. Int J Artif Organs. 2003 May 18;26(5):421–7.

31. Petersen TH, Calle EA, Colehour MB, Niklason LE. Matrix composition and mechanics of decellularized lung scaffolds. Cells Tissues Organs. 2012 Feb;195(3):222–31.

32. O'Neill JD, Anfang R, Anandappa A, Costa J, Javidfar J, Wobma HM, et al. Decellularization of human and porcine lung tissues for pulmonary tissue engineering. Ann Thorac Surg. 2013 Sep;96(3):1046–56.

33. Petersen TH, Calle EA, Zhao L, Lee EJ, Gui L, Raredon MB, et al. Tissue-engineered lungs for in vivo implantation. Science (80-). 2010 Jul 30;329(5991):538–41.

34. Ye J-S, Stoltz J-F, Isla N de, Liu Y, Yin Y-F, Zhang L. An approach to preparing decellularized whole liver organ scaffold in rat. Biomed Mater Eng. 2015;25(1):159–66.

35. Wainwright JM, Czajka CA, Patel UB, Freytes DO, Tobita K, Gilbert TW, et al. Preparation of cardiac extracellular matrix from an intact porcine heart. Tissue Eng Part C Methods. 2010 Jun;16(3):525–32.

36. Ott HC, Matthiesen TS, Goh S, Black LD, Kren SM, Netoff TI, et al. Perfusion-decellularized matrix: using nature's platform to engineer a bioartificial heart. Nat Med. 2008 Feb 13;14(2):213–21.

37. Badylak SF, Tullius R, Kokini K, Shelbourne KD, Klootwyk T, Voytik SL, et al. The use of xenogeneic small intestinal submucosa as a biomaterial for Achille's tendon repair in a dog model. J Biomed Mater Res. 1995 Aug;29(8):977–85.

38. Guler S, Aslan B, Hosseinian P, Aydin HM. Supercritical carbon dioxide-assisted decellularization of aorta and cornea. Tissue Eng Part C Methods. 2017 Sep;23(9):540–7.

39. Kajbafzadeh A-M, Khorramirouz R, Nabavizadeh B, Ladi Seyedian S-S, Akbarzadeh A, Heidari R, et al. Whole organ sheep kidney tissue engineering and in vivo transplantation: Effects of perfusion-based decellularization on vascular integrity. Mater Sci Eng C. 2019 May;98:392–400.

40. Grand View Research. Extracellular matrix (ECM) patches market analysis report by raw material (bovine, porcine), by application (soft tissue repair, vascular repair & reconstruction), by region, and segment

forecasts, 2018 - 2025 [Internet]. Grand View Research; 2018 [cited 2019 Aug 5]. Report No.: GVR-2-68038-422-2. Available from: https://www.grandviewresearch.com/industry-analysis/extracellular-matrix-ecm-patches-market

41. Porzionato A, Stocco E, Barbon S, Grandi F, Macchi V, De Caro R. Tissue-engineered grafts from human decellularized extracellular matrices: A systematic review and future perspectives. Int J Mol Sci. 2018 Dec 18;19(12):4117.

42. The Insight Partners. Extracellular matrix market to 2027 - Global analysis and forecasts by application (vascular repair and reconstruction, dural repair, wound healing, cardiac repair, pericardial repair, soft tissue repair) [Internet]. The Insight Partners; 2019 [cited 2019 Aug 5]. Report No.: TIPRE00004925. Available from: https://www.theinsightpartners.com/reports/extracellular-matrix-market/

43. Grand View Research. Orthobiologics market analysis by product (DBM, allograft, BMP, viscosupplementation, synthetic bone substitutes, stem cell), by application (spinal fusion, reconstructive surgery, trauma repair), by end use, and segment forecasts, 2018 - 2025 [Internet]. Grand View Research; 2017 [cited 2019 Aug 5]. Report No.: GVR-1-68038-360-7. Available from: https://www.grandviewresearch.com/industry-analysis/orthobiological-products-market

44. Dong X, Wei X, Yi W, Gu C, Kang X, Liu Y, et al. RGD-modified acellular bovine pericardium as a bioprosthetic scaffold for tissue engineering. J Mater Sci Mater Med. 2009 Nov 9;20(11):2327–36.

45. Syed O, Walters NJ, Day RM, Kim H, Knowles JC. Evaluation of decellularization protocols for production of tubular small intestine submucosa scaffolds for use in oesophageal tissue engineering. Acta Biomater. 2014 Dec;10(12):5043–54.

46. Crapo PM, Gilbert TW, Badylak SF. An overview of tissue and whole organ decellularization processes. Biomaterials. 2011 Apr;32(12):3233–43.

47. Deeken CR, White AK, Bachman SL, Ramshaw BJ, Cleveland DS, Loy TS, et al. Method of preparing a decellularized porcine tendon using tributyl phosphate. J Biomed Mater Res Part B Appl Biomater. 2011 Feb;96B(2):199–206.

48. Bernstein H, Bernstein C, Payne CM, Dvorakova K, Garewal H. Bile acids as carcinogens in human gastrointestinal cancers. Mutat Res. 2005 Jan;589(1):47–65.

49. Meezan E, Hjelle JT, Brendel K, Carlson EC. A simple, versatile, nondisruptive method for the isolation of morphologically and chemically pure basement membranes from several tissues. Life Sci. 1975 Dec;17(11):1721–32.

50. Ozeki M, Narita Y, Kagami H, Ohmiya N, Itoh A, Hirooka Y, et al. Evaluation of decellularized esophagus as a scaffold for cultured esophageal epithelial cells. J Biomed Mater Res Part A. 2006 Jul 26;79A(4):771–8.

51. Bloch O, Erdbrügger W, Völker W, Schenk A, Posner S, Konertz W, et al. Extracellular matrix in deoxycholic acid decellularized aortic heart valves. Med Sci Monit. 2012;18(12):BR487–92.

52. Xu CC, Chan RW, Tirunagari N. A biodegradable, acellular xenogeneic scaffold for regeneration of the vocal fold lamina propria. Tissue Eng. 2007 Mar;13(3):551–66.

53. Ishida Y, Sakakibara S, Terashi H, Hashikawa K, Yamaoka T. Development of a novel method for decellularizing a nerve graft using a hypertonic sodium chloride solution. Int J Artif Organs. 2014 Nov 26;37(11):854–60.

54. Genovese L, Zawada L, Tosoni A, Ferri A, Zerbi P, Allevi R, et al. Cellular localization, invasion, and turnover are differently influenced by healthy and tumor-derived extracellular matrix. Tissue Eng Part A. 2014 Jul;20(13–14):2005–18.

55. Ross EA, Williams MJ, Hamazaki T, Terada N, Clapp WL, Adin C, et al. Embryonic stem cells proliferate and differentiate when seeded into kidney scaffolds. J Am Soc Nephrol. 2009 Nov;20(11):2338–47.

56. Cox B, Emili A. Tissue subcellular fractionation and protein extraction for use in mass-spectrometry-based proteomics. Nat Protoc. 2006 Nov 22;1(4):1872–8.

57. Merritt EK, Hammers DW, Tierney M, Suggs LJ, Walters TJ, Farrar RP. Functional assessment of skeletal muscle regeneration utilizing homologous extracellular matrix as scaffolding. Tissue Eng Part A. 2010

Apr;16(4):1395–405.

58. Yang M, Chen C-Z, Wang X-N, Zhu Y-B, Gu YJ. Favorable effects of the detergent and enzyme extraction method for preparing decellularized bovine pericardium scaffold for tissue engineered heart valves. J Biomed Mater Res Part B Appl Biomater. 2009 Oct;91B(1):354–61.

59. Meyer SR, Chiu B, Churchill TA, Zhu L, Lakey JRT, Ross DB. Comparison of aortic valve allograft decellularization techniques in the rat. J Biomed Mater Res Part A. 2006 Nov;79A(2):254–62.

60. Zhou J, Fritze O, Schleicher M, Wendel H-P, Schenke-Layland K, Harasztosi C, et al. Impact of heart valve decellularization on 3-D ultrastructure, immunogenicity and thrombogenicity. Biomaterials. 2010 Mar;31(9):2549–54.

61. Dahl SLM, Koh J, Prabhakar V, Niklason LE. Decellularized native and engineered arterial scaffolds for transplantation. Cell Transplant. 2003;12(919):659–66.

62. Korossis S, Berry HE, Watterson KG, Fisher J. Tissue engineering of cardiac valve protheses I: Development and histological characterization of an acellular porcine scaffold. J Heart Valve Dis. 2002 Jul;11(4):457–62.

63. Seddon AM, Curnow P, Booth PJ. Membrane proteins, lipids and detergents: Not just a soap opera. Biochim Biophys Acta - Biomembr. 2004 Nov 3;1666(1–2):105–17.

64. Cortijo J, Dixon JS, Foster RW, Small RC. Influence of some variables in the Triton X-100 method of skinning the plasmalemmal membrane from guinea pig trachealis muscle. J Pharmacol Methods. 1987 Nov;18(3):253–66.

65. Shupe T, Williams M, Brown A, Willenberg B, Petersen BE. Method for the decellularization of intact rat liver. Organogenesis. 2010;6(2):134–6.

66. Cartmell JS, Dunn MG. Effect of chemical treatments on tendon cellularity and mechanical properties. J Biomed Mater Res. 2000 Jan;49(1):134–40.

67. Sullivan DC, Mirmalek-Sani S-H, Deegan DB, Baptista PM, Aboushwareb T, Atala A, et al. Decellularization methods of porcine kidneys for whole organ engineering using a high-throughput system. Biomaterials. 2012 Nov;33(31):7756–64.

68. Uygun BE, Soto-Gutierrez A, Yagi H, Izamis M-L, Guzzardi MA, Shulman C, et al. Organ reengineering through development of a transplantable recellularized liver graft using decellularized liver matrix. Nat Med. 2010 Jul 13;16(7):814–20.

69. Roosens A, Somers P, De Somer F, Carriel V, Van Nooten G, Cornelissen R. Impact of detergent-based decellularization methods on porcine tissues for heart valve engineering. Ann Biomed Eng. 2016 Sep 2;44(9):2827–39.

70. Nakayama KH, Batchelder CA, Lee CI, Tarantal AF. Decellularized rhesus monkey kidney as a three-dimensional scaffold for renal tissue engineering. Tissue Eng Part A. 2010 Jul;16(7):2207–16.

71. Rieder E, Kasimir M-T, Silberhumer G, Seebacher G, Wolner E, Simon P, et al. Decellularization protocols of porcine heart valves differ importantly in efficiency of cell removal and susceptibility of the matrix to recellularization with human vascular cells. J Thorac Cardiovasc Surg. 2004 Feb;127(2):399–405.

72. Woods T, Gratzer PF. Effectiveness of three extraction techniques in the development of a decellularized bone–anterior cruciate ligament–bone graft. Biomaterials. 2005 Dec;26(35):7339–49.

73. Bodnar EG, Olsen E, Florio R, Dobrin J. Damage of porcine aortic valve tissue caused by the surfactant sodiumdodecylsulphate. Thorac Cardiovasc Surg. 1986 Apr 29;34(02):82–5.

74. Courtman DW, Pereira CA, Kashef V, McComb D, Lee JM, Wilson GJ. Development of a pericardial acellular matrix biomaterial: Biochemical and mechanical effects of cell extraction. J Biomed Mater Res. 1994 Jun;28(6):655–66.

75. Gilpin SE, Guyette JP, Gonzalez G, Ren X, Asara JM, Mathisen DJ, et al. Perfusion decellularization of human and porcine lungs: Bringing the matrix to clinical scale. J Hear Lung Transplant. 2014 Mar;33(3):298–308.

76. Du L, Wu X, Pang K, Yang Y. Histological evaluation and biomechanical characterisation of an acellular porcine cornea scaffold. Br J Ophthalmol. 2011 Mar 1;95(3):410–4.

77. Gui L, Chan SA, Breuer CK, Niklason LE. Novel utilization of serum in tissue decellularization. Tissue Eng Part C Methods. 2010 Apr;16(2):173–84.

78. Ingram LO. Mechanism of lysis of escherichia coli by ethanol and other chaotropic agentst. J Bacteriol. 1981;146(1):331–6.

79. Prasertsung I, Kanokpanont S, Bunaprasert T, Thanakit V, Damrongsakkul S. Development of acellular dermis from porcine skin using periodic pressurized technique. J Biomed Mater Res Part B Appl Biomater. 2008 Apr;85B(1):210–9.

80. Vyavahare N, Hirsch D, Lerner E, Baskin JZ, Schoen FJ, Bianco R, et al. Prevention of bioprosthetic heart valve calcification by ethanol preincubation. Circulation. 1997 Jan 21;95(2):479–88.

81. Sawada K, Terada D, Yamaoka T, Kitamura S, Fujisato T. Cell removal with supercritical carbon dioxide for acellular artificial tissue. J Chem Technol Biotechnol. 2008 Jun;83(6):943–9.

82. Flynn LE. The use of decellularized adipose tissue to provide an inductive microenvironment for the adipogenic differentiation of human adipose-derived stem cells. Biomaterials. 2010 Jun;31(17):4715–24.

83. Brown BN, Freund JM, Han L, Rubin JP, Reing JE, Jeffries EM, et al. Comparison of three methods for the derivation of a biologic scaffold composed of adipose tissue extracellular matrix. Tissue Eng Part C Methods. 2011 Apr;17(4):411–21.

84. Jorge-Herrero E, Fernández P, Gutiérrez M, Castillo-Olivares JL. Study of the calcification of bovine pericardium: analysis of the implication of lipids and proteoglycans. Biomaterials. 1991 Sep;12(7):683–9.

85. Gratzer PF, Harrison RD, Woods T. Matrix alteration and not residual sodium dodecyl sulfate cytotoxicity affects the cellular repopulation of a decellularized matrix. Tissue Eng. 2006 Oct;12(10):2975–83.

86. Lumpkins SB, Pierre N, McFetridge PS. A mechanical evaluation of three decellularization methods in the design of a xenogeneic scaffold for tissue engineering the temporomandibular joint disc. Acta Biomater. 2008 Jul;4(4):808–16.

87. Casali DM, Handleton RM, Shazly T, Matthews MA. A novel supercritical CO2-based decellularization method for maintaining scaffold hydration and mechanical properties. J Supercrit Fluids. 2018 Jan;131:72–81.

88. Jamur MC, Oliver C. Cell fixatives for immunostaining. In: Oliver C, Jamur MC, editors. Immunocytochemical methods and protocols. 3rd ed. New York: Humana Press; 2010. p. 55–61.

89. Piet MP, Chin S, Prince AM, Brotman B, Cundell AM, Horowitz B. The use of tri(n-butyl)phosphate detergent mixtures to inactivate hepatitis viruses and human immunodeficiency virus in plasma and plasma's subsequent fractionation. Transfusion. 1990 Sep;30(7):591–8.

90. Horowitz B, Bonomo R, Prince AM, Chin SN, Brotman B, Shulman RW. Solvent/detergent-treated plasma: a virus-inactivated substitute for fresh frozen plasma. Blood. 1992 Feb 1;79(3):826–31.

91. Bottagisio M, Pellegata AF, Boschetti F, Ferroni M, Moretti M, Lovati AB. A new strategy for the decellularisation of large equine tendons as biocompatible tendon substitutes. Eur Cells Mater. 2016 Jul 8;32:58–73.

92. Pridgen BC, Woon CYL, Kim M, Thorfinn J, Lindsey D, Pham H, et al. Flexor tendon tissue engineering: Acellularization of human flexor tendons with preservation of biomechanical properties and biocompatibility. Tissue Eng Part C Methods. 2011 Aug;17(8):819–28.

93. Elder BD, Kim DH, Athanasiou KA. Developing an articular cartilage decellularization process toward facet joint cartilage replacement. Neurosurgery. 2010 Apr;66(4):722–7.

94. Schenke-Layland K, Vasilevski O, Opitz F, König K, Riemann I, Halbhuber KJ, et al. Impact of decellularization of xenogeneic tissue on extracellular matrix integrity for tissue engineering of heart valves. J Struct Biol. 2003 Sep;143(3):201–8.

95. Bader A, Steinhoff G, Strobl K, Schilling T, Brandes G, Mertsching H, et al. Engineering of human

vascular aortic tissue based on a xenogeneic starter matrix. Transplantation. 2000 Jul 15;70(1):7–14.

96. Lee K-I, Lee J-S, Kim J-G, Kang K-T, Jang J-W, Shim Y-B, et al. Mechanical properties of decellularized tendon cultured by cyclic straining bioreactor. J Biomed Mater Res Part A. 2013 Nov;101(11):3152–3158.

97. Ozasa Y, Amadio PC, Thoreson AR, An K-N, Zhao C. Repopulation of intrasynovial flexor tendon allograft with bone marrow stromal cells: An ex vivo model. Tissue Eng Part A. 2014 Feb;20(3–4):566–74.

98. Whitlock PW, Smith TL, Poehling GG, Shilt JS, Van Dyke M. A naturally derived, cytocompatible, and architecturally optimized scaffold for tendon and ligament regeneration. Biomaterials. 2007 Oct;28(29):4321–9.

99. Spurr SJ, Gipson IK. Isolation of corneal epithelium with Dispase II or EDTA. Effects on the basement membrane zone. Investig Ophthalmol Vis Sci. 1985 Jun;26(6):818–27.

100. Hopkinson A, Shanmuganathan VA, Gray T, Yeung AM, Lowe J, James DK, et al. Optimization of amniotic membrane (AM) denuding for tissue engineering. Tissue Eng Part C Methods. 2008 Dec;14(4):371–81.

101. Ning L-J, Jiang Y-L, Zhang C-H, Zhang Y, Yang J-L, Cui J, et al. Fabrication and characterization of a decellularized bovine tendon sheet for tendon reconstruction. J Biomed Mater Res Part A. 2017 Aug;105(8):2299–311.

102. Abedin E, Lari R, Shahri NM, Fereidoni M. Development of a demineralized and decellularized human epiphyseal bone scaffold for tissue engineering: A histological study. Tissue Cell. 2018 Dec;55:46–52.

103. Gardin C, Ricci S, Ferroni L, Guazzo R, Sbricoli L, De Benedictis G, et al. Decellularization and delipidation protocols of bovine bone and pericardium for bone grafting and guided bone regeneration procedures. Liu X, editor. PLoS One. 2015 Jul 20;10(7):e0132344.

104. Xing Q, Yates K, Tahtinen M, Shearier E, Qian Z, Zhao F. Decellularization of fibroblast cell sheets for natural extracellular matrix scaffold preparation. Tissue Eng Part C Methods. 2015 Jan;21(1):77–87.

105. Ngangan A V., McDevitt TC. Acellularization of embryoid bodies via physical disruption methods. Biomaterials. 2009 Feb;30(6):1143–9.

106. Ning L-J, Zhang Y, Chen X-H, Luo J-C, Li X-Q, Yang Z-M, et al. Preparation and characterization of decellularized tendon slices for tendon tissue engineering. J Biomed Mater Res Part A. 2012 Jun;100A(6):1448–56.

107. Jackson DW, Grood ES, Wilcox P, Butler DL, Simon TM, Holden JP. The effects of processing techniques on the mechanical properties of bone-anterior cruciate ligament-bone allografts. Am J Sports Med. 1988 Mar 23;16(2):101–5.

108. Brown BN, Barnes CA, Kasick RT, Michel R, Gilbert TW, Beer-Stolz D, et al. Surface characterization of extracellular matrix scaffolds. Biomaterials. 2010 Jan;31(3):428–37.

109. Sellaro TL, Ranade A, Faulk DM, McCabe GP, Dorko K, Badylak SF, et al. Maintenance of human hepatocyte function in vitro by liver-derived extracellular matrix gels. Tissue Eng Part A. 2010 Mar;16(3):1075–82.

110. Freytes DO, Stoner RM, Badylak SF. Uniaxial and biaxial properties of terminally sterilized porcine urinary bladder matrix scaffolds. J Biomed Mater Res Part B Appl Biomater. 2008 Feb;84B(2):408–14.

111. Fujisato T, Minatoya K, Yamazaki S, Meng Y, Niwaya K, Kishida A, et al. Preparation and recellularization of tissue engineered bioscaffold for heart valve replacement. In: Mori H, Matsuda H, editors. Cardiovascular regeneration therapies using tissue engineering approaches. 1st ed. Tokyo: Springer; 2005. p. 83–94.

112. Funamoto S, Nam K, Kimura T, Murakoshi A, Hashimoto Y, Niwaya K, et al. The use of high-hydrostatic pressure treatment to decellularize blood vessels. Biomaterials. 2010 May;31(13):3590–5.

113. Hashimoto Y, Funamoto S, Sasaki S, Honda T, Hattori S, Nam K, et al. Preparation and characterization of decellularized cornea using high-hydrostatic pressurization for corneal tissue engineering. Biomaterials. 2010 May;31(14):3941–8.

114. Moerman F. High hydrostatic pressure inactivation of vegetative microorganisms, aerobic and anaerobic spores in pork Marengo, a low acidic particulate food product. Meat Sci. 2005 Feb;69(2):225–32.

115. Eckert CA, Knutson BL, Debenedetti PG. Supercritical fluids as solvents for chemical and materials processing. Nature. 1996 Sep;383(6598):313–8.

116. Antons J, Marascio MGM, Aeberhard P, Weissenberger G, Hirt-Burri N, Applegate L, et al. Decellularised tissues obtained by a CO2-philic detergent and supercritical CO2. Eur Cells Mater. 2018 Sep 4;36:81–95.

117. Halfwerk FR, Rouwkema J, Gossen JA, Grandjean JG. Supercritical carbon dioxide decellularised pericardium: Mechanical and structural characterisation for applications in cardio-thoracic surgery. J Mech Behav Biomed Mater. 2018 Jan;77:400–7.

118. Enomoto A, Nakamura K, Nagai K, Hashimoto T, Hakoda M. Inactivation of food microorganisms by high-pressure carbon dioxide treatment with or without explosive decompression. Biosci Biotechnol Biochem. 1997 Jan 12;61(7):1133–7.

119. Soares GC, Learmonth DA, Vallejo MC, Davila SP, González P, Sousa RA, et al. Supercritical CO2 technology: The next standard sterilization technique? Mater Sci Eng C. 2019 Jun;99:520–40.

120. Gratzer PF. Decellularized extracellular matrix. In: Narayan R, editor. Encyclopedia of biomedical engineering. 1st ed. Amsterdam: Elsevier; 2019. p. 86–96.

121. Gilbert TW, Sellaro TL, Badylak SF. Decellularization of tissues and organs. Biomaterials. 2006 Mar 7;27(19):3675–83.

122. Bracey D, Seyler T, Jinnah A, Lively M, Willey J, Smith T, et al. A decellularized porcine xenograft-derived bone scaffold for clinical use as a bone graft substitute: A critical evaluation of processing and structure. J Funct Biomater. 2018 Jul 12;9(3):45.

123. Aamodt JM, Grainger DW. Extracellular matrix-based biomaterial scaffolds and the host response. Biomaterials. 2016 Apr;86:68–82.

124. Simon CG, Yaszemski MJ, Ratcliffe A, Tomlins P, Luginbuehl R, Tesk JA. ASTM international workshop on standards and measurements for tissue engineering scaffolds. J Biomed Mater Res Part B Appl Biomater. 2015 Jul;103(5):949–59.

125. Nagata S, Hanayama R, Kawane K. Autoimmunity and the clearance of dead cells. Cell. 2010 Mar;140(5):619–30.

126. Vadori M, Cozzi E. The immunological barriers to xenotransplantation. Tissue Antigens. 2015 Oct;86(4):239–53.

127. Wong ML, Griffiths LG. Immunogenicity in xenogeneic scaffold generation: Antigen removal vs. decellularization. Acta Biomater. 2014 May;10(5):1806–16.

128. Sandor M, Xu H, Connor J, Lombardi J, Harper JR, Silverman RP, et al. Host response to implanted porcine-derived biologic materials in a primate model of abdominal wall repair. Tissue Eng Part A. 2008 Dec;14(12):2021–31.

129. Gilbert TW, Freund JM, Badylak SF. Quantification of DNA in biologic scaffold materials. J Surg Res. 2009 Mar;152(1):135–9.

130. Brown BN, Valentin JE, Stewart-Akers AM, McCabe GP, Badylak SF. Macrophage phenotype and remodeling outcomes in response to biologic scaffolds with and without a cellular component. Biomaterials. 2009 Mar;30(8):1482–91.

131. Ellingsworth LR, DeLustro F, Brennan JE, Sawamura S, McPherson J. The human immune response to reconstituted bovine collagen. J Immunol. 1986 Feb 1;136(3):877–82.

132. Griffiths LG, Choe LH, Reardon KF, Dow SW, Christopher Orton E. Immunoproteomic identification of bovine pericardium xenoantigens. Biomaterials. 2008 Sep;29(26):3514–20.

133. Simon P, Kasimir MT, Seebacher G, Weigel G, Ullrich R, Salzer-Muhar U, et al. Early failure of the tissue engineered porcine heart valve SYNERGRAFT™ in pediatric patients. Eur J Cardio-Thoracic Surg. 2003 Jun;23(6):1002–6.

134. Gilpin A, Yang Y. Decellularization strategies for regenerative medicine: From processing techniques to applications. Biomed Res Int. 2017;2017:1–13.

135. Kawecki M, Łabuś W, Klama-Baryla A, Kitala D, Kraut M, Glik J, et al. A review of decellurization methods caused by an urgent need for quality control of cell-free extracellular matrix' scaffolds and their role in regenerative medicine. J Biomed Mater Res Part B Appl Biomater. 2018 Feb;106(2):909–23.

136. European Commission. Comission Directive 2003/94/EC laying down the principles and guidelines of good manufacturing practice in respect of medicinal products for human use and investigational medicinal products for human use. Brussels: European Commission; 2003.

137. Council of the European Union. Council Directive 93/42/EEC concerning medical devices. Brussels: Council of the European Union; 1993.

138. European Parliament, Council of the European Union. Directive 2004/23/Ec on setting standards of quality and safety for the donation, procurement, testing, processing, preservation, storage and distribution of human tissues and cells. Strasbourg: European Parliament and Council; 2004.

139. Grosskinsky U. Biomaterial regulations for tissue engineering. Desalination. 2006 Nov;199(1–3):265–7.

140. Scarrit ME. A review of cellularization strategies for tissue engineering of whole organs. Front Bioeng Biotechnol. 2015 Mar;3:1–17.

141. ASTM F2150-02e1, Standard Guide for Characterization and Testing of Biomaterial Scaffolds Used in Tissue-Engineered Medical Products [Internet]. ASTM International; 2002 [cited 2019 Aug 6]. Available from: http://www.astm.org/cgi-bin/resolver.cgi?F2150-02e1

142. ISO 9001:2000: Quality management systems - Requirements [Internet]. International Organization for Standardization; 2000 [cited 2019 Aug 6]. Available from: https://www.iso.org/standard/21823.html

143. ISO 13485:2003: Medical devices - Quality management systems - Requirements for regulatory purposes [Internet]. International Organization for Standardization; 2003 [cited 2019 Aug 6]. Available from: https://www.iso.org/standard/36786.html

144. ISO 10993-5:2009: Biological evaluation of medical devices - Part 5: Tests for in vitro cytotoxicity [Internet]. International Organization for Standardization; 2009 [cited 2019 Aug 6]. Available from: https://www.iso.org/standard/36406.html

145. Clarke B. Normal bone anatomy and physiology. Clin J Am Soc Nephrol. 2008 Nov;3(Supplement 3):S131–9.

146. Boskey AL. Bone composition: relationship to bone fragility and antiosteoporotic drug effects. Bonekey Rep. 2013 Dec 4;2.

147. Boyde A. Scanning electron microscopy of bone. In: Idris AI, editor. Bone Research Protocols. 3rd ed. New York: Humana Press; 2019. p. 571–616.

148. Cheng CW, Solorio LD, Alsberg E. Decellularized tissue and cell-derived extracellular matrices as scaffolds for orthopaedic tissue engineering. Biotechnol Adv. 2014 Mar;32(2):462–84.

149. Finkemeier CG. Bone-grafting and bone-graft substitutes. J Bone Jt Surgery-American Vol. 2002 Mar;84(3):454–64.

150. Younger EM, Chapman MW. Morbidity at bone graft donor sites. J Orthop Trauma. 1989;3(3):192–5.

151. Thavornyutikarn B, Chantarapanich N, Sitthiseripratip K, Thouas GA, Chen Q. Bone tissue engineering scaffolding: computer-aided scaffolding techniques. Prog Biomater. 2014 Dec 17;3(2–4):61–102.

152. Drosos GI, Kazakos KI, Kouzoumpasis P, Verettas D-A. Safety and efficacy of commercially available demineralised bone matrix preparations: A critical review of clinical studies. Injury. 2007 Sep;38(Supplement 4):S13–21.

153. Gruskin E, Doll BA, Futrell FW, Schmitz JP, Hollinger JO. Demineralized bone matrix in bone repair: History and use. Adv Drug Deliv Rev. 2012 Sep;64(12):1063–77.

154. Hashimoto Y, Funamoto S, Kimura T, Nam K, Fujisato T, Kishida A. The effect of decellularized

bone/bone marrow produced by high-hydrostatic pressurization on the osteogenic differentiation of mesenchymal stem cells. Biomaterials. 2011 Oct;32(29):7060–7.

155. Sawkins MJ, Bowen W, Dhadda P, Markides H, Sidney LE, Taylor AJ, et al. Hydrogels derived from demineralized and decellularized bone extracellular matrix. Acta Biomater. 2013 Aug;9(8):7865–73.

156. Smith CA, Richardson SM, Eagle MJ, Rooney P, Board T, Hoyland JA. The use of a novel bone allograft wash process to generate a biocompatible, mechanically stable and osteoinductive biological scaffold for use in bone tissue engineering. Reilly G, editor. J Tissue Eng Regen Med. 2015 May 15;9(5):595–604.

157. Lee DJ, Diachina S, Lee YT, Zhao L, Zou R, Tang N, et al. Decellularized bone matrix grafts for calvaria regeneration. J Tissue Eng. 2016 Jan 5;7:204173141668030.

158. Karalashvili L, Chichua N, Menabde G, Atskvereli L, Grdzelidze T, Machavariani A, et al. Decellularized bovine bone graft for zygomatic bone reconstruction. Med Case Reports. 2018;4(1):1–5.

159. You L, Weikang X, Lifeng Y, Changyan L, Yongliang L, Xiaohui W, et al. In vivo immunogenicity of bovine bone removed by a novel decellularization protocol based on supercritical carbon dioxide. Artif Cells, Nanomedicine, Biotechnol. 2018 Nov 5;46(sup2):334–44.

160. Sladkova M, Cheng J, Palmer M, Chen S, Lin C, Xia W, et al. Comparison of decellularized cow and human bone for engineering bone grafts with human induced pluripotent stem cells. Tissue Eng Part A. 2019 Feb;25(3–4):288–301.

161. Chen K, Lin X, Zhang Q, Ni J, Li J, Xiao J, et al. Decellularized periosteum as a potential biologic scaffold for bone tissue engineering. Acta Biomater [Internet]. 2015;19(February):46–55. Available from: http://dx.doi.org/10.1016/j.actbio.2015.02.020

162. Guobao C, Yonggang L. Decellularized Bone Matrix Scaffold for Bone Regeneration. Decellularized Scaffolds Organog. 2017;1577:239–54.

163. Suto K, Urabe K, Naruse K, Uchida K, Matsuura T, Mikuni-Takagaki Y, et al. Repeated freeze–thaw cycles reduce the survival rate of osteocytes in bone-tendon constructs without affecting the mechanical properties of tendons. Cell Tissue Bank. 2012 Mar 30;13(1):71–80.

164. Polo-Corrales L, Latorre-Esteves M, Ramirez-Vick JE. Scaffold design for bone regeneration. J Nanosci Nanotechnol. 2014 Jan 1;14(1):15–56.

165. Marcos-Campos I, Marolt D, Petridis P, Bhumiratana S, Schmidt D, Vunjak-Novakovic G. Bone scaffold architecture modulates the development of mineralized bone matrix by human embryonic stem cells. Biomaterials. 2012 Nov;33(33):8329–42.

166. Oftadeh R, Perez-Viloria M, Villa-Camacho JC, Vaziri A, Nazarian A. Biomechanics and mechanobiology of trabecular bone: A review. J Biomech Eng. 2015 Jan 1;137(1).

167. Amini AR, Adams DJ, Laurencin CT, Nukavarapu SP. Optimally porous and biomechanically compatible scaffolds for large-area bone regeneration. Tissue Eng Part A. 2012 Jul;18(13–14):1376–88.

168. Karageorgiou V, Kaplan D. Porosity of 3D biomaterial scaffolds and osteogenesis. Biomaterials. 2005 Sep;26(27):5474–91.

169. Liu G, Sun J, Li Y, Zhou H, Cui L, Liu W, et al. Evaluation of partially demineralized osteoporotic cancellous bone matrix combined with human bone marrow stromal cells for tissue engineering: An in vitro and in vivo study. Calcif Tissue Int. 2008 Sep 15;83(3):176–85.

170. Keaveny TM, Morgan EF, Niebur GL, Yeh OC. Biomechanics of trabecular bone. Annu Rev Biomed Eng. 2001 Aug;3(1):307–33.

171. Lin ASP, Barrows TH, Cartmell SH, Guldberg RE. Microarchitectural and mechanical characterization of oriented porous polymer scaffolds. Biomaterials. 2003 Feb;24(3):481–9.

172. Kim S-H, Shin J-W, Park S-A, Kim YK, Park MS, Mok JM, et al. Chemical, structural properties, and osteoconductive effectiveness of bone block derived from porcine cancellous bone. J Biomed Mater Res. 2004 Jan 15;68B(1):69–74.

173. Linde F, Hvid I, Madsen F. The effect of specimen geometry on the mechanical behaviour of trabecular

bone specimens. J Biomech. 1992 Apr;25(4):359–68.

174. Keaveny TM, Borchers RE, Gibson LJ, Hayes WC. Trabecular bone modulus and strength can depend on specimen geometry. J Biomech. 1993 Aug;26(8):991–1000.

175. Zioupos P. Ageing Human Bone: Factors Affecting its Biomechanical Properties and the Role of Collagen. J Biomater Appl. 2001 Jan 27;15(3):187–229.

176. Xing S, Liu C, Xu B, Chen J, Yin D, Zhang C. Effects of various decellularization methods on histological and biomechanical properties of rabbit tendons. Exp Ther Med. 2014 Aug;8(2):628–34.

177. Garnero P. The contribution of collagen crosslinks to bone strength. Bonekey Rep. 2012 Sep 19;1:182.

178. Depalle B, Qin Z, Shefelbine SJ, Buehler MJ. Influence of cross-link structure, density and mechanical properties in the mesoscale deformation mechanisms of collagen fibrils. J Mech Behav Biomed Mater. 2015 Dec;52:1–13.

179. ACell Vet [Internet]. [cited 2019 Jun 17]. Available from: https://acell.com/vet/

180. AlloMax™ Surgical Graft [Internet]. [cited 2019 Jun 17]. Available from: https://www.crbard.com/davol/en-US/products/AlloMax-Surgical-Graft

181. AlloMend - AlloSource [Internet]. [cited 2019 Jun 21]. Available from: https://www.allosource.org/products/allomend/

182. Allopatch HD® [Internet]. [cited 2019 Jun 17]. Available from: https://www.conmed.com/en/products/orthopedics/mtf-allografts-and-biologics/biologic-scaffolds/allopatch-hd-acellular-human-dermis

183. AlloSkin™ AC Acellular Dermal Matrix - AlloSource [Internet]. [cited 2019 Jun 21]. Available from: https://www.allosource.org/products/alloskin-ac-acellular-dermal-matrix/

184. Architect® | Harbor MedTech [Internet]. [cited 2019 Jun 21]. Available from: http://www.harbormedtech.com/architect/

185. Arthrex - ArthroFLEX® Decellularized Dermal Allograft [Internet]. [cited 2019 Jun 17]. Available from: https://www.arthrex.com/orthobiologics/arthroflex

186. Avance® Nerve Graft | Axogen [Internet]. [cited 2019 Jun 21]. Available from: https://www.axogeninc.com/avance-nerve-graft/

187. Axis™ Dermis [Internet]. [cited 2019 Jun 17]. Available from: https://www.coloplastmd.com/products/allograft/

188. Axoguard® Nerve Protector [Internet]. Available from: https://www.axogeninc.com/axoguard-nerve-protector/

189. Biodesign® Duraplasty Graft [Internet]. [cited 2019 Jun 17]. Available from: https://www.cookmedical.com/products/3165f1ce-66d0-4a7a-bf36-1584698e7174/

190. BIOVANCE® Human Amniotic Membrane Allograft [Internet]. [cited 2019 Jun 21]. Available from: https://www.woundsource.com/product/biovance-human-amniotic-membrane-allograft

191. CardioGRAFT® Aortic Heart Valve [Internet]. [cited 2019 Jun 17]. Available from: https://www.lifenethealth.org/cardiac

192. Chondrofix® Osteochondral Allograft [Internet]. [cited 2019 Jun 21]. Available from: https://www.zimmerbiomet.com/medical-professionals/biologics/product/chondrofix.html

193. Cor™ PATCH – Cor Matrix [Internet]. [cited 2019 Jun 17]. Available from: http://www.cormatrix.com/corpatch

194. Cortiva®, Cortiva® 1mm and Cortiva®1mm Tailored Allograft Dermis - Products - RTI Surgical Holdings, Inc. [Internet]. [cited 2019 Jun 21]. Available from: http://www.rtix.com/en_us/products/product-implant/cortiva-cortiva-1mm-and-cortiva1mm-tailored-allograft-dermis

195. CryoPatch SG - CryoLife, Inc. [Internet]. [cited 2019 Jun 21]. Available from: https://www.cryolife.com/products/cardiac-allografts/cryopatch-sg/

196. CryoValve SG Pulmonary Human Heart Valve [Internet]. [cited 2019 Jun 17]. Available from: https://www.cryolife.com/products/cardiac-allografts/cryovalve-sg-pulmonary-human-heart-valve/

197. DermACELL® | Stryker [Internet]. [cited 2019 Jun 17]. Available from: https://www.stryker.com/us/en/endoscopy/products/dermacell.html

198. Dermacell AWM Wound Management; Surgical Reconstruction (WMSR) | LifeNet Health [Internet]. [cited 2019 Jun 21]. Available from: https://www.lifenethealth.org/skin-and-wound-allograft-institute

199. DermaMatrix™ Acellular Dermis [Internet]. [cited 2019 Jun 17]. Available from: https://www.aegisdentalnetwork.com/id/products/synthes-cmf-dentoalveolar-surgery/dermamatrix-acellular-dermis

200. Soft Tissue Management | DermaSpan™ Acellular Dermal Matrix | Zimmer Biomet [Internet]. [cited 2019 Jun 21]. Available from: https://www.zimmerbiomet.com/medical-professionals/biologics/product/dermaspan-acellular-dermal-matrix.html

201. Dermavest® — AediCell [Internet]. [cited 2019 Jun 21]. Available from: https://www.aedicell.com/products

202. DURA-GUARD [Internet]. [cited 2019 Jun 17]. Available from: https://ecatalog.baxter.com/ecatalog/loadproduct.html?cid=20016&lid=10001&hid=20001&pid=821640

203. DuraMatrix Suturable [Internet]. [cited 2019 Jun 17]. Available from: https://cmf.stryker.com/products/duramatrix-suturable

204. Durepair Dura Regeneration Matrix [Internet]. [cited 2019 Jun 17]. Available from: https://www.medtronic.com/us-en/healthcare-professionals/products/neurological/cranial-repair/durepair-dura-regeneration-matrix.html

205. DynaMatrix® Plus - Keystone Dental [Internet]. [cited 2019 Jun 21]. Available from: https://www.keystonedental.com/dynamatrixplus

206. FlexHD [Internet]. [cited 2019 Jun 17]. Available from: https://www.mtfbiologics.org/our-products/detail/flexhd-structural

207. Fortiva® Porcine Dermis - Products - RTI Surgical Holdings, Inc. [Internet]. [cited 2019 Jun 21]. Available from: http://www.rtix.com/en_us/products/product-implant/fortiva-porcine-dermis

208. Glyaderm [Internet]. [cited 2019 Jun 17]. Available from: http://www.glyaderm.org/

209. GRAFTJACKET™ | Wright Medical Group [Internet]. [cited 2019 Jun 17]. Available from: http://www.wright.com/healthcare-professionals/graftjacket

210. HuMend™ Acellular Dermal Matrix [Internet]. [cited 2019 Jun 17]. Available from: https://www.integralife.com/humend-acellular-dermal-matrix/product/surgical-reconstruction-plastic-reconstructive-surgery-hospital-or-humend-acellular-dermal-matrix

211. Integra® Reinforcement Matrix [Internet]. [cited 2019 Jun 17]. Available from: https://www.integralife.com/integra-reinforcement-matrix/product/nerve-tendon-integra-reinforcement-matrix

212. Hancock II and Hancock II Ultra Bioprostheses [Internet]. [cited 2019 Jun 17]. Available from: https://www.medtronic.com/us-en/healthcare-professionals/products/cardiovascular/heart-valves-surgical/hancock-ii-hancock-ii-ultra-bioprostheses.html

213. Matrix HD® Allograft; Matrix HD® Allograft Fenestrated; 3mm, 5mm Matrix HD® Allograft - Products - RTI Surgical Holdings, Inc. [Internet]. [cited 2019 Jun 21]. Available from: http://www.rtix.com/en_us/products/product-implant/matrix-hd-allograft-matrix-hd-allograft-fenestrated-3mm-5mm-matrix-hd-allograft

214. Matrix Patch [Internet]. [cited 2019 Jun 17]. Available from: https://autotissue.de/products/

215. MatriStem UBM™ Overview – ACell [Internet]. [cited 2019 Jun 17]. Available from: https://acell.com/ecmubm-overview/

216. Medeor® [Internet]. [cited 2019 Jun 21]. Available from: https://www.dsm.com/markets/medical/en_US/products-page/extracellular-matrix-technology/medeor-matrix.html

217. Meso BioMatrix® Surgical Mesh - Extracellular Matrix (ECM) - Products & Technologies - DSM [Internet]. [cited 2019 Jun 17]. Available from: https://www.dsm.com/markets/medical/en_US/products-page/extracellular-matrix-technology/meso-biomatrix-surgical-mesh/european-union.html

218. MIRODERM Biologic Wound Matrix — MIROMATRIX MEDICAL Inc [Internet]. [cited 2019 Jun 17]. Available from: https://www.miromatrix.com/miroderm

219. MIROMESH Page — MIROMATRIX MEDICAL Inc [Internet]. [cited 2019 Jun 17]. Available from: https://www.miromatrix.com/miromesh-2

220. Medtronic Bioprostheses for Replacement of Aortic and/or Mitral Heart Valves [Internet]. [cited 2019 Jun 17]. Available from: https://www.medtronic.com/us-en/healthcare-professionals/products/cardiovascular/heart-valves-surgical/mosaic-mosaic-ultra-bioprostheses.html

221. OASIS® Wound Matrix products for HCPs [Internet]. [cited 2019 Jun 17]. Available from: https://www.oasiswoundmatrix.com/

222. OraGRAFT® Ilium Strip [Internet]. [cited 2019 Jun 21]. Available from: https://www.lifenethealth.org/dental

223. PERI-GUARD [Internet]. [cited 2019 Jun 17]. Available from: https://ecatalog.baxter.com/ecatalog/loadproduct.html?cid=20016&lid=10001&hid=20001&loadroot=true&categoryId=&pid=821800

224. Surgical Aortic Pericardial Valves [Internet]. [cited 2019 Jun 17]. Available from: https://www.edwards.com/gb/devices/heart-valves/aortic-pericardial

225. PerioDerm™ Acellular Dermis - Inside Dentistry - aegisdentalnetwork.com [Internet]. [cited 2019 Jun 17]. Available from: https://www.aegisdentalnetwork.com/id/products/dentsply-implants/perioderm-acellular-dermis

226. Permacol™ Surgical Implant [Internet]. [cited 2019 Jun 17]. Available from: https://www.medtronic.com/covidien/en-us/products/hernia-repair/permacol-surgical-implant.html

227. PriMatrix Product - Integra LifeSciences [Internet]. [cited 2019 Jun 17]. Available from: https://www.primatrix.com/products/by-brand/

228. ProxiCor for Pericardial Closure - Aziyo [Internet]. [cited 2019 Jun 21]. Available from: http://www.aziyo.com/cardiothoracic-repair/

229. Strattice RTM [Internet]. [cited 2019 Jun 17]. Available from: http://hcp.stratticetissuematrix.com/en

230. SureDerm®- Acellular Dermal Matrix [Internet]. [cited 2019 Jun 21]. Available from: http://www.hansbiomed.com/eng/product/allograft/skin_surederm.asp

231. SurgiMend® 1.0 - 4.0 Collagen Matrix [Internet]. [cited 2019 Jun 17]. Available from: https://www.integralife.com/surgimend-10-40-collagen-matrix/product/surgical-reconstruction-hernia-abdominal-wall-surgimend-1-0-4-0-collagen-matrix

232. Suspend® [Internet]. [cited 2019 Jun 21]. Available from: https://www.coloplast.us/suspend-en-us.aspx

233. Tutopatch® Bovine Pericardium ; Tutomesh® Fenestrated Bovine Pericardium - Products - RTI Surgical Holdings, Inc. [Internet]. [cited 2019 Jun 21]. Available from: http://www.rtix.com/en_us/products/product-implant/tutopatch-bovine-pericardium--tutomesh-fenestrated-bovine-pericardium

234. VASCU-GUARD [Internet]. [cited 2019 Jun 17]. Available from: https://ecatalog.baxter.com/ecatalog/loadproduct.html?cid=20016&lid=10001&hid=20001&loadroot=true&categoryId=&pid=821605

235. VERITAS | Homepage [Internet]. [cited 2019 Jun 17]. Available from: http://www.veritascollagenmatrix.com/index.html

236. XCM BIOLOGIC® Tissue Matrix | DePuy Synthes Companies [Internet]. [cited 2019 Jun 21]. Available from: https://www.depuysynthes.com/hcp/cmf/products/qs/xcm-biologic-tissue-matrix-2#tab3

237. XenMatrix™ AB Surgical Graft | Bard has joined BD [Internet]. [cited 2019 Jun 17]. Available from: https://www.crbard.com/davol/en-US/products/XenMatrix-AB-Surgical-Graft

238. Zimmer® Collagen Repair Patch [Internet]. [cited 2019 Jun 17]. Available from: http://www.zimmer.co.uk/medical-professionals/products/biologics-sports-medicine/collagen-repair-patch.html

239. Remlinger NT, Czajka CA, Juhas ME, Vorp DA, Stolz DB, Badylak SF, et al. Hydrated xenogeneic decellularized tracheal matrix as a scaffold for tracheal reconstruction. Biomaterials. 2010 May;31(13):3520–6.

240. Reing JE, Brown BN, Daly KA, Freund JM, Gilbert TW, Hsiong SX, et al. The effects of processing methods upon mechanical and biologic properties of porcine dermal extracellular matrix scaffolds. Biomaterials. 2010 Nov;31(33):8626–33.

241. Hodde J, Hiles M. Virus safety of a porcine-derived medical device: Evaluation of a viral inactivation method. Biotechnol Bioeng. 2002 Jul 20;79(2):211–6.

242. Gilbert TW, Wognum S, Joyce EM, Freytes DO, Sacks MS, Badylak SF. Collagen fiber alignment and biaxial mechanical behavior of porcine urinary bladder derived extracellular matrix. Biomaterials. 2008 Dec;29(36):4775–82.

243. Price AP, England KA, Matson AM, Blazar BR, Panoskaltsis-Mortari A. Development of a decellularized lung bioreactor system for bioengineering the lung: The matrix reloaded. Tissue Eng Part A. 2010 Aug;16(8):2581–91.

244. Mendoza-Novelo B, Avila EE, Cauich-Rodríguez J V., Jorge-Herrero E, Rojo FJ, Guinea G V., et al. Decellularization of pericardial tissue and its impact on tensile viscoelasticity and glycosaminoglycan content. Acta Biomater. 2011 Mar;7(3):1241–8.

245. Goissis G, Suzigan S, Parreira DR, Maniglia JV, Braile DM, Raymundo S. Preparation and characterization of collagen-elastin matrices from blood vessels intended as small diameter vascular grafts. Artif Organs. 2000 Mar;24(3):217–23.

246. Stern MM, Myers RL, Hammam N, Stern KA, Eberli D, Kritchevsky SB, et al. The influence of extracellular matrix derived from skeletal muscle tissue on the proliferation and differentiation of myogenic progenitor cells ex vivo. Biomaterials. 2009 Apr;30(12):2393–9.

247. Gorschewsky O, Klakow A, Riechert K, Pitzl M, Becker R. Clinical comparison of the tutoplast allograft and autologous patellar tendon (bone-patellar tendon-bone) for the reconstruction of the anterior cruciate ligament. Am J Sports Med. 2005 Aug 30;33(8):1202–9.

248. Márquez SP, Martínez VS, McIntosh Ambrose W, Wang J, Gantxegui NG, Schein O, et al. Decellularization of bovine corneas for tissue engineering applications. Acta Biomater. 2009 Jul;5(6):1839–47.

249. Rao N, Agmon G, Tierney MT, Ungerleider JL, Braden RL, Sacco A, et al. Engineering an injectable muscle-specific microenvironment for improved cell delivery using a nanofibrous extracellular matrix hydrogel. ACS Nano. 2017 Apr 25;11(4):3851–9.

250. Levy RJ, Vyavahare NR, Ogle MF, Ashworth PE, Bianco RW, Schoen FJ. Inhibition of cusp and aortic wall calcification in ethanol- and aluminum-treated bioprosthetic heart valves in sheep: Background, mechanisms, and synergism. J Heart Valve Dis. 2003 Mar;12(2):209–16.

251. Choi Y-J, Kim TG, Jeong J, Yi H-G, Park JW, Hwang W, et al. 3D cell printing of functional skeletal muscle constructs using skeletal muscle-derived bioink. Adv Healthc Mater. 2016 Oct;5(20):2636–45.

252. Montoya CV, McFetridge PS. Preparation of ex vivo-based biomaterials using convective flow decellularization. Tissue Eng Part C Methods. 2009 Jun;15(2):191–200.

253. Harrison RD, Gratzer PF. Effect of extraction protocols and epidermal growth factor on the cellular repopulation of decellularized anterior cruciate ligament allografts. J Biomed Mater Res Part A. 2005 Dec 15;75A(4):841–54.

254. Simsa R, Padma AM, Heher P, Hellström M, Teuschl A, Jenndahl L, et al. Systematic in vitro comparison of decellularization protocols for blood vessels. Soncini M, editor. PLoS One. 2018 Dec 17;13(12):e0209269.

255. Grauss RW, Hazekamp MG, Oppenhuizen F, Munsteren CJ van, Groot ACG, DeRuiter MC. Histological evaluation of decellularised porcine aortic valves: Matrix changes due to different decellularisation methods. Eur J Cardio-Thoracic Surg. 2005 Apr;27(4):566–71.

256. Guo S-Z, Ren X-J, Wu B, Jiang T. Preparation of the acellular scaffold of the spinal cord and the study of biocompatibility. Spinal Cord. 2010 Jul 12;48(7):576–81.

257. Xiang J-X, Zheng X-L, Gao R, Wu W-Q, Zhu X-L, Li J-H, et al. Liver regeneration using decellularized splenic scaffold: A novel approach in tissue engineering. Hepatobiliary Pancreat Dis Int. 2015 Oct;14(5):502–8.

258. Mazza G, Rombouts K, Rennie Hall A, Urbani L, Vinh Luong T, Al-Akkad W, et al. Decellularized human liver as a natural 3D-scaffold for liver bioengineering and transplantation. Sci Rep. 2015 Oct 7;5(1):13079.

259. Zhong Y, Jiang A, Sun F, Xiao Y, Gu Y, Wu L, et al. A comparative study of the effects of different decellularization methods and genipin-cross-linking on the properties of tracheal matrices. Tissue Eng Regen Med. 2019 Feb 8;16(1):39–50.

260. Hudson TW, Zawko S, Deister C, Lundy S, Hu CY, Lee K, et al. Optimized acellular nerve graft is immunologically tolerated and supports regeneration. Tissue Eng. 2004 Nov;10(11–12):1641–51.

261. Choi JS, Williams JK, Greven M, Walter KA, Laber PW, Khang G, et al. Bioengineering endothelialized neo-corneas using donor-derived corneal endothelial cells and decellularized corneal stroma. Biomaterials. 2010 Sep;31(26):6738–45.

262. White LJ, Taylor AJ, Faulk DM, Keane TJ, Saldin LT, Reing JE, et al. The impact of detergents on the tissue decellularization process: A ToF-SIMS study. Acta Biomater. 2017 Mar;50:207–19.

263. Sasaki S, Funamoto S, Hashimoto Y, Kimura T, Honda T, Hattori S, et al. In vivo evaluation of a novel scaffold for artificial corneas prepared by using ultrahigh hydrostatic pressure to decellularize porcine corneas. Mol Vis. 2009 Oct 13;15:2022–8.

264. Lin P, Chan WCW, Badylak SF, Bhatia SN. Assessing porcine liver-derived biomatrix for hepatic tissue engineering. Tissue Eng. 2004 Jul;10(7–8):1046–53.

265. Cortiella J, Niles J, Cantu A, Brettler A, Pham A, Vargas G, et al. Influence of acellular natural lung matrix on murine embryonic stem cell differentiation and tissue formation. Tissue Eng Part A. 2010 Aug;16(8):2565–80.

266. Ott HC, Clippinger B, Conrad C, Schuetz C, Pomerantseva I, Ikonomou L, et al. Regeneration and orthotopic transplantation of a bioartificial lung. Nat Med. 2010 Aug 13;16(8):927–33.

267. DeQuach JA, Mezzano V, Miglani A, Lange S, Keller GM, Sheikh F, et al. Simple and high yielding method for preparing tissue specific extracellular matrix coatings for cell culture. Leipzig ND, editor. PLoS One. 2010 Sep 27;5(9):e13039.

268. Cebotari S, Tudorache I, Jaekel T, Hilfiker A, Dorfman S, Ternes W, et al. Detergent decellularization of heart valves for tissue engineering: Toxicological effects of residual detergents on human endothelial cells. Artif Organs. 2010 Mar;34(3):206–10.

269. Chen R-N, Ho H-O, Tsai Y-T, Sheu M-T. Process development of an acellular dermal matrix (ADM) for biomedical applications. Biomaterials. 2004 Jun;25(13):2679–86.

270. Dongen JA, Getova V, Brouwer LA, Liguori GR, Sharma PK, Stevens HP, et al. Adipose tissue-derived extracellular matrix hydrogels as a release platform for secreted paracrine factors. J Tissue Eng Regen Med. 2019 Jun;13(6):973–85.

271. Conconi MT, Coppi P De, Liddo R Di, Vigolo S, Zanon GF, Parnigotto PP, et al. Tracheal matrices,

obtained by a detergent-enzymatic method, support in vitro the adhesion of chondrocytes and tracheal epithelial cells. Transpl Int. 2005 Jun;18(6):727–34.

272. Henderson PW, Nagineni V V., Harper A, Bavinck N, Sohn AM, Krijgh DD, et al. Development of an acellular bioengineered matrix with a dominant vascular pedicle. J Surg Res. 2010 Nov;164(1):1–5.

273. Conconi MT, Coppi P De, Bellini S, Zara G, Sabatti M, Marzaro M, et al. Homologous muscle acellular matrix seeded with autologous myoblasts as a tissue-engineering approach to abdominal wall-defect repair. Biomaterials. 2005 May;26(15):2567–74.

274. Roberts TS, Drez D, McCarthy W, Paine R. Anterior cruciate ligament reconstruction using freeze-dried, ethylene oxide-sterilized, bone-patellar tendon-bone allografts. Am J Sports Med. 1991 Jan 23;19(1):35–41.

275. Jackson DW, Grood ES, Arnoczky SP, Butler DL, Simon TM. Cruciate reconstruction using freeze dried anterior cruciate ligament allograft and a ligament augmentation device (LAD). Am J Sports Med. 1987 Nov 23;15(6):528–38.

276. Lehr EJ, Rayat GR, Chiu B, Churchill T, McGann LE, Coe JY, et al. Decellularization reduces immunogenicity of sheep pulmonary artery vascular patches. J Thorac Cardiovasc Surg. 2011 Apr;141(4):1056–62.

277. Kheir E, Stapleton T, Shaw D, Jin Z, Fisher J, Ingham E. Development and characterization of an acellular porcine cartilage bone matrix for use in tissue engineering. J Biomed Mater Res Part A. 2011 Nov;99A(2):283–94.

278. Gulati AK. Evaluation of acellular and cellular nerve grafts in repair of rat peripheral nerve. J Neurosurg. 1988 Jan;68(1):117–23.

279. Jackson DW, Grood ES, Arnoczky SP, Butler DL, Simon TM. Freeze dried anterior cruciate ligament allografts. Am J Sports Med. 1987 Jul 23;15(4):295–303.

280. Jackson DW, Windler GE, Simon TM. Intraarticular reaction associated with the use of freeze-dried, ethylene oxide-sterilized bone-patella tendon-bone allografts in the reconstruction of the anterior cruciate ligament. Am J Sports Med. 1990 Jan 23;18(1):1–11.

281. Utomo L, Pleumeekers MM, Nimeskern L, Nürnberger S, Stok KS, Hildner F, et al. Preparation and characterization of a decellularized cartilage scaffold for ear cartilage reconstruction. Biomed Mater. 2015 Jan 13;10(1):015010.

282. Wicha MS, Lowrie G, Kohn E, Bagavandoss P, Mahn T. Extracellular matrix promotes mammary epithelial growth and differentiation in vitro. Proc Natl Acad Sci U S A. 1982 May;79(10):3213–7.

283. Seo Y, Jung Y, Kim SH. Decellularized heart ECM hydrogel using supercritical carbon dioxide for improved angiogenesis. Acta Biomater. 2018 Feb;67:270–81.

284. Wang JK, Luo B, Guneta V, Li L, Foo SEM, Dai Y, et al. Supercritical carbon dioxide extracted extracellular matrix material from adipose tissue. Mater Sci Eng C. 2017 Jun;75:349–58.

285. Boer EC de, Geldof F, Gerritse TJ, Winkelhorst EW. Supercritical CO2 decellularized porcine pericardium is a promising material for an ascending aortic prosthesis. University of Twente; 2015.

286. Cho D, Chung S, Eo J, Kim NP. Super-critical-CO2 de-ECM process. MRS Adv. 2018 Jun 26;3(40):2391–7.